Nanoscale structural and mechanical properties of lipid bilayers in air environment

Propietats estructurals i mecàniques a la nanoescala de les bicapes lipídiques en aire

Aurora Dols Pérez

UNIVERSITAT DE BARCELONA
Facultat de Física
Departament d'Electrònica

Nanoscale structural and mechanical properties of lipid bilayers in air environment

Propietats estructurals i mecàniques a la nanoescala de les bicapes lipídiques en aire

Programa de Doctorat:
Nanociències

Línea de recerca:
Nanobiotecnologia

Autor:
Aurora Dols Pérez

Director de Tesi:
Gabriel Gomila Lluch

Se hace y sale

Pere Company

Index

Chapter 0. Outline

Nanotechnology is one of the main examples of interdisciplinarity that exists in science. It covers the study of phenomena occurring at the nanoscale in all fields of science; such as Physics, Biology or Chemistry. In order to progress forward, Nanotechnology has required a considerable effort in combining the various disciplines into a common objective. It has not only been essential to develop new techniques to study certain physicochemical properties or to discover new cellular structures or machinery, but also to make an effort to adapt and merge the research of all fields to a crossed interdisciplinary result. For this reason, sometimes, it has been necessary to adapt nanoscale techniques to the samples to be studied (e.g. biological samples) as well as to adapt the samples to the techniques with which they had to be studied. The versatility of the Nanotechnology approach to science has commonly generated perplexity or lack of understanding from researchers following a very orthodox way of reasoning. But it has shown, it rises with a wealth of new results, progress and a better acceptance.

My work of the last four years has been devoted to the development of sample preparation procedures to get in touch the study of cell membranes with the application of a wider range of physical nanoscale techniques. In particular, the objective was to develop a technique to create model membranes systems stable in air environment with similar structural, compositional and mechanical properties to hydrated samples. Our hypothesis of work was that in this particular problem a lot of information could be gained by adapting the samples to the nanoscale techniques with respect to what is lost from the point of view of biological relevance. According to the results presented in this work we think that we succeeded in our aim.

0.1 Structure of the thesis

The work of thesis is organized into 8 chapters. After this brief outline, in Chapter 1 I will give a short introduction about basic knowledge about cell membranes, model lipid membranes and lipid phases, followed by a description of nanoscale techniques potentially usable for its study, and which ones are used in practice. We will conclude that the nanoscale study of biomembranes is severely limited by the need of the sample to be under liquid environment. We will then explore possible methods to prepare biomembranes stable in air environment and will conclude that no simple and reproducible technique is currently available for these purpose. Based on this analysis, we will set the objectives of the present work of thesis. In Chapter 2 we will describe the general aspects of the experimental techniques used in this thesis, namely spin-coating and Atomic Force Microscopy (AFM). After these introductory chapters the results of the thesis will be presented. They are separated in term of the type of lipids used to prepare the sample and its complexity. Accordingly, we will start the analysis for the simple case of a monocomponent sample consisting of unsaturated phospholipids (Chapter 3), followed by the study of monocomponent saturated phospholipids (Chapter4). Then, we will move to the study of multicomponent samples (Chapter 5) both with binary and ternary mixture. Finally, Chapter 6 will present the main conclusions of this work thesis and some future perspectives, together with the summary in catalan. Chapter 7 contains an appendix with the acronyms, list of publications and congress presentations derived from this work. We end up the work of thesis with the list of references (Chapter 8)

Chapter 1. Introduction

Summary: In this chapter the main objectives of this thesis are presented. We start by providing an overview about basic concepts in the study of cell membranes and model membrane systems. Following, a description of techniques for membrane characterization with special attention to nanoscale imaging and spectroscopic scanning probe techniques. Finally, we analyze the limitations of the present approaches and set the objectives of this thesis.

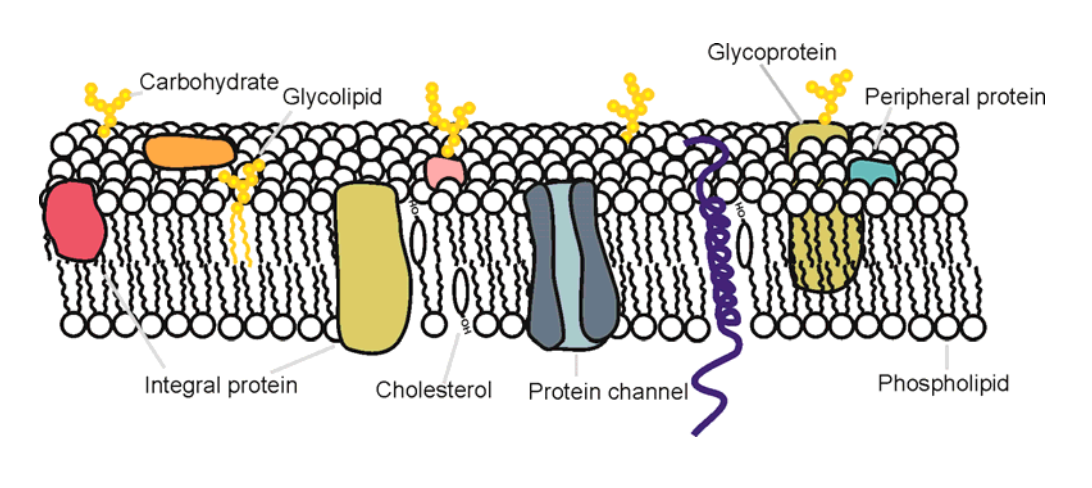

1.1 Cell Membrane

The plasma membrane is a biological membrane that surrounds the cell, being the interface between the interior of the cell and the environment. Besides the plasma membrane, one can find other internal membranes delimiting internal structures of the cell in some organisms[1].

The plasma membrane is a 2-D structure of great fluidity and its main functions are to delimit the cell, providing flexibility, a selective barrier, support to certain activities and interaction with other cells.

According to the fluid mosaic model proposed by Singer and Nicholson, membranes are 2D fluid structures of lipids with proteins embedded in it, and the molecules can diffuse freely through them[2] (Figure 1-1). Their composition consists mainly of lipids and proteins although some carbohydrates are also present (5-10% of the membrane mass). The weight percentage of proteins is greater than the lipid content; however the molar percentage of lipids is much greater, around 50 lipids/protein. For this reason often plasma membranes are called *lipid bilayers*.

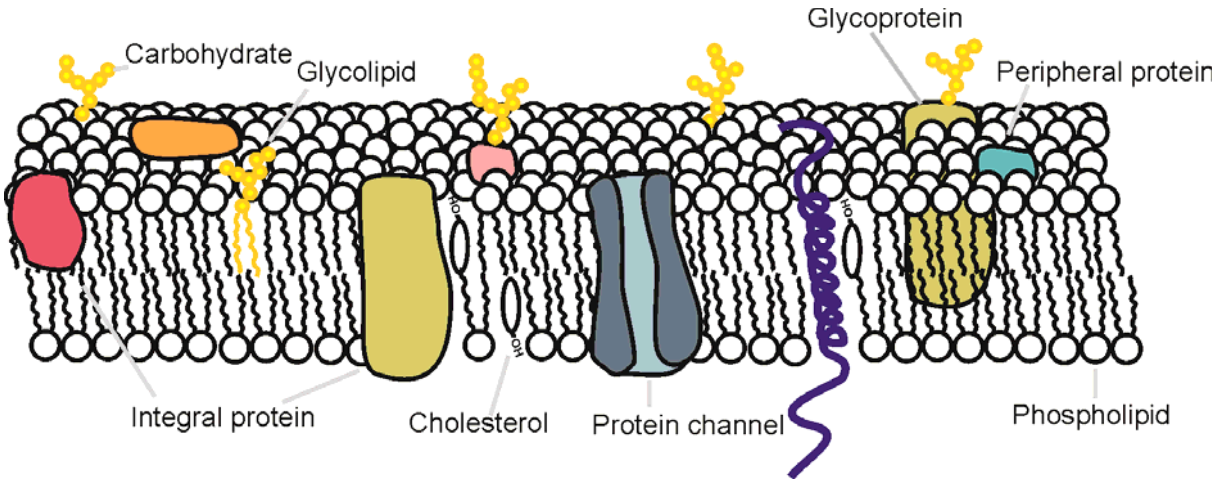

Figure 1-1. Model of plasma membrane. Integral proteins are inserted into the lipid bilayer made of phospholipids; most of them are transmembrane proteins such as protein channels. Some peripheral proteins are bound to the membrane. The extracellular part of the membrane is often glycosylated.

The membrane proteins are classified in two main groups: peripheral proteins and integral proteins (which includes transmembrane proteins and protein channels).

Among lipids, the most abundant component are phospholipids, which play a critical structural function for the membrane as matrix forming the bilayer structure. Phospholipids are amphiphilic molecules consisting of

a polar head, oriented toward the hydrophilic exterior and interior of the cell, and with hydrophobic tails oriented towards the central region of the bilayer.

There are different types of phospholipids forming biological membranes, the most important being the group of phosphoglycerides. They consist of a glycerol esterified with two fatty acids and a third component that forms the hydrophilic head. The head may be formed of a choline (in the case of phosphocholines), or alcohols such as ethanolamine or serine, or derivatives of sugars such as inositol. The hydrocarbon chains usually consist of between 12 and 24 carbon atoms and may be saturated or unsaturated (presenting some double bonds), or may have a chain of each type (Figure 1-2).

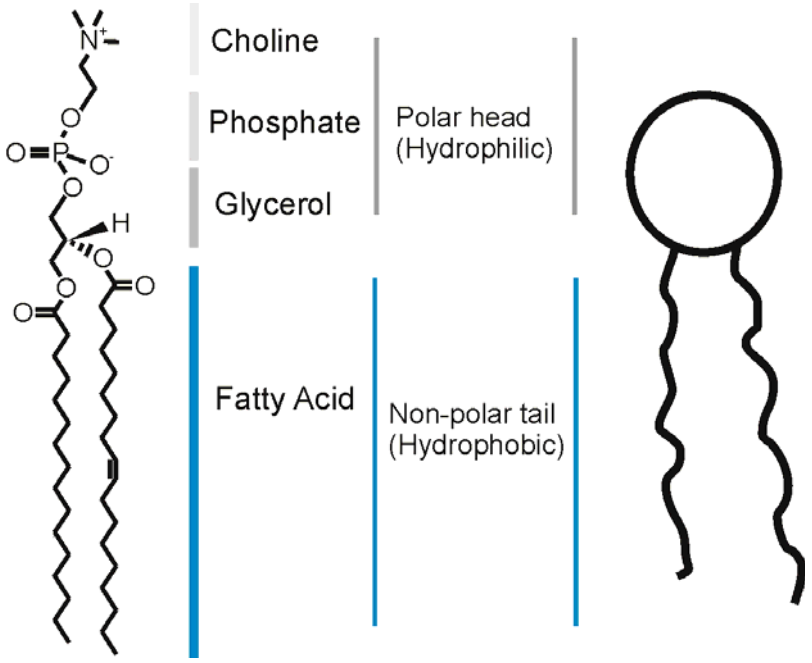

Figure 1-2. Schematic representation of the phospholipid (phosphocholine) structure and composition

Another important phospholipid is sphingomyelin, which instead of glycerol, contains a sphingosine esterified with choline (Figure1-3).

Finally, another relevant type of lipid refers to sterols, whose main representative is cholesterol. Cholesterol is the most abundant and widely distributed sterol in animal tissues[3]. One of the roles of cholesterol in eukaryotic cells is to modulate some physical properties of the membrane[4]. Cholesterol is predominantly a hydrocarbonated molecule, consists of a hydrocarbonated chain and rings in which there is a hydroxyl group which gives the amphiphilic character to the molecule (Figure1-3). Because of this rigid ring structure, cholesterol does not form bilayers itself, but usually, it is inserted between phospholipids with the hydroxyl group near the phospholipid polar head (see Figure 1-1).

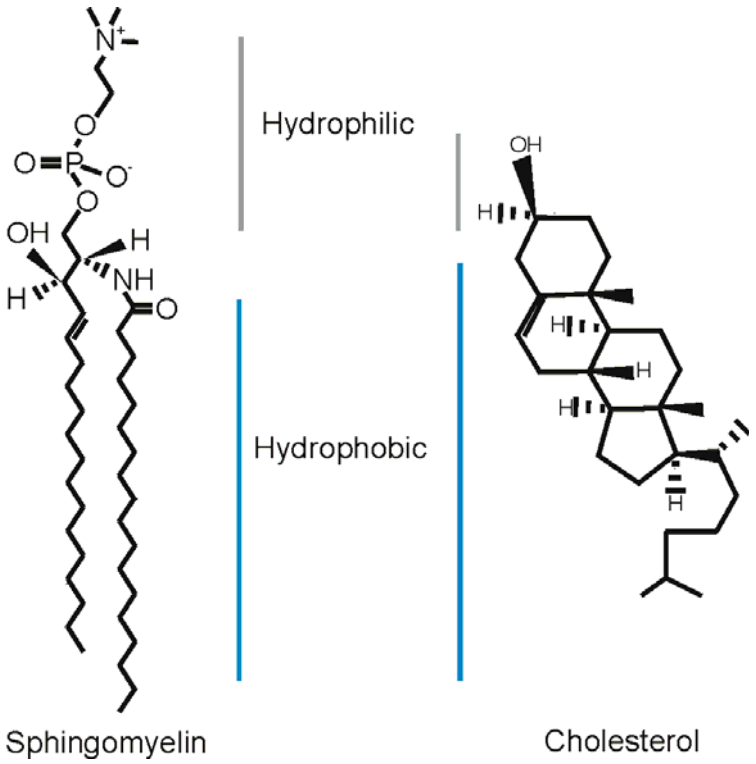

Figure 1-3 Schematic representation of sphingomyelin and cholesterol structure and composition

The distribution of the bilayer components in a biological membrane is not homogeneous; differences exist between leaflets and also laterally in the same layer. Phosphatidylcholines and sphingomyelin are predominantly in the outer leaflet while phophatidylserines and

phosphatidylethanolamines are in the inner leaflet[5]. Laterally, the *fluid mosaic model* emphasized the autonomy and diffusional mobility of membrane lipids and proteins[2]. Later, however, experimental evidence indicated that the lateral motion was not free[6]. More recent models suggest that membranes are mixtures with defined domains and disorganized lipids[7]. This lateral organization results from preferential packing of some lipids because of their thermodynamic characteristics.

In a system in thermodynamic equilibrium, the reason for domain formation is simply the differential interaction between membrane components, that are their mutual *likes* and *dislikes*. One important example of lipid domains are *lipid rafts*, which are composed of lipids, like cholesterol and sphingolipids, and are thought to be the place onto which specific proteins attach within the bilayer[8, 9].

1.2 Model membranes

Due to the inherent complexity of natural membranes, studies with model membranes are essential and can provide important information about membrane properties and interactions[10]. These model membranes are simple model systems with a known composition and known global structure. They can be bilayers forming vesicles in a suspension (unsupported) or bilayers supported onto a substrate[11] (Figure 1-4). In many cases their composition is lipidic, but they can contain also some proteins or fragments of natural membranes[10, 12].

The most used **unsupported Lipid Bilayers** are Vesicles and Black Lipid Membranes (BLM) (Figure 1-4).

Vesicles are spherical enclosed structures of lipid bilayers that are formed spontaneously under certain conditions due to the amphiphilic character of the lipids used (e.g. when water is added to dried layers of phospholipids). These vesicles could be unilamellar or multilamellar (with several concentric bilayers) with variable ranging sizes. They are usually classified as Multilamellar Large Vesicles (MLVs), Giant Unilamellar vesicles (GUVs) (1-10µm), Large Unilamellar vesicles (LUVs) (50-200nm) and Small Unilamellar Vesicles (SUVs) (18-20nm).

Secondly, Black Lipid Membranes are formed by painting with a lipid solution a hole in a hydrophobic support that separates two aqueous solutions, thus the bilayer is spontaneously formed. The lipid membrane is then self-standing and has a size of less than $1mm^2$ [13].

Supported Lipid Bilayers (SLB) are typically produced by vesicle fusion or by Langmuir transfer to the desired substrate[14] (Figure 1-4).

SLBs formed by vesicle fusion arise when LUVs or SUVs suspensions are deposited onto a substrate and incubated under certain conditions.

The vesicles are adsorbed to the substrate and they rupture and fuse, forming a single bilayer. The time of incubation, the required temperature and the concentration of lipid depend upon the characteristics of the substrate, the lipid type used and the desired coverage. In general, in order to obtain a total coverage of the substrate, the incubation time should be long (>20min) and the temperature should be above the transition temperature (Tm) of the lipid. The fusion mechanism of vesicles continues being a subject of study[15, 16]

An alternative method to produce SLB is the use of the Langmuir-Blodgget technique. The Langmuir-Blodgett (LB) technique is based in transferring a floating organic molecule (lipid) monolayer from the water surface, a Langmuir film, onto a substrate. The lipid layer can be formed by transference onto a substrate by dipping it slowly perpendicularly to the water surface, this is the LB technique, or by horizontal contacting of the substrate on the Langmuir film, this is the Langmuir-Schaefer (LS) technique[17]. Using these techniques the lateral pressure of the layers can be controlled and the composition of the different layers could be different[12, 18]. One advantage of the LB technique with respect to others is the possibility to form layers of different number of layers (as monolayers or multilayers) and not only bilayers.

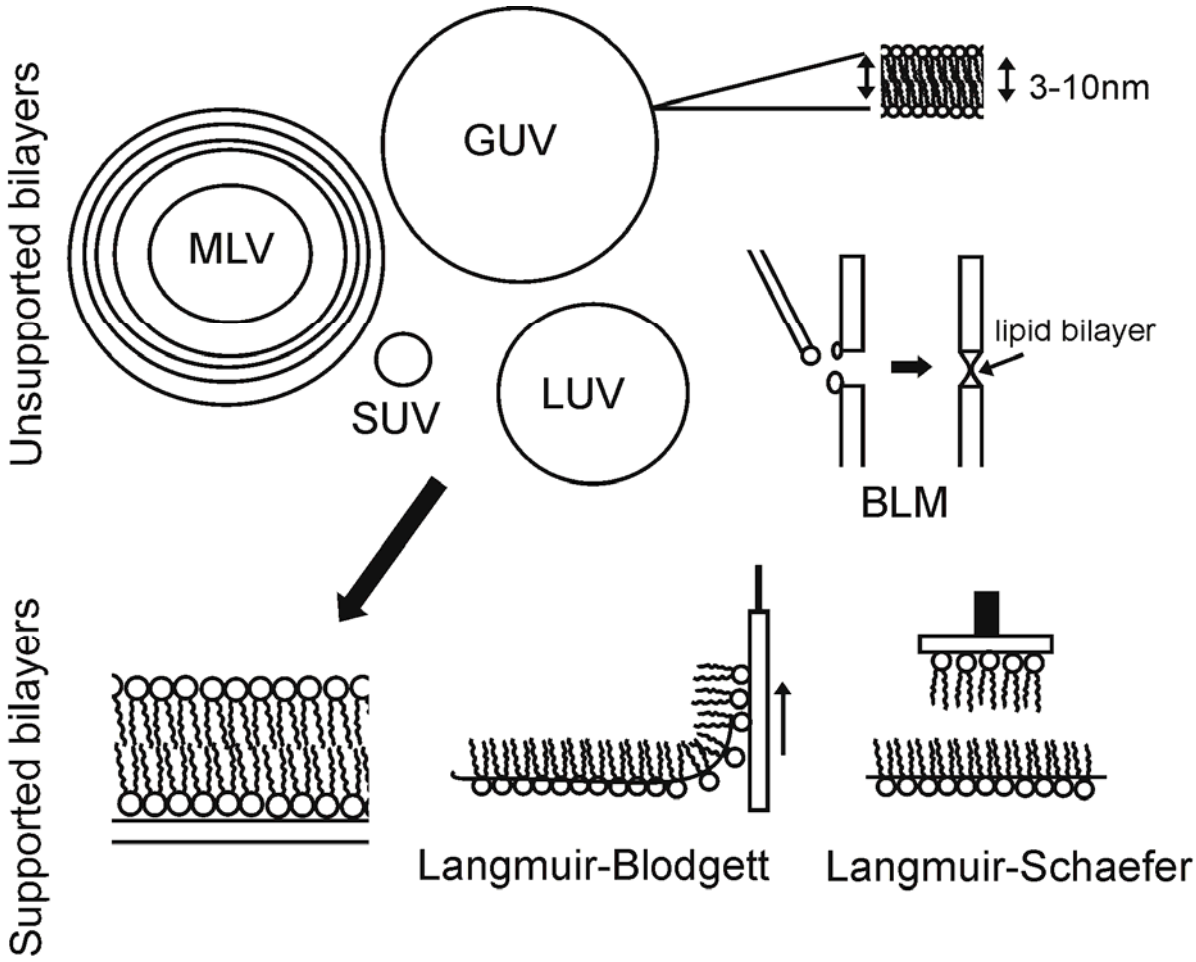

Figure 1-4 Schematic representation of the main model membranes. Unsupported bilayers: Vesicles (Multilamellar vesicles (MLV), Giant Unilamellar Vesicles (GUV), Large Unilamellar Vesicles (LUV) and Small Unilamellar Vesicles (SUV)) and Black Lipid Membranes (BLM). Supported Bilayers formed by vesicle fusion or Langmuir technique (Langmuir-Blodgett or Langmuir-Schaefer).

1.3 Lipid Phases

The membrane lipids have the capacity to adopt different phases and conformations. In general, these phases are classified into two different groups: lamellar phases and non-lamellar phases. The particular phase depends on the lipid used, its concentration, the temperature, the pressure, the composition of the solution and the presence of other lipids.

Some of the more relevant lamellar and non-lamellar phases of lipids in membranes are listed below:

- Lamellar phases: The conventional lipid bilayer corresponds with a lamellar conformation.
    - **Solid or Gel (L_β or S):** In the gel phase lipids are ordered and tightly-packed. The surface of the bilayers is flat and, usually, the thickness of the layer formed is the highest among the other phases (Figure 1-5).
    - **Fluid or Liquid disordered (L_α or L_d):** This is a fluid phase in which chains are disordered. Usually the area per molecule is higher and the thickness of the layer formed is thinner than in other phases[19]. The appearance of the bilayers is flat and the lateral diffusion of the lipids is increased with respect to the gel phase (Figure 1-5).
    - **Liquid ordered (L_o):** Liquid ordered is a phase with characteristics between solid and liquid. It presents an increased mobility compared with gel phase, but the lipids are highly ordered[20, 21] The thickness is between S and L_d. This phase requires the presence of an sterol, and it is also enriched in lipids with saturated chains like phosphocholines or sphingomyelins[22] (Figure 1-5).
    - **Interdigitated (L_β I or L_β I_T):** the interdigitated phase has a gel-like structure but with a reduced thickness (1-2 nm

lower than gel phase), due to the interpenetration of the acyl chains from one bilayer leaflet to the other. This can be induced by the addition of alcohols or by a rapid change in the temperature (among others)[23, 24] (Figure 1-5).

- **Ripple phase (P_β):** this phase is characterized by periodic undulations of the surface. This phase forms prior to the main chain melting. The ripples are proposed to be formed by periodic arrangements of interdigitated and gel phase[25] (Figure 1-5).

- Non-lamellar phases:

  - **Inverted Hexagonal (H_{II}):** this is the most biologically relevant non-lamellar phase. It consists of lipids organized into cylinders surrounding water cores[26-28] (Figure 1-5).

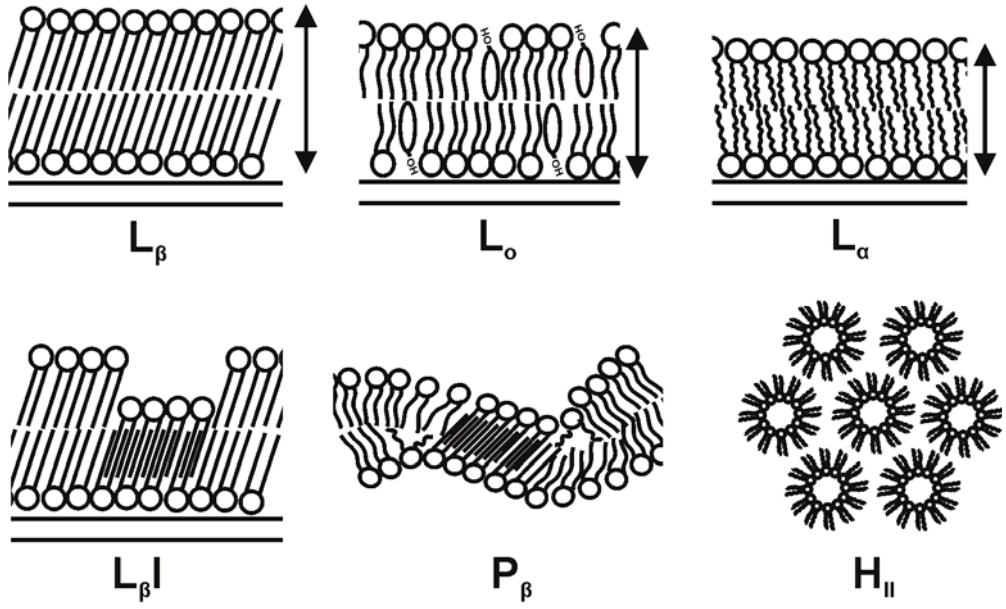

Figure 1-5. Cartoon illustration of the different lipid phases: Gel phase (L_β), Liquid ordered phase (L_o) where cholesterol is shown as ellipses, Liquid disordered or fluid phase (L_α), Interdigitated phase (L_β I), ripple phase (P_β) (cartoon based in reference [25]) and Inverted Hexagonal phase (H_{II})

One important parameter in the study of lipid phases is the Transition temperature (Tm), which is the temperature required to induce a change of phase in the lipids. Above the transition temperature the lipid is in one phase and below it, a different phase. The most common transition temperature is the one that defines the change between liquid disordered phase and solid phase. Below Tm the lipid is in gel phase and above it is in liquid phase. In general, increasing the temperature causes and increase of the rotation of the hydrocarbon chains, provoking a decrease in the order of the chains and changing their lateral interactions[29]. In general lipids with low melting temperatures have short acyl chains or present double bonds (e.g. Dilauroylphosphatidylcholine (DLPC) or Dioleoylphosphatidylcholine (DOPC)) whereas lipids with high melting temperature present long, saturated acyl chains (e.g. Dipalmitoylphosphatidylcholine (DPPC) or Sphingomyelin (SM)). Some examples of transition temperatures for some of the lipids used in this work of thesis are shown in Table 1-1.

Phospholipid	Tm (ºC)
DOPC (18:1)	-20
DLPC (12:0)	-1
DMPC (14:0)	23
DPPC (16:0)	41
DSPC (18:0)	55

Table 1-1. Examples of some transition temperatures Tm as a function of the chain characteristics. (Number of C: number of double bonds)[1]

[1] Acronyms list in Chapter7

Usually the phase properties of lipid bilayers are represented in phase diagrams. Phase diagrams are graphic representations with the purpose to show the distinct phases present in a lipid sample under different conditions (usually temperature and composition), in other words, phase diagrams show the possible phase states of a lipidic system at thermodynamic equilibrium. An extensive literature spanning several decades exists on lipid phase diagrams [30]. The most common phase diagrams are the temperature-composition (TC) diagrams (Figure 1-6), but the temperature-humidity diagrams for certain lipids are also feasible.

The simplest TC diagrams correspond to binary lipids in which the behavior of two components is described as a function of their relative concentration and temperature. Ternary phase diagrams are also possible, but considerably more complex. Usually, they are constructed for equimolar proportions of two of the components or for different ratios of the three lipids (triangular representation, Figure 1-6), although recently different representations have emerged[20, 31]

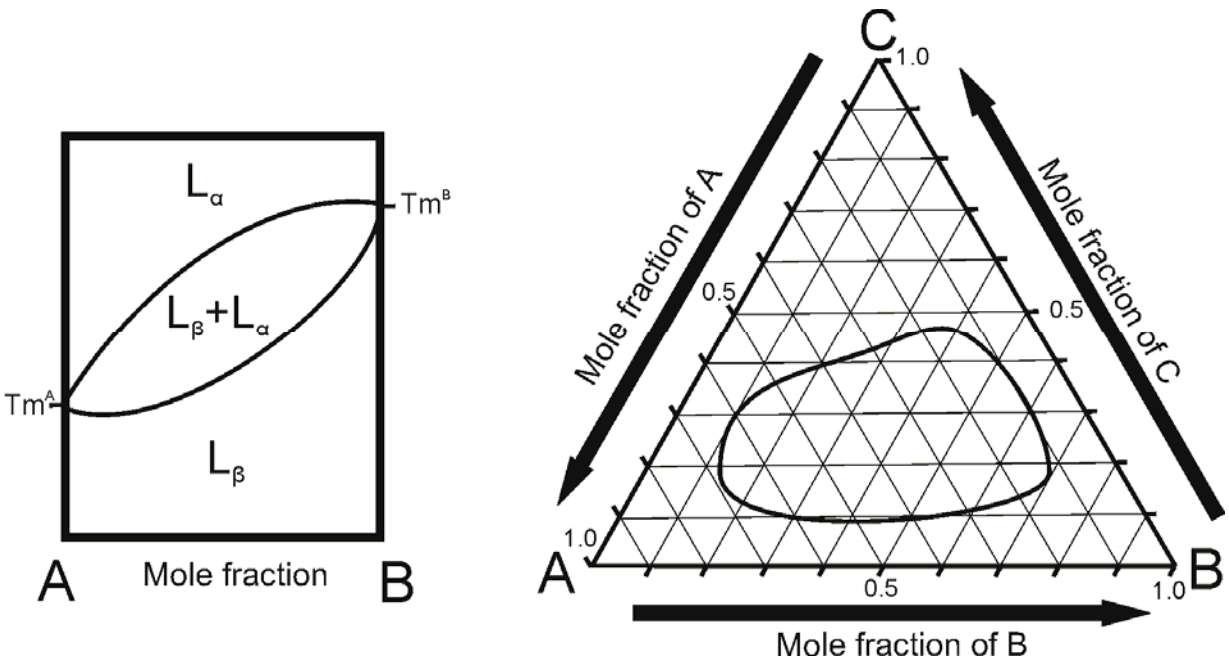

Figure 1-6 Schematic phase diagrams for a binary and a ternary membrane composed of lipids**.**

1.4 Nanoscale techniques for lipid membrane studies

Several techniques allow studying biomembranes accurately, but only some of them allow obtaining local information with nanoscale spatial resolution. Accessing such spatial resolution is fundamental for many investigations on biomembranes, such as the lateral size of the membrane structures, e.g. lipid rafts, are in the order of 10nm-100 nm while their differences in height are in the order of 1-2 nm. Therefore nanoscale techniques are especially suitable for the study of biomembranes.

Nanometric techniques, in general, allow visualizing samples with high spatial resolution (sample topography). In addition they provide information on its physical and chemical properties, as for instance mechanical properties such as force of rupture, adhesion, Young modulus; electrical properties such as electrical conductivity, surface charge, dielectric constant; or chemical properties such as material composition.

Most of the nanometric techniques used in the study of lipid bilayers are of the scanning probe microscopy (SPM) type. SPM is a branch of microscopies used for surface imaging with a resolution down to the atomic level, although the resolution varies from technique to technique and from sample to sample. SPMs are based in the use of a probe that scans the sample at close distance and use a given physical interaction to reveal local characteristics of the specimen. The probe-sample distance is controlled by a feedback-control which adapts the vertical scanner position as a function of the interaction sensed by the probe (some SPM can image different interactions simultaneously). The image is reconstructed as a function of the scanner movement.

Different SPMs have been developed as a function of the measured probe-sample interaction. The most used techniques are Near-Field Scanning Optical Microscopy, Scanning Tunneling Microscopy and

Atomic Force Microscopy. A brief description of them is presented in what follows, especially in relation to the study of biomembranes.

Near-Field Scanning Optical Microscopy (NSOM) is a nanoscale technique that allows the realization of optical images with a spatial resolution below the diffraction limit of conventional optical microscopes (far field optical microscopes) which have a resolution limited to ~300nm for visible excitation. NSOM uses an optical probe to image the sample at distances much smaller than the wavelength of light in the so called near-field regime, where by taking advantage of the evanescent waves, the resolution is no longer limited by the classical diffraction limit, but rather by the size of the aperture of the probe. This technique can operate in liquid (e.g. buffer) or in air, and like conventional optical microscopy, very often needs the use of staining or labeling methods (e.g. fluorescence) to provide the desired contrast.

One of the main advantages of NSOM is its ability to provide information on the composition of the sample through appropriate labeling, in addition to provide topographic information of the sample through shear-force feed-back methods[32]. One disadvantage is that the labeling can induce artifacts on the sample[33]. In addition, it is a technique relatively difficult to use in a routine basis due to difficulties in preparing good quality small scale probes, get stable working conditions in liquid environment and the need of a relatively complex precise measuring optical set-up.

Scanning Tunneling Microscopy (STM) was the first SPM invented by Binning and Rohrer in 1982[34].This technique senses the dc tunneling current between the sample and a sharp conducting probe. The measurements requires in general a conductive specimen (or a very thin sample on top of a conductive substrate)[35]. As a general rule the technique needs to be applied in air or vacuum, although systems able to work under liquid conditions with specific probes have been also developed (providing lower performance than their equivalents in air).

On what concerns membrane studies based on STM, its number is very limited due to the insulating nature of the membranes and the need of STM to be operated under air or vacuum conditions[36].

Atomic Force Microscopy (AFM) is a SPM technique that senses the atomic forces (e.g. van der Waals force) of attraction or repulsion between the sample and a sharp probe. The AFM probes have a long cantilever with a tip, which interacts with the sample, located at the free end of the cantilever. The interaction force between the sample and the tip induces the bending of the cantilever that can be measured by an optical detection system. (More details in Chapter 2).

AFM can work with both conductive and insulator samples, and can be operated both in air and liquid conditions. Probes can be made of insulator or of conductive materials and are easily available from probe manufacturers. Usually, AFM is used to image the topography of the samples, as well as, to determine its mechanical properties through force-spectroscopy measurements (more details in Chapter 2). AFM has been largely used in the study of supported lipid membranes.

On the negative side, AFM is relatively limited to discriminate the sample composition when used in its conventional form.

Beyond imaging and mechanical studies, there exists a number of AFM based techniques which can provide additional physical or chemical information on the samples under study. Some of these AFM-based techniques are described below:

- **Conductive Atomic Force Microscopy (C-AFM):** With C-AFM, the DC current flowing through the sample in response to a DC voltage applied between a conductive tip and the substrate is measured locally. This allows the conductivity of a sample be imaged during the topography measurements, which have to be done in "contact mode". Apart from a conduction image, it is also possible to obtain I/V curves at given points of the sample.

This technique has to be operated in air, preferably in dry air conditions to avoid the water layer present in humid ambient. For this reason, their application on membranes has been limited (like the case of STM) and only some studies have been published in samples that are very resistant to dried conditions, such as the *purple membrane*[37]

- **Kelvin Probe Force Microscopy (KPFM):** This is an AFM-based technique that allows measuring the surface potential of a sample. This is related to the charges that are in the surface of the sample. This technique is also limited to the use of samples in air[38] and hence its use on biomembranes has been limited.

- **Nanoscale Impedance Microscopy (NIM):** This technique is an AC-current sensing technique that is able to measure the local electrical impedance of a sample $Z(\omega)$. NIM permits to obtain an impedance image for a fixed frequency simultaneously with topography. The main goal of this technique is to provide in addition to the conductive information on the sample, also local dielectric properties, through capacitive measurements.

  This technique can be used satisfactorily in the study of membranes stable in air conditions (e.g. *purple membrane* [39]) but it is limited to the use of samples in dry air conditions.

- **Electrostatic Force Microscopy (EFM):** This technique is based in the detection of the attractive force that arises between a conductive probe and the sample when an electric voltage is applied between them. The electrostatic force is sensed by the probe and can be monitored as a function of the bending of the cantilever, allowing the extraction of the surface potential and the dielectric properties of the sample.

The study of biomembranes with this technique is also limited to the samples that are stable in dry air conditions (e.g. *purple membrane*[40]) due to the need to be operated under air environment.

Scattering type-NSOM: In recent years, aperture-less (also called scattering type) NSOM systems have been developed to be able to operate with conventional conductive Atomic Force Microscopy probes in modified AFM set ups. These systems couple an AFM with a Fourier Transform Infra Red detector to allow both topographic imaging as well as IR imaging. This allows obtaining information on the chemical, optical and electrical properties of the sample at the nanoscale. At present, these systems can only be operated in dry air conditions and, to our knowledge, no reports on biomembranes have been provided.

Beyond conventional SPM techniques, in recent years other nanoscale techniques have been developed which are relevant for biomembrane studies. Among them, the more relevant one has been

Nano- Secondary Ion Mass Spectrometry (NanoSIMS). This technique is based in the use of Secondary ion mass spectrometry (SIMS) with an improved resolution that permits to identify the components of a sample with a resolution on the order of 50nm [41]. One of the requirements of the technique is that the sample has to be labeled isotopically and ultra-high vacuum is necessary during the measurement.

Some studies demonstrate satisfactory results with freeze-dried model lipid membranes and may even quantify the proportion of different lipid in a domain [41-43].

In summary, we have seen that there are an impressive number of nanoscale techniques potentially applicable to the study of biomembranes and that could provide local information on its topography, chemical composition and electrical, mechanical and optical properties. However, only a few of them have been applied to the study of biomembranes. The reason being that biomembranes are believed to require a liquid environment to keep their properties intact, and only a few of the nanoscale techniques mentioned can be operated under liquid conditions (the practical exceptions are conventional AFM and NSOM). In spite of the efforts made in recent years, there is not a clear perspective that all the techniques will be one day able to operate under liquid environment.

As an alternative approach, it has been proposed to develop sample preparation methods for biomembranes enabling their study under dry air conditions (examples have been given for C-AFM, NIM or NanoSIMS). However, drying biomembranes and keeping their properties almost intact is far from being simple, as we describe in next section.

1.5 Drying biomembrane techniques

As mentioned above, there are several nanoscale techniques that could be used to obtain important physicochemical properties of the membranes. However, due to technical limitations they can only be operated in dried air conditions or vacuum. For this reason it is important to know if biomembranes can be prepared under these conditions and how a dehydration procedure affects the membrane properties.

Effects of dehydration on biomembranes

The structure and function of biological membranes are considered dependent of the water presence and dehydration may cause an irreversible damage [44]. The main problem is that during dehydration the lipids tend to orient themselves at the interface between the aqueous solution and the air disrupting the bilayer structure, thus causing aggregates and the delamination of the sample [45-47]. Therefore, simple drying of the membrane samples generally causes an irreversible damage. An example of the characteristic effect of simple dehydration of a lipid bilayer is shown in Figure 1-7 for the case of a supported lipid bilayer of DPPC on mica. Therefore, in order to avoid irreversible damage on the membrane upon drying, special drying procedures need to be used. Some of the more relevant procedures for membrane drying are described in what follows.

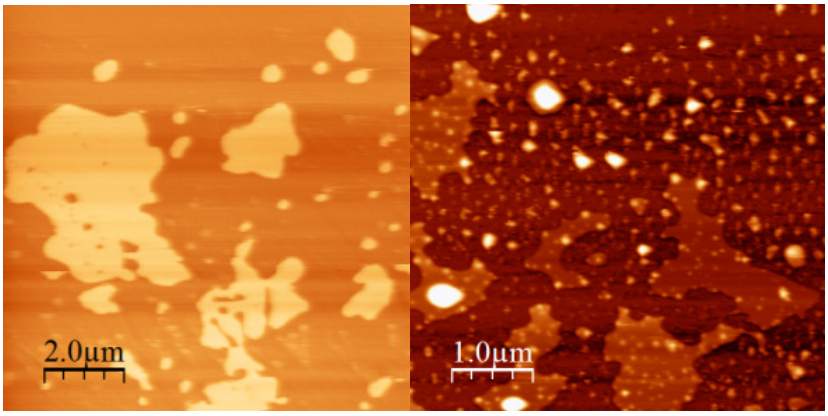

Figure 1-7 AFM topography images of a supported lipid bilayer of DPPC in liquid media (A) and after simple dehydration (B).

Existing biomembrane dehydration techniques

An essential requirement of dehydration is that the water must be removed from the biomembrane without the disruption of the sample structure. The dehydration of the lipid bilayers properly is a topic that is currently under study because of its great importance for the creation of biosensors and the need to obtain information on properties that are not measurable in liquid medium. Some of the techniques used are based on the use of protectants or coatings, the creation of hybrid layers or the use of special drying processes (e.g. freeze-drying).

- **Protectants or coatings**

The use of protectants is based in the mechanism of some organisms to survive and preserve their structures against severe dehydrations. These desiccation-tolerant organisms usually produce large amounts of disaccharides in the dehydration process. The actuation mechanism of these disaccharides and other protectants is not completely understood but some hypotheses were proposed to explain this phenomenon[47].

The main hypothesis is that after dehydration the sample is completely covered by the protectant, maintaining a thin layer of water between the bilayer heads and the protectant. This layer protects the bilayers against a complete dehydration and promotes the function recovery after the rehydration of the membrane (Figure 1-8).

Some examples of protectants used in SLBs are: trehalose, sucrose, DMSO, glucose and dextran. [47-49]

The main disadvantage of this technique is the presence of the protectant network on the dry sample. The added substances in the solution tend to precipitate at the time of dehydration and it is very difficult to obtain a homogeneous coverage of the sample, with some regions being damaged by the dehydration and some others covered by a protectant layer or precipitates. Then the protectant layer could mask the membrane which is being studied (Figure 1-8)

For coatings the principle is the same, to form a water-retaining layer to maintain the membrane structure (Figure 1-8). Examples include the formation of bilayers which incorporate poly ethylene glycol (PEG)[50], proteins[45] or s-layer[51]. Similarly to the use of protectants the main disadvantage of this technique is the formation of a layer completely covering the sample, thus limiting the access of most of the nanoscale characterization techniques that can be used.

- **Tethered bilayers**

In this approach the membrane is covalently linked to a support (Figure 1-8). Usually the inner leaflet of the membrane is the bounded part although in some cases the linker can cross the membrane conferring more stability against delamination [11, 52, 53].

Occasionally this technique needs the use of some protective molecule as the protectants or coating to preserve the upper layer.

The main disadvantage is the presence of molecules that are not components of the original membranes, which can potentially affect its intrinsic properties.

- **Freeze-drying**

The freeze-drying method consists of flash-freezing the sample followed by careful removal of bulk water, as performed in standard freeze-fracture and cryoelectron microscopy experiments (Figure 1-8). Different protocols can be used but in general the sample is immersed in liquid nitrogen to frozen completely the sample converting the liquid in a frozen amorphous state. Afterwards, the sample is subjected to a low pressure maintaining the temperature in order to sublimate the water.

This procedure has allowed the preparation of dry lipid layers with apparent good quality, also preserving even phase separated lipids domains, as revealed with the TOF-SIMS technique[41-43].

The main problem of this procedure is the control of the speed in the freezing step and often artifacts are produced.

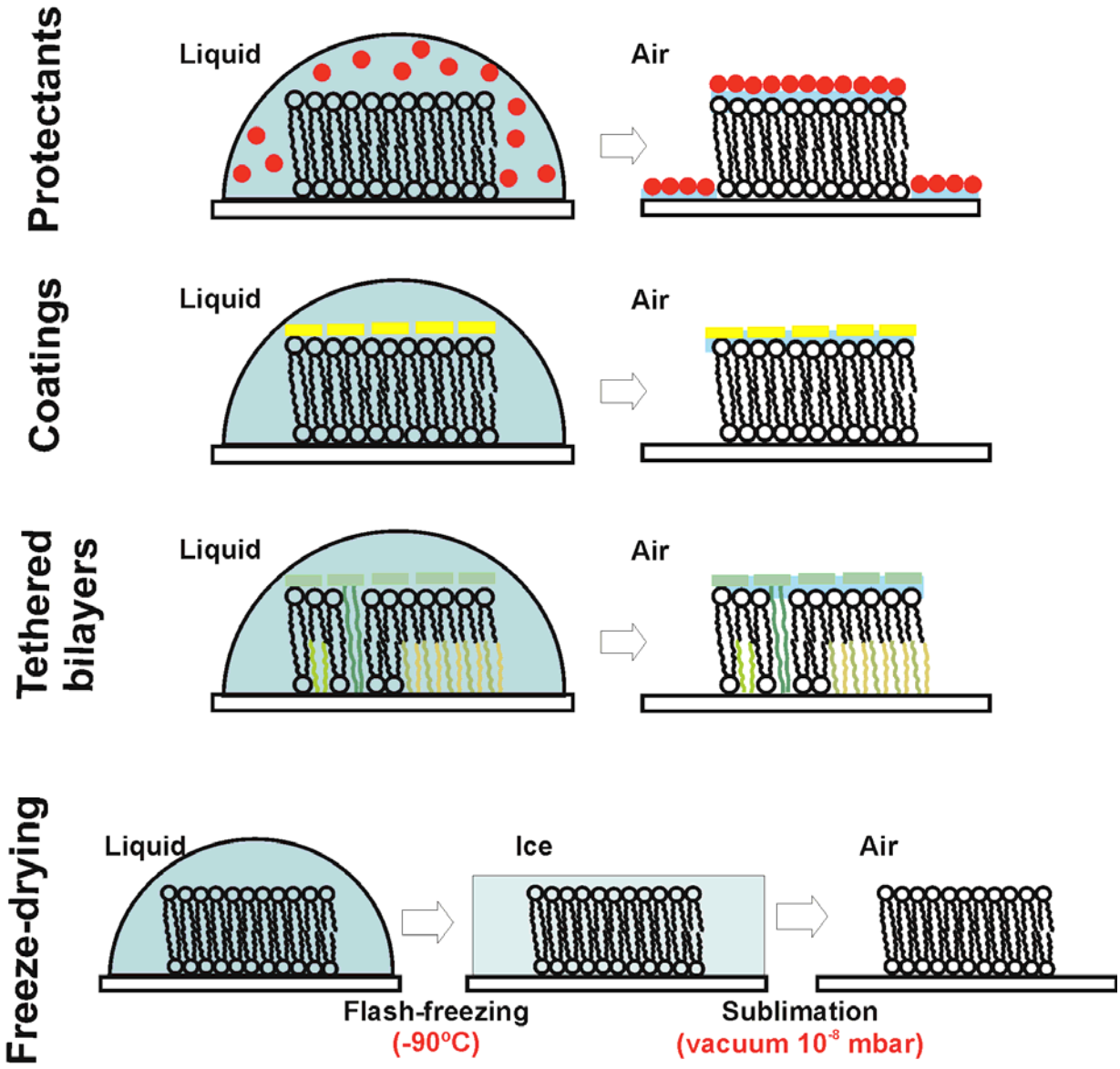

Figure 1-8 Schematic representation of the different techniques used to dehydrate membranes (use of protectants, use of coatings, tethered bilayers and freeze-drying)

In summary, in spite of numerous efforts, currently there is no simple and reproducible technique to prepare membrane samples stable in dry air conditions.

1.6 Objective of this thesis

As explained in this chapter, Cell membranes are 2-D heterogeneous fluid systems that show nanoscale structures of great interest because of its importance in membrane functions. Due to the inherent complexity of natural membranes, the study of model membranes is essential to obtain important information about membranes.

The small lateral size and tiny variation of the height of the lipid structures require the use of nanoscale characterization techniques. However, the requirement of liquid environment to preserve the integrity of the membrane limits the number of techniques that can be applied in the study of the physical and chemical properties of biomembranes. In practice, atomic force microscopy (AFM) is the most used technique[54-63] for its ability to be operated under liquid environment, but many other techniques exist that works in dry environment and that are widely applied on dry samples in biology and materials science. Examples of important techniques that we have described include Secondary Ion Mass Spectrometry (Nano-SIMS) [41-43] , which probe material composition at the nanoscale, and a number of electrical characterization techniques such as conductive Atomic Force Microscopy (C-AFM) [37] and Scanning Tunneling Microscopy (STM) [36], which measure electrical conductivity; Nanoscale Impedance Microscopy (NIM) [39] and Electrostatic Force Microscopy (EFM)[40] , which probe dielectric properties at the nanoscale. Thus, so far many physical properties of biomembranes have remained unknown due to difficulties in operating these techniques in liquid.

To overcome this limitation, it would be advantageous to produce lipid models that remain stable in air and with structural and physical properties as close as possible to the ones observed in aqueous environment.

To this aim, simple drying of lipid bilayers is useless because it induces irreversible instabilities that modify the bilayer structure[45, 64]. Adding molecules such as lyoprotectants has been proposed to preserve the

bilayer during the dehydration[47,48] but they show a tendency to precipitate during dehydration. Freeze-drying of lipid layers has shown to give good-quality layers that preserve phase-separated lipid domains[41-43], but this approach is not easily reproducible without expertise.

So it is necessary to develop novel techniques for drying the samples without the inconveniences of the existing techniques.

Precisely, the main objective of this thesis is to develop a preparation procedure for lipid membranes (both single and multi-component) which makes them stable in dry air conditions and to show physicochemical properties as close as possible to their equivalents in liquid environment.

In order to validate the equivalence between dried membranes and hydrated ones we have chosen AFM to characterize the structural and mechanical properties of the prepared samples. This technique and type of measurements can be done both in dry air and liquid conditions, and therefore, the results of topography and force spectroscopy can be compared in both media.

In particular, I addressed four main objectives:

1- To prepare monocomponent and multicomponent supported lipid bilayers stable in dry air conditions.

2- To study the nanoscale structural characteristics of the ultrathin layers formed (monocomponent and multicomponent) in dry air environment.

3- To study the nanoscale mechanical properties of the lipid bilayers in dry air environment as a function of the composition.

4- To establish the similarities and dissimilarities between the nanoscale structural and mechanical properties of dry lipid membranes and of hydrated lipid membranes.

Chapter 2. Experimental techniques.

Summary: Chapter 2 explains the experimental techniques used in this thesis. A brief description of the techniques used for sample preparation and for sample characterization (namely spin-coating and Atomic Force Microscopy) is provided.

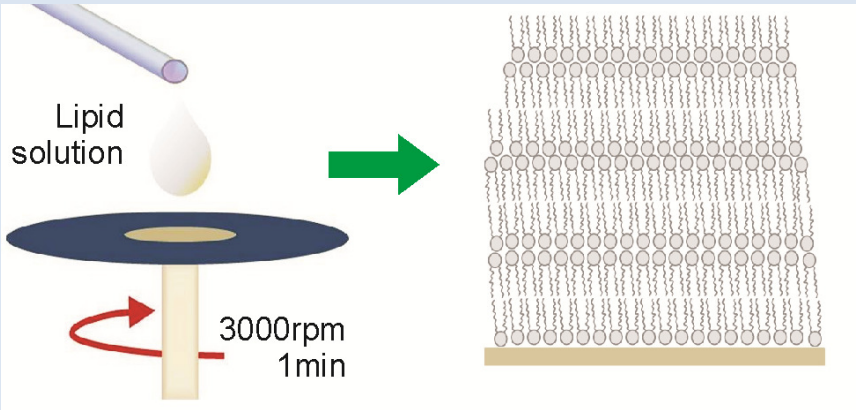

2.1 Sample preparation: Spin-coating

During this work of thesis we have considered different techniques for the preparation of air-stable Supported Lipid bilayers (SLBs) and also considered the use of different substrates. We started considering the formation of hydrated lipid bilayers by means of the liposome fusion technique and the posterior drying of the sample, either by simple vacuum dehydration or by means of the more elaborated freeze-drying technique described in the Chapter 1. Although some partial successful results were obtained, none of these techniques provided reliable and reproducible results, thus not being suitable for posterior systematic studies (in section 2.4 Appendix we provide a summary of the results obtained by means of these techniques).

After these initial studies, we considered the use of the spin-coating technique after analyzing in detail the results reported by Simonsen and coworkers [65]. At the end, this has been the technique that allowed us to

derive most of the results presented in the present thesis and that are described in detail here.

Spin-coating is a technique widely used to create thin films on substrates. Briefly, a solution is placed on a substrate and then it is rotated at a high speed. Due to centrifugal forces, the fluid spreads onto the substrate and forms a very thin layer of material on the substrate whose thickness depends on the properties of the solution and on the speed of rotation.

Normally the spin-coating process is divided into four stages:

1. **Deposition:** the solution is deposited on the substrate.
2. **Spin up:** this is the acceleration step in which the substrate is accelerated to the desired speed.
3. **Spin off:** the excess amount of solution is flung off the substrate surface during the rotation until enough solution is eliminated to increase the viscosity and the flow ceases. This is the spin-coating stage.
4. **Evaporation:** once the flow ceases, it starts the evaporation of the solvent and the thinning of the layer.

Spin-coating of lipids on solid supports has been proven as an excellent technique to obtain lipid multilayers, which usually are rehydrated to obtain lipid bilayers of high quality[59, 65-73]. Originally this technique has been used to prepare samples for X-ray reflectivity[66], but after it has been adapted to prepare samples for use with AFM and confocal microscopy[65] and it is increasingly being used to obtain lipid bilayers [59, 65-67, 74, 75].

In spin-coating the preparation of samples is easy, fast and with a high reproducibility. Therefore, it constitutes an interesting approach for the preparation of dry lipid bilayers for nanoscale investigations, even if the orientation of the lipids chains in dry bilayers is reported to be inverted with respect to their analogues in hydrated environment[65].

However, until now, little is known about the nanoscale properties of supported dry spin-coated lipid bilayers [65, 71-73], especially in the low concentration range where ultrathin films are formed (down to a single lipid bilayer). For this reason, it is necessary to find the suitable concentrations and operation conditions to obtain ultrathin layers.

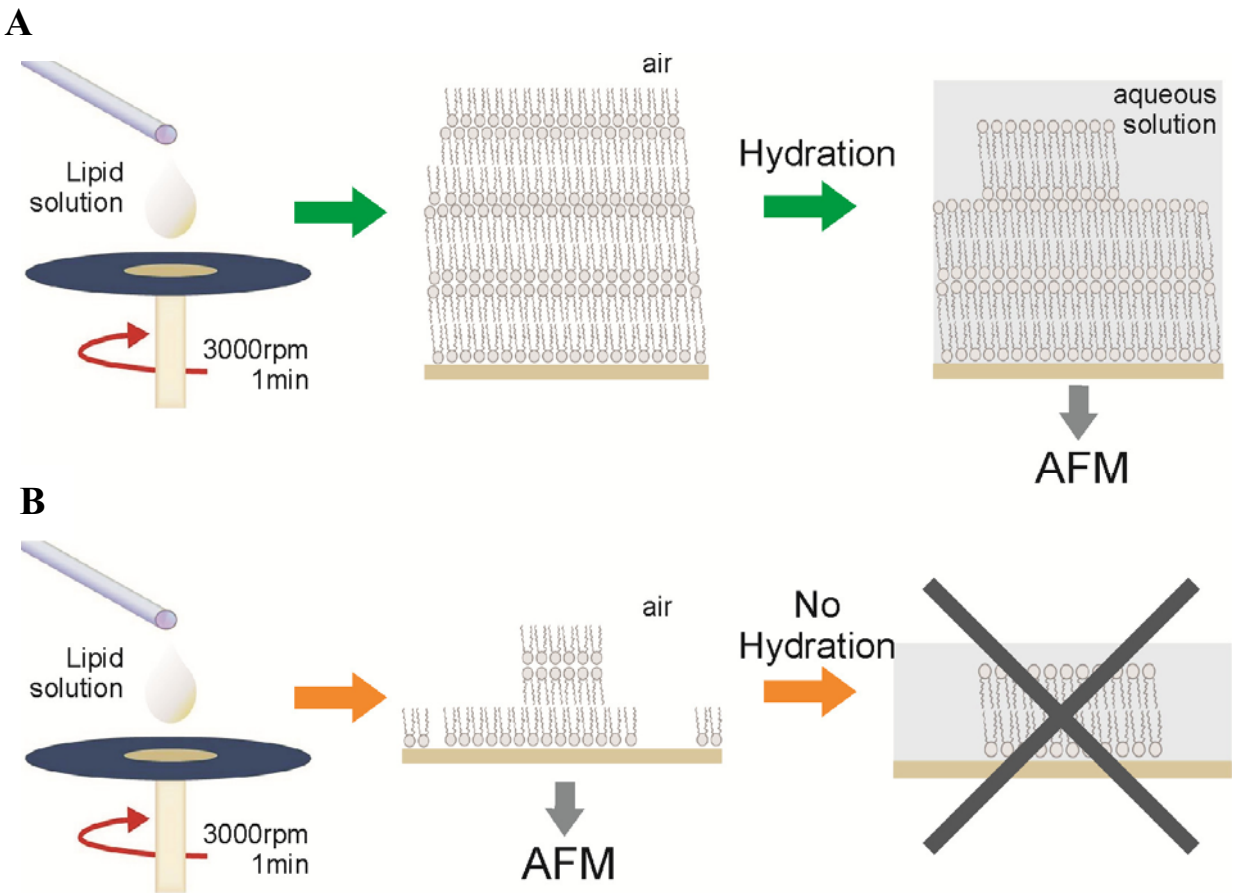

Figure 2-1. Schematic representation of preparation of lipid layers by the spin-coating technique. A drop of lipid solution on a substrate is spun 1min at 3000rpm and after some hours, for the total evaporation of the solvent, one obtains a sample with inverted bilayers on top. In the case of rehydrated samples (a) then a solution is added which makes the lipids to recover the usual orientation (b), the coating solution concentration has to be chosen adequately to provide after the spin-coating process already a few layers samples.

To prepare dry samples the procedure is the same as the one used to prepare rehydrated lipid bilayers, but with the difference that the lipid concentration has to be adjusted to provide ultrathin layers and that the rehydration step is avoided (Figure 2-1). We note that on rehydrated samples the control of the concentration of lipids in the coating solution is not so critical. During this work of thesis, we have shown that lipid concentrations below 1 mM provide the desired ultrathin spin coated layers, compared with concentrations used in the formation of rehydrated samples(>3mM).

2.2 General experimental methods for sample preparation.

The general materials used in this thesis for the sample preparation with the spin-coating technique are described in below. Later on, for each particular application we give the particular details about the methods applicable to each case.

- **Lipids:** The lipids used to create the model membranes are mostly Phosphatidylcholines (DOPC, POPC, DLPC, DMPC, DPPC, DSPC) although Sphingomyelin (SM) and Cholesterol (Chol) were also used. These lipids have been chosen because they are the main components of eukaryotic cell membranes [76] and because they are the ones usually used in hydrated model lipid membranes, thus allowing a direct comparison between the properties of dry and hydrated samples. As mentioned before, the concentration of lipids in the solution was kept relatively low in the mM range in order to ensure the formation of ultrathin layers.

- **Solvent:** In our case the solvent used depends of the lipid dissolved but, in general, we used a hexane/methanol (98:2, v/v) solution. This solvent, previously used for Simonsen and coworkers [65], met the requirements necessary to prepare lipid samples by spin-coating since it wets adequately the substrate surface, the lipids are well soluble in it and it is volatile.

- **Substrate:** The substrate used as support for the lipid layers is muscovite Mica (Figure 2-2). This is a phyllosilicate mineral of aluminum and potassium with chemical formula $(KF)_2$ $(Al_2O_3)_3$ $(SiO_2)_6$ (H_2O). Mica has a layered structure and an atomically flat surface that can be produced by mechanical exfoliation. Due to its flatness and the low roughness, and easy of availability, it is the substrate most widely used in AFM in general, and in the

study of SLBs in particular. We have considered other substrates like glass, silicon dioxide, graphite or gold but most results have been obtained with mica substrates.

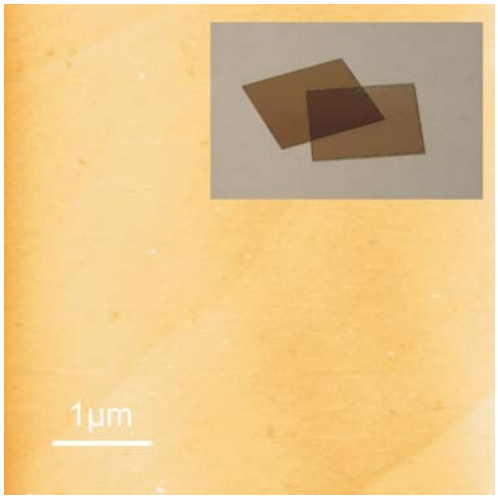

Figure2-2 AFM topography image of a mica layer. Inset: appearance of the mica sheets used.

2.3 Sample characterization: Atomic Force Microscopy

Sample characterization has been carried out by means of Atomic Force Microscopy (AFM). As mentioned briefly in Chapter 1, AFM is a scanning probe technique that allows mapping the sample with lateral and vertical resolution in the range of nanometer (from subnanometers to tens of nanometers) by measuring the interaction force sensed by a very sharp probe.

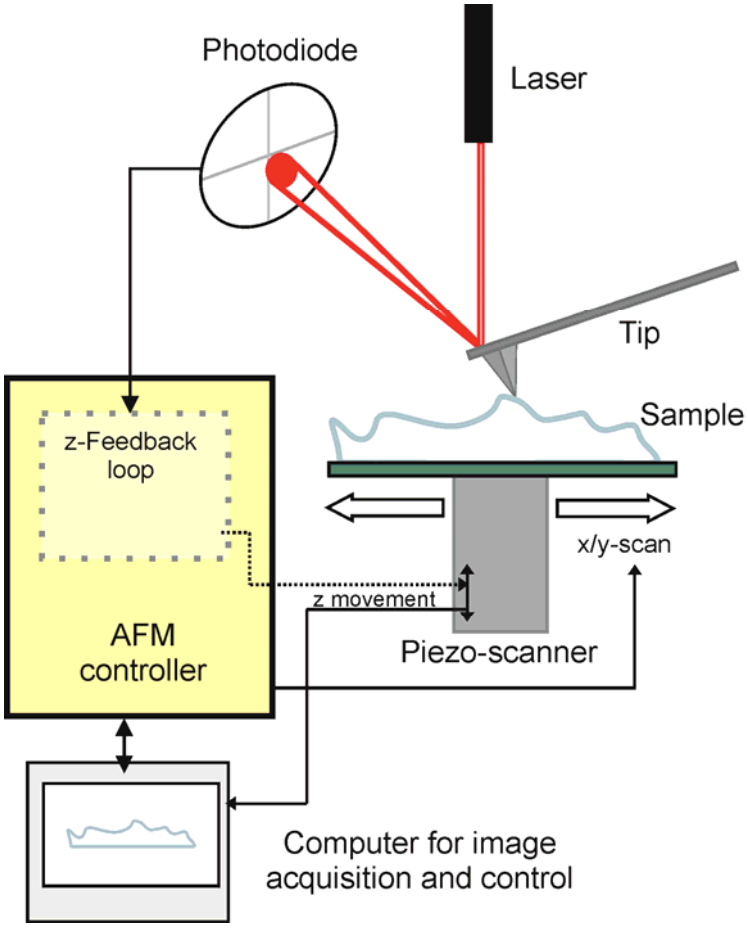

Figure 2-3. Simplified diagram for a AFM set up showing the main components of an AFM

An AFM contains five basic components (see Figure 2-3): A probe consisting of a cantilever with a sharp tip, a laser directed to the end of the cantilever of the probe, a photodetector to monitor the deflection of

the probe, a piezo-electric scanner and a controller with a feedback electronic system.

The interaction force between the sample and the tip induces the bending of the cantilever which can be measured due to the use of the laser and the photodiode. The laser is focused at the end of the cantilever and the signal is reflected to the photodiode. The position of the spot in the photodiode will depend on the deflection of the cantilever. During the formation of an image, the feedback system will change the scanner elongation (in z direction) to maintain constant the force between the tip and the sample. The final image is the reconstruction by the acquired movement of the scanner in the z direction as a function of the position of the tip (in x/y).

Topographic AFM modes.

Of the various existing AFM topographic modes, in this work of thesis we have mainly used two of them:

- **Contact mode**: It is the basic operating mode. This mode works in the repulsive regime of Van der Waals forces. The tip is maintained at a constant force using the signal of the deflection, the feedback loop and the movement of the piezo-scanner in z. This vertical motion together with the scan in x/y of the sample permits to map the sample topography in x, y and z.

  This mode has to be used with soft cantilevers (spring constant <0.1 N/m) and tends to damage soft samples, such as biological samples, if the lateral shear force is not controlled by adjusting properly the scan speed and the feedback parameters.

- **Dynamic mode:** it works by oscillating the cantilever near its resonance frequency and keeping the amplitude of oscillation constant when the tip interacts with the sample (the amplitude of oscillation decreases when the tip gets closer to the sample). The

feedback controller adjusts the piezoscanner elongation to maintain the oscillation amplitude constant while the sample is scanned, and from it the topographical image is reconstructed.

This mode reduces the interaction between the sample and the tip and it is considered more appropriate for measurements in soft samples like lipid membranes.

Force spectroscopy

Beyond imaging, AFM can also be used to map the mechanical properties of the samples. Usually, this information is obtained from force spectroscopy measurements, in which force-distance curves are measured on selected locations of the sample. A force-distance curve (fz) is a representation of the tip-sample interaction forces versus the piezo-scanner displacement in z direction. To obtain this information the sample is moved along a certain range in the z axis while the deflection signal of the cantilever is captured. The force of the tip-sample interaction is related to the cantilever deflection through the Hooke's law:

$$F = k_c \cdot \Delta D \qquad \text{(I)}$$

where k_c is the equivalent spring constant of the cantilever and ΔD the measured cantilever deflection.

In most equipments the recorded fz curves gives the force between tip and sample as a function of the piezo displacement in the z direction and not as a function of the real distance between the sample and the tip. In order to get the distance between tip and sample, the force curve has to be analyzed in order to identify the point of interaction between tip and sample, which is then taken as the zero position.

In the study of lipid membranes the force curves are usually represented as a function of the sample deformation or indentation (δ), rather than as a function of tip sample distance (Figure 2-4). The sample deformation is defined as:

$$\delta = \Delta z - \Delta D \qquad \text{(II)}$$

where Δz is the piezoscanner displacement and ΔD the cantilever deflection, defined above. Usually the first contact point is considered to have zero indentation, δ=0, so that positive values of δ correspond with tip-sample contact while negative values correspond with non-contact region.

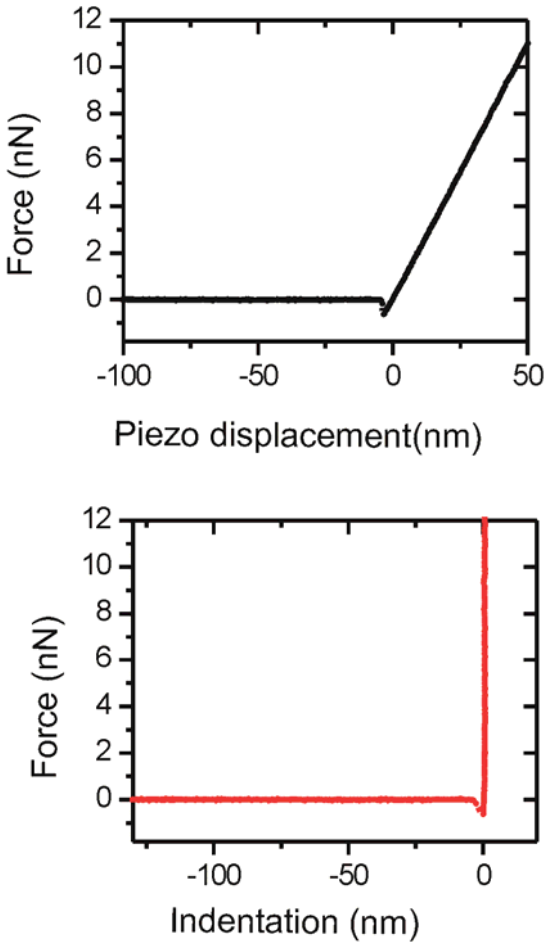

Figure 2-4 Representative Force versus piezo-scanner displacement curve (black) and Force versus Indentation curve (red)

Approach and retract curves provide different information about the tip-sample interaction. In general the approach fz curves are divided into three regions: (1) the non-contact region, (2) the jump-to-contact region and (3) the tip-sample contact region. For the retract fz curves, similar regions are observed with the presence of a jump-off region (2') instead of a jump-to-contact region (see Fig. 2-5):

Non-contact region: the tip is far from the sample and there is no interaction between tip and sample. Then, there is no deflection.

Jump-to-contact: When the tip-sample force gradient exceeds the cantilever stiffness it causes the instability in the cantilever position and produces the jump-to-contact event[77]. This depends on the tip, the sample and the medium, and could be not observable depending on the conditions of the measurements.

Contact region: This region can provide information about the properties of the sample. One example is the deformation or rigidity of the sample when the tip pushes the sample or, even, the force that the sample is able to withstand before its rupture.

Jump-off: This event is related with the adhesion between the tip and the sample, which can depend on a variety of factors, such as chemical affinity, environmental humidity, tip-sample interaction, sample deformability and elongability, etc..

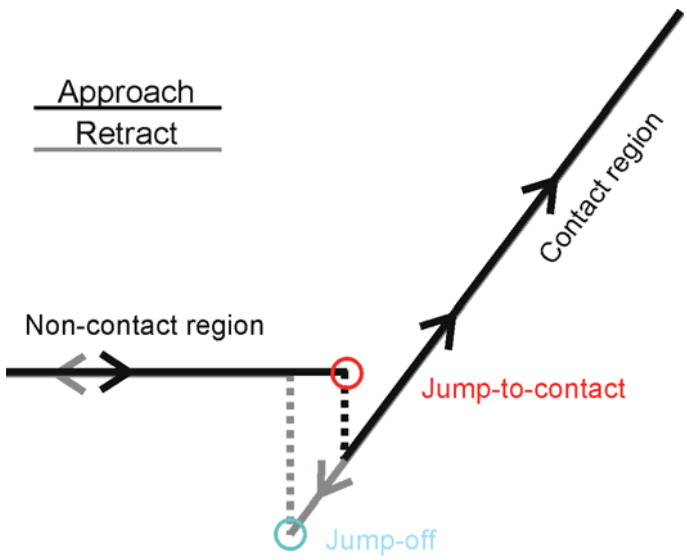

Figure 2-5. Schematic representation of the fz curve regions: non-contact region, the jump-to-contact region (red) and the tip-sample contact region in the approach curve (black). For the retract fz curves (grey), the most important region is the jump-off (blue).

In the case of supported lipid bilayers, the most distinctive feature of the approach fz curves is that they usually reveal an abrupt and discontinuous event in the tip-sample contact region[78]. This event corresponds with the spontaneous rupture of the membrane and the sudden penetration of the tip through the bilayer. The force at which this event occurs is the breakthrough force. Breakthrough forces are considered unambiguous signatures of the resistance of a bilayer to rupture and provide a way to quantify the mechanical stability of a biomembrane [79, 80].

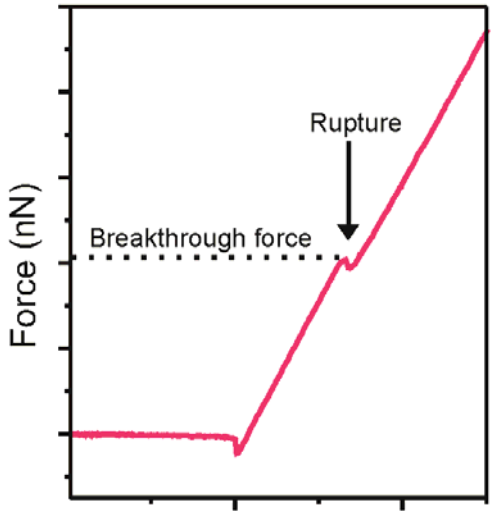

Figure 2-6. Schematic representation of a fz curve made on a lipid layer. The rupture event is signaled as well as the corresponding breakthrough force

In this thesis the breakthrough force is the parameter used to evaluate the stability of dried lipid layers, and to identify different components and phases in the formed dry lipid bilayers. This parameter not only allows us to compare with the values obtained in liquid, but leads to values that had not been described until now for dry membranes.

Finally, we note that in order to obtain reliable quantitative force values the spring constant of the cantilevers need to be known. In the present thesis the spring constant of the cantilever has been determined from calibrated values provided by the manufacturer. These values have been verified to be in excellent agreement with values obtained by calibrating the spring constant by using the thermal noise method, as shown in Figure 2-7.

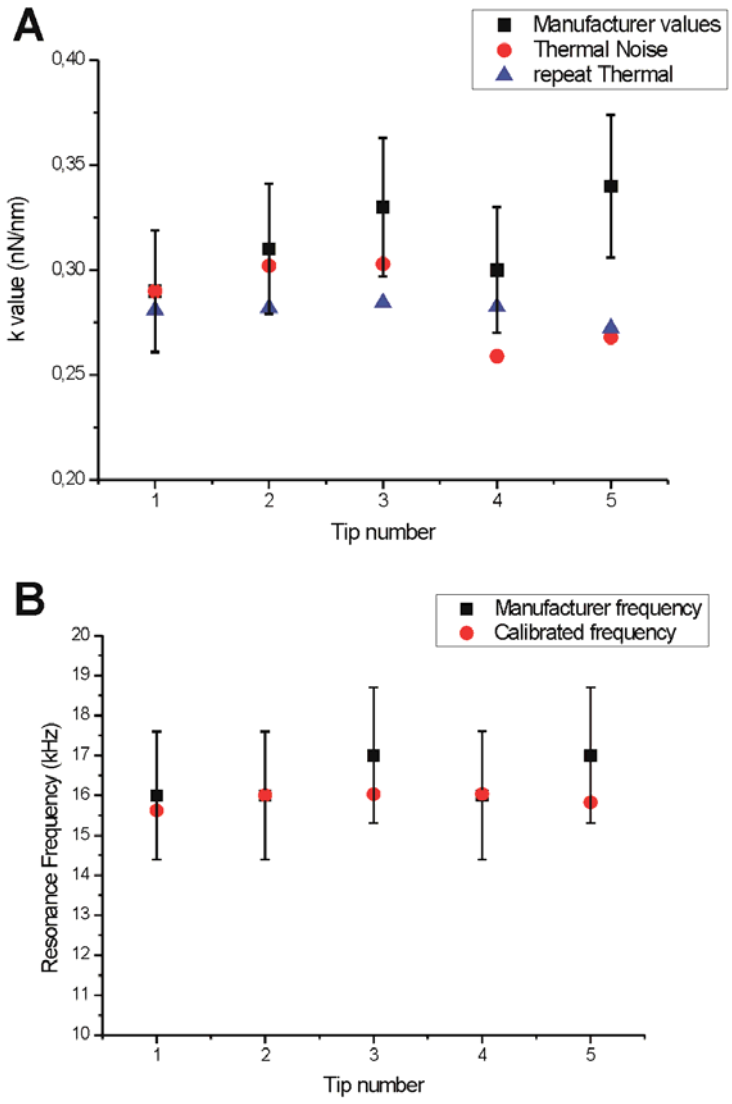

Figure 2-7 (A) Comparison of the spring constant value of different probes given by the manufacturer and obtained by us in two different calibrations following the thermal noise method. (B) Comparison of the resonance frequency given by the manufacturer and that obtained during the calibration process.

2.4 Appendix: Results with sample preparation techniques different from spin coating

As we mentioned at the beginning of this chapter, during this work of thesis we have considered other sample preparation methods besides the spin-coating technique, which did not showed reproducible enough for systematic studies. Drying the samples was attempted using different techniques and different substrates were tested in parallel to the sample preparation. The aim was to solve at the same time the limitations of some techniques concerning substrate requirements (e.g. conductive substrates). A list of the different approaches followed is described in Figure 2-8. The main results obtained with these techniques are described briefly below.

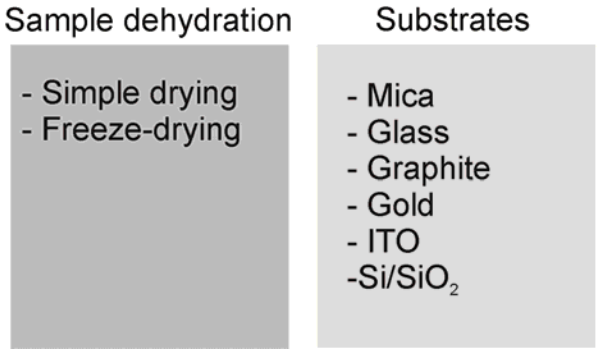

Figure 2-8. Sample dehydration methods used before the spin-coating method and Substrates used for the bilayer formation using the vesicle fusion technique

2.4.1 Vesicle fusion technique and drying

To evaluate the different techniques of dehydration it was necessary to create hydrated SLBs with an easy and reproducible method. For this reason we chose the preparation of hydrated SLBs by the well-known vesicle fusion technique on mica substrates[81]. After their characterization by AFM in liquid (Figure 2-9A), different protocols were used to

dehydrate them. The first attempt was to evaporate the liquid of the sample by simple drying in a vacuum chamber. Representative results of this procedure are presented in Figure 2-9B. As can be seen, the bilayers presented damages and accumulations of material in accordance with the literature[45-48], then this approach was discarded.

The second procedure used was the freeze-drying technique, previously used by Kraft and coworkers[41-43]. This approach showed a low reproducibility and a long sample preparation time. After this freeze-drying process the samples are expected to maintain their structure[41] but, in most of our results, a partial peel off of the upper leaflet and the formation of an additional layer on top of it was observed. The lipid patches were transformed from bilayers to mono- and trilayer patches as can be seen in Fig. 2-9C-D. Due to its low reproducibility this method was discarded.

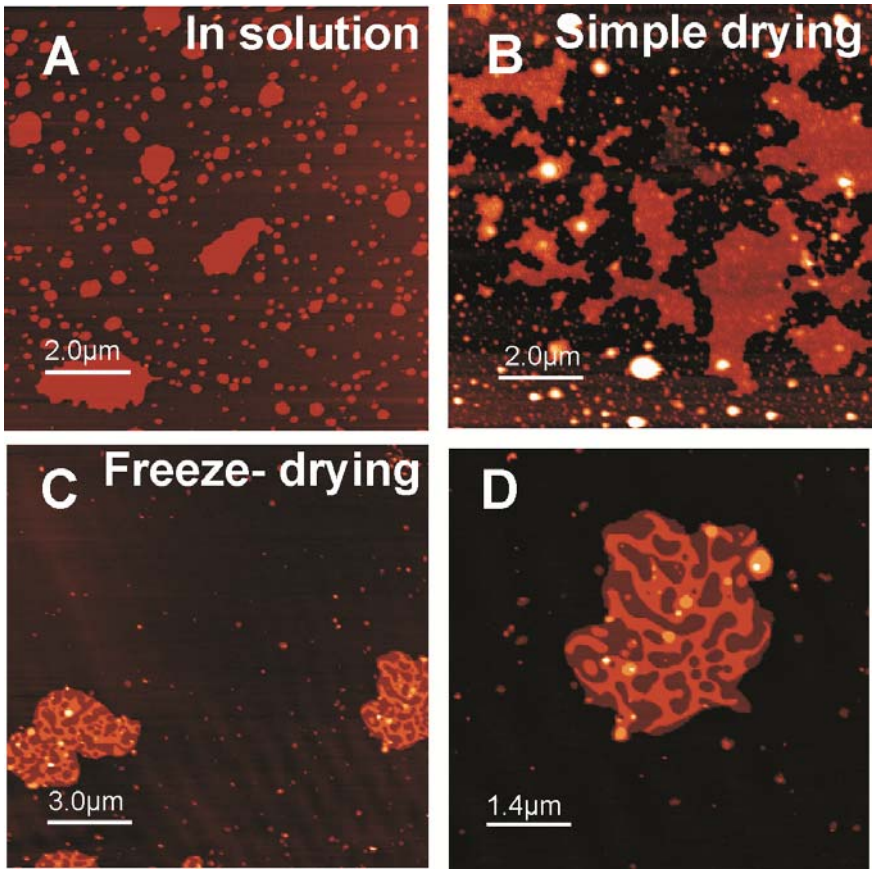

Figure 2-9 AFM topography images of lipid samples prepared by vesicle fusion on mica imaged in solution (A), and imaged after simple drying (B) and after freeze-drying (C) and (D).

2.4.2 Use of substrates others than mica

As it is mentioned in the previous chapter, mica is not a suitable substrate in all the techniques because some have special requirements for the substrate like transparency or conductance. For this reason, the preparation of dry lipid bilayers was attempted also on other substrates. As before, the first step was the preparation of lipid bilayers by the vesicle fusion technique of these different substrates. As we show below, this first step already allowed us to discard a number of substrates due to the difficulty to form stable lipid bilayers even in liquid environment due to poor adsorption properties.

The substrates considered for vesicle deposition and lipid bilayer formation are listed below together with their most relevant properties for vesicle adsorption. In Figure 2-10 we show topographic images of the bare substrates.

List of substrates considered during the thesis:

- Glass: hydrophilic and transparent material. Useful for experiments combined with optical methods.

- Gold: different gold substrates were considered; sputtered gold substrates, crystalline gold and flat gold produced by the replica technique. All of them are conductive but as a function of the fabrication process the hydrophilicity and the roughness of the surface changes thus potentially affecting the vesicle deposition. Gold substrates being conductive are useful for experiments requiring electrical characterization methods.

- Graphite: High Ordered Pyrolytic Graphite (HOPG) was used due to the flatness of its surface and its conductive character. The principal drawback is that it is hydrophobic.

- Ito: Indium Tin Oxide is a hydrophilic, conductive and transparent material that can be acquired commercially. It has the

advantage of being potentially useful for combined electrical and optical characterization.

- Silicon: It is the main material in the electronic industry and hence with potential interest in the development of hybrid bioelectronic devices. Both in air ambient and in liquid media presents a thin layer of silicon dioxide that makes the surface hydrophilic.

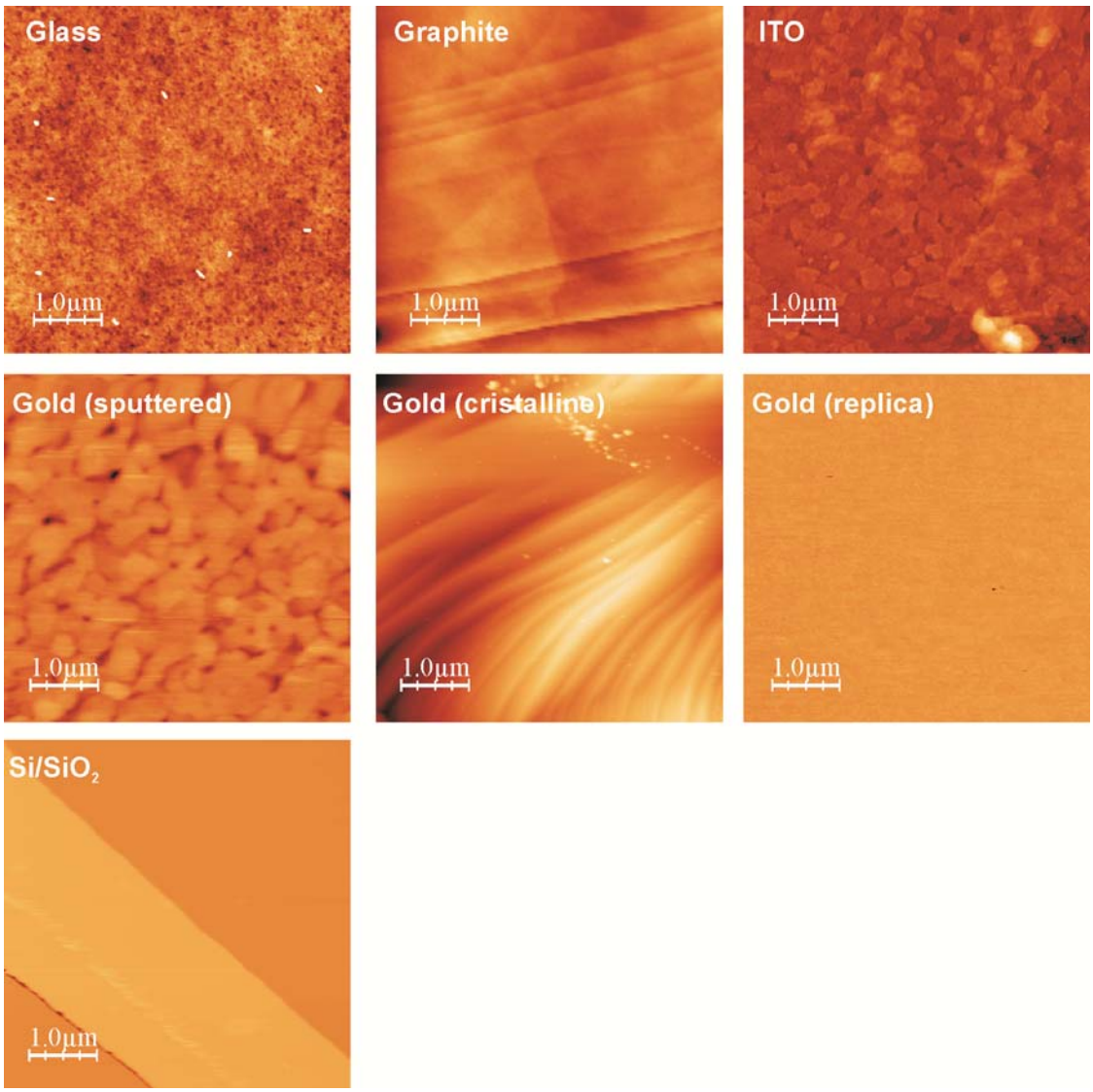

Figure 2-10. AFM topography images of different substrates studied (Glass, Graphite, ITO, Gold (sputtered, crystalline and prepared by the replica method) and Si/SiO2)

Of these substrates, ITO and Gold obtained by sputtering were discarded from the very beginning because of its roughness (see Fig. 2-10).

The best coverage and appearance of the lipid bilayers was obtained with glass and Si/SiO_2 (Figure 2-11). With graphite and gold results were much less satisfactory and reproducible, although from time to time reasonable results were obtained. Neither Glass or Silicon offered significant advantages with respect to mica for the purposes of the present thesis, so that these substrates were not further considered. However, we believe that most of the results reported for mica would remain valid also for Glass and Silicon.

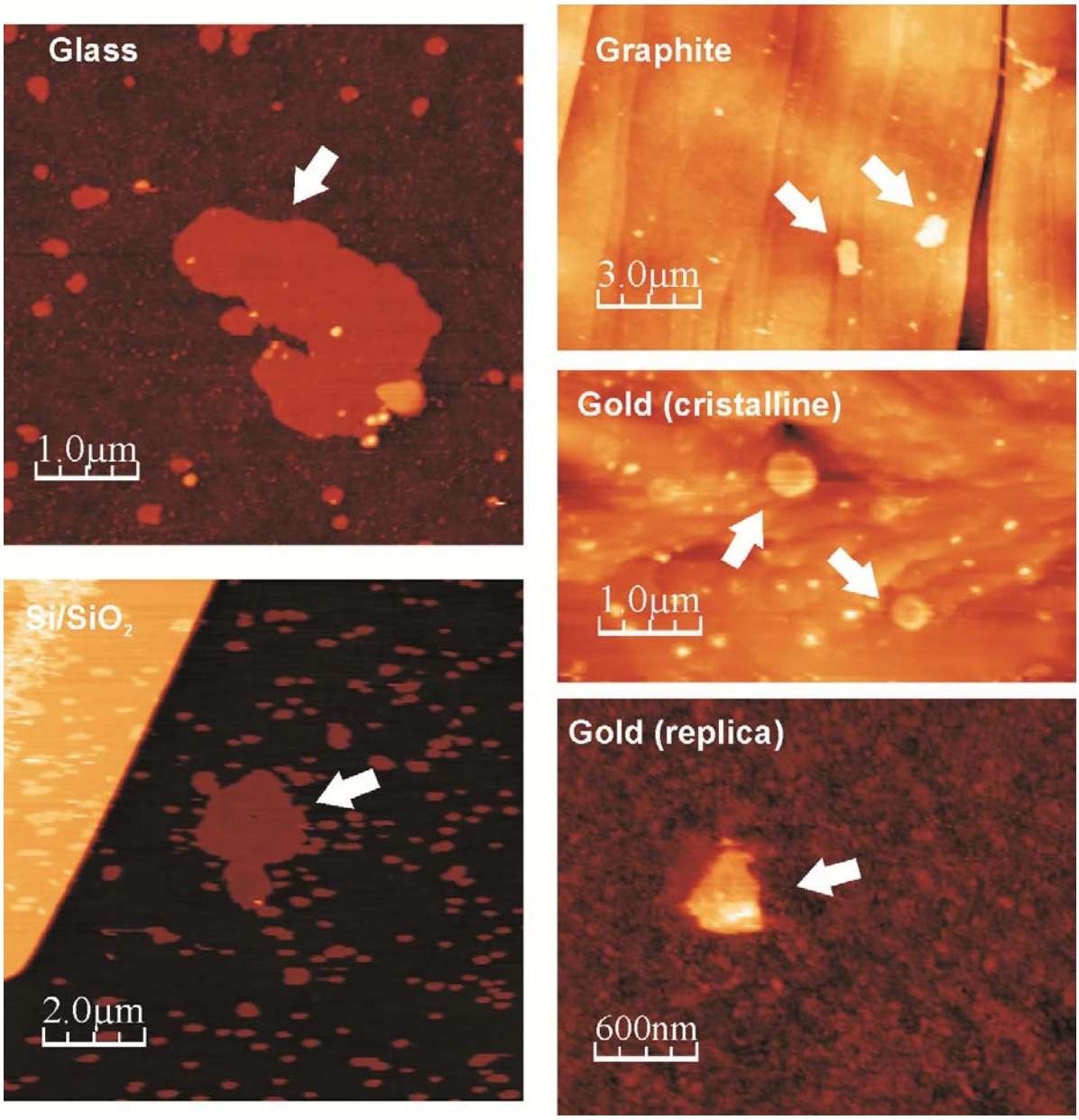

Figure 2-11 AFM topography images in liquid media of lipid bilayers formed by the vesicle fusion technique on different substrates: Glass, Graphite, Gold (crystalline and prepared by the replica method) and Si/SiO_2.

Chapter 3. Nanoscale structural and mechanical properties of monocomponent ultrathin spin-coated lipid layers in dry air environment: unsaturated phosphocholine

Summary: In the present chapter the formation and nanoscale structural and mechanical properties of ultrathin dry spin-coated lipid layers on mica is investigated. Lipid bilayers are obtained with the use of dilute Dioleoylphosphatidylcholine (DOPC) solutions (< 1 mM) and show to display an excellent quality and morphological stability in dry air environment. A complete Atomic Force Microscopy (AFM) study of the formed dry lipid layers is carried out, including topographic and nanomechanical characterization. The present study is the first nanomechanical study of dry single lipid bilayers. We demonstrate that dry DOPC bilayers exhibit mechanical properties comparable with hydrated fluid bilayers and close to the mechanical properties of DOPC lipid bilayers in pure water, but distinct from DOPC lipid bilayers in buffer solutions. (*)

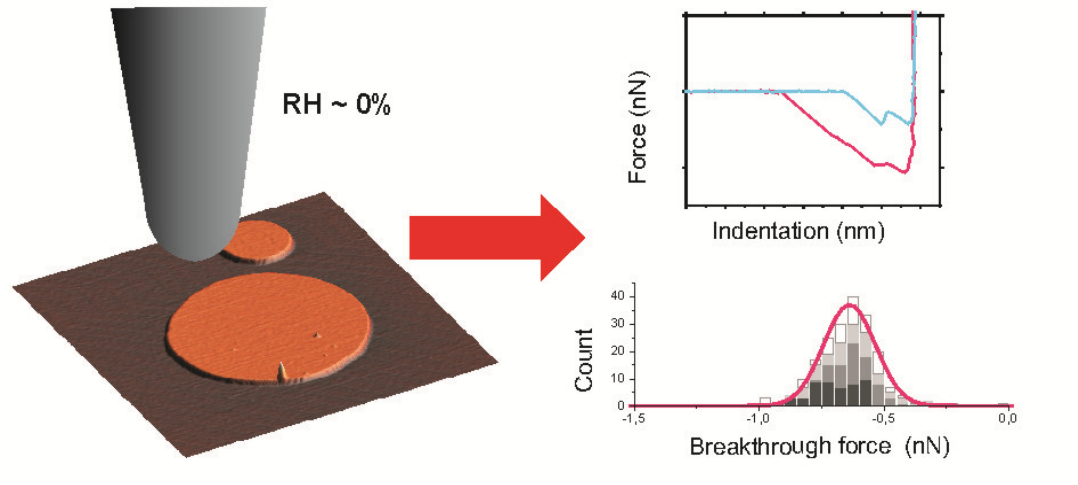

(*)This chapter reproduces almost literally the article : *Ultrathin Spin-Coated Dioleoylphosphatidylcholine Lipid Layers in Dry Conditions: A Combined Atomic*

Force Microscopy and Nanomechanical Study, Langmuir 27, 13165-13172 (2011) by Aurora Dols-Perez, Laura Fumagalli, Adam Cohen Simonsen, and Gabriel Gomila.

In this article I was in charge of performing the experiments and processing the results. In this part of the work I followed some technical suggestions from L. Fumagalli and A.C. Simonsen. The article was written by me with the collaboration of the other co-authors.

3.1 Introduction

As we mentioned in the Introduction to this work of thesis there is a need to produce lipid bilayer samples stable in air environment and with physicochemical properties as close as possible to their equivalent in liquid media. The first example considered is the case of a monocomponent lipid bilayer made of the phosphocholine dioleoylphosphatidylcholine (DOPC) and prepared by the spin coating technique. Atomic force microscopy (AFM) has been used to study the structural and mechanical properties of the lipid layers in dry air environment (RH ≈ 0%) at the nanoscale. It is shown that for concentrations in the 0.1-1 mM range the structure of the DOPC spin-coated samples consists of an homogeneous lipid monolayer ~1.3 nm thick covering the whole substrate on top of which lipid bilayer (or multilayer) micro- and nanometric patches and rims are formed. The thickness of the bilayer structures is found to be ~4.5 nm (or multiples of this value for multilayer structures), while the lateral dimensions range from micrometers to tens of nanometer depending on the lipid concentration. The force required to break a bilayer (breakthrough force) is found to be ~0.24 nN. No dependence of the mechanical values on the lateral dimensions of the bilayer structures is evidenced. Remarkably, the thickness and breakthrough force values of the bilayers measured in dry environment are very similar to values reported in the literature for supported DOPC bilayers in pure water.

3.2 Materials and Methods

Materials

1,2-Dioleoyl-sn-glycero-3-phosphocholine (DOPC), was purchased from Sigma-Aldrich and used without further purification. Hexane LC-MS grade was used as solvent (Sigma-Aldrich) in all of the experiments. Samples at concentrations ranging from 1mM to 5μM were prepared. Throughout the chapter, the reported concentration of the samples refers to the concentration of lipid in the coating solution. Substrates used were high-grade freshly cleaved mica (Ted Pella, Inc.).

Sample preparation

Air-stable lipid layers have been obtained by the spin-coating technique detailed in Chapter 2 following the methodology developed by Simonsen *et al* [65]. In our case the use of methanol is not necessary because of the good solubility of DOPC in hexane. Briefly, a droplet of lipid stock solution was deposited on the high-grade freshly cleaved mica and spun with a spinner (WS-650MZ-23NPP/LITE, Laurell Technologies Corporation) for 1min at 3000rpm immediately after the deposition of the solution. Then the samples were placed under vacuum in a desiccator during 15-20 hours to fully evaporate the solvents. The mica substrates with the lipid layers were glued onto a metallic disc and stored in a desiccator until the AFM measurement (maximum storage time of 2 days after spin-coating procedure)

Atomic force microscopy measurements

Topographic images and force-distance curves were acquired with a Nanotec Electronica AFM using Silicon tips PPP-CONTR (Nanosensors) with a nominal spring constant of 0.2 N/m, resonance frequency of 13kHz and nominal radius < 7nm. Experiments were performed at room temperature in a glass chamber with <1% relative humidity controlled by dry N_2(g) flow. Before imaging the piezoscanner was left scanning at least 10 hours to avoid piezoscanner drift during the experiment. Due to

the softness of the samples topographic images were obtained in dynamic mode at the resonance frequency (~13 kHz) and a scan rate between 0.7-0.9 Hz. The sample thickness of the lipid structures was extracted from both single line profiles and from height histograms of the pixels over the different areas. The value reported is the difference between the values extracted from each area [82]. Histogram analysis allows a higher precision in the measurements, including the sample roughness.

Force-distance curves (that we refer to as force curves or Fz) were acquired at selected locations of the samples. All curves were acquired at the same approach-retract velocity (~1.6μm/s) to avoid velocity-dependent effects which were not the focus of this study[83]. A total of ~150-200 curves were obtained for each selected sample area, with 512 points per curve. The force curves were taken in sequences of 20 curves at the same position to examine the reproducibility of the measurements, since it is known that irreproducibility can indicate plastic deformations[68]. Prior to and after force measurements, topographic images were acquired to ensure the correct positioning of the probe and to evaluate possible sample modifications. Measured deflections (in V) were converted into nm by calibrating the photodetector sensitivity from the long distance part of an approach curve taken on a point of the sample containing no bilayers. The photodetector sensitivity (V/nm) was evaluated for each curve and compared with the reference curve to rule out possible artifacts. The forces acting on the probe are calculated as usual through the Hooke's law $F = k_c \cdot \Delta D$ where k_c is the equivalent spring constant of the cantilever and ΔD the measured cantilever deflection. The manufacturer's calibration values for individual cantilevers were used as spring constant values for force spectroscopy analysis. The lipid layer deformation is calculated as usual through the indentation (also called penetration), δ, where $\delta = \Delta z - \Delta D$, with Δz being the piezoscanner displacement. In the curves analyzed, the first contact point was considered as $\delta = 0$ so that all points in which there is a tip-sample contact correspond to positive values of δ. The total indentation from the contact point to the "hard contact" represents the thickness of

the sample. Topography image processing was carried out using WSxM 5.0 Develop 1.1 (Nanotec Electronica) [84] software, used for image flattening and removal of isolated lines. Force curves were analyzed with a custom made software. Independent sets of experiments with different probes and samples have been done, providing results in quantitative agreement within the experimental error, thus demonstrating an excellent reproducibility of the results and reliability of the procedure followed here.

3.3 Results

Topography of ultrathin, dry spin-coated lipid layers

The topography of ultrathin dry DOPC layers in spin-coated samples has been studied for different concentrations of lipid in the coating solution. Representative results are shown in Figure 3-1.

In the concentration range that we studied, 0.1 mM-1 mM, the samples displayed a uniform background with micro/nanostructures on top of it consisting of rims and patches. The thickness of these nanostructures is 4.6 ± 0.2 nm, obtained from histogram analysis. Only for the higher concentrations (0.75 mM and 0.5 mM) a few isolated structures with larger thicknesses are observed, with thickness of ~9 nm, ~20nm and ~25 nm (see Figure 3-1A, 3-1B and 3-1E). These values match well with integer multiples of the thickness of the lowest nanostructures hence suggesting to correspond to multilayer stacks.

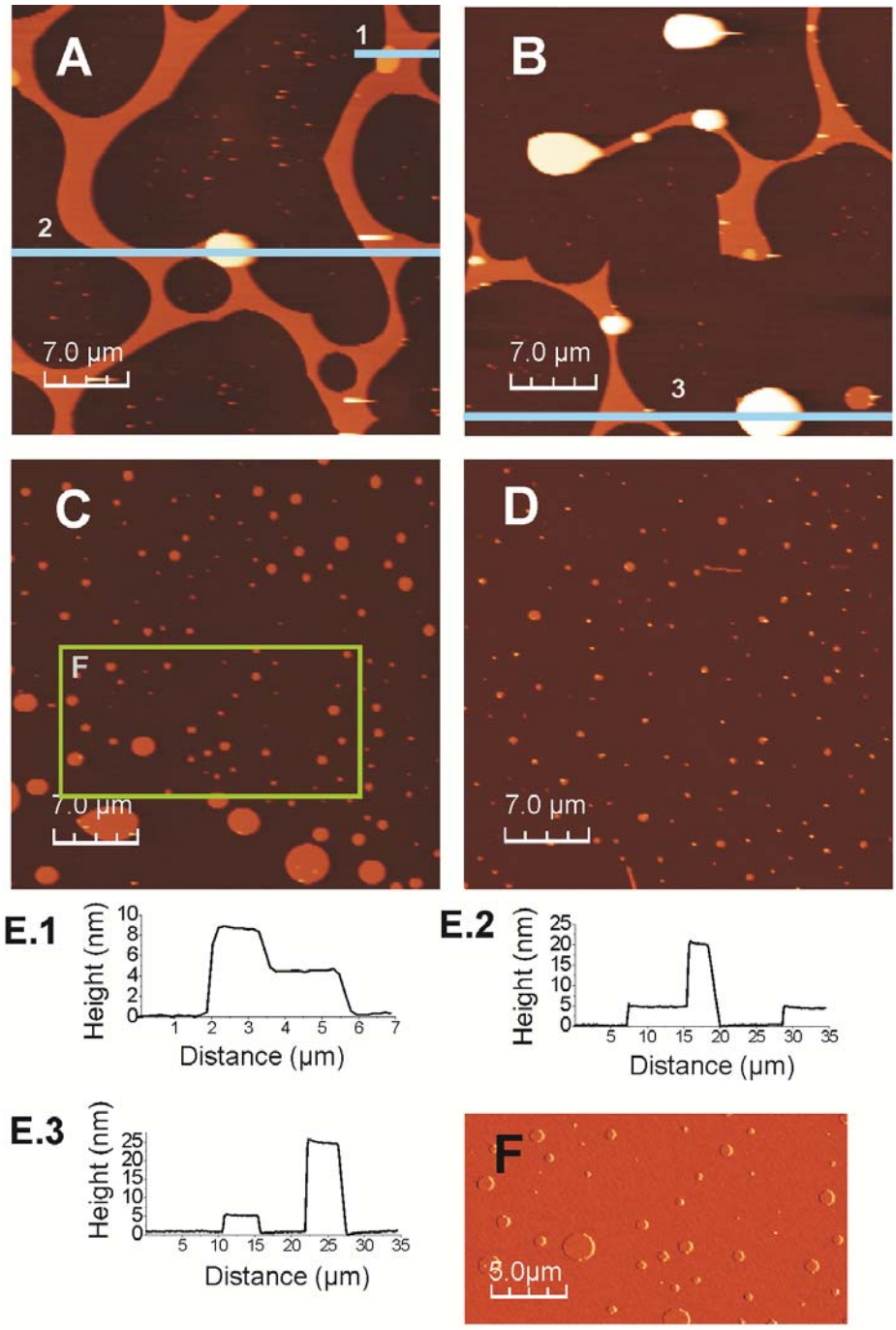

Figure 3-1 AFM topography images of spin-coated samples of DOPC in air prepared with different concentrations of lipid in the coating solution in the range 0.1mM-1mM. (A) 0.75mM, (B) 0.5mM, (C) 0.25mM and (D) 0.1mM. (35 x 35 μm^2, Z-scale: 30nm). (E) Profiles corresponding to the cross-section line shown in image A(1, 2 are E.1 and E.2 respectively) and B (3 is E.3), (F) phase image of the marked area in image C.

The morphology of the nanostructures observed in Figure 3-1A (concentration 0.75 mM) corresponds to a continuous network of rims with occasional isolated patches located on top of them. This filamentous structure is reminiscent of a layer covering the whole substrate containing large holes. As the concentration decreases (0.5 mM) the continuous filamentous network shrinks and starts breaking up, and at the same time, some isolated patches start appearing (Figure 3-1B). For even lower concentrations (0.25 mM) practically all rims structures disappear and the sample consists of isolated disc-shaped patches with the same thickness as the filamentous structures described before and with a diameter ranging from hundreds of nanometers to a few micrometers (Figure 3-1C). Finally, at a concentration of 0.1 mM, (Figure 3-1D), the sample display again only nanopatches but of much smaller dimensions (below hundreds of nanometers down to tens of nanometer). The thickness of the rims and patches observed in Figure3-1A-D is comparable to the expected thickness of a DOPC bilayer, from which we conclude that the structures observed in the figures are DOPC bilayers that for higher concentrations would cover the whole sample.

In order to identify the nature and properties of the background present in Figures 3-1A-D, additional information is required. Phase images (Figure 3-1F) and root mean square roughness (RMS) (0.072nm versus 0.078nm, background and patches respectively) do not show any significant difference between the background and the patches or rims.

Figure 3-2 AFM topography images of the background area of spin-coating samples of DOPC in air prepared with different concentrations of lipid in the coating solution in the range 0.005mM-1mM. (A) 0.75mM, (B) 0.1mM, (C) 0.025mM and (D) 0.005mM. (500 x 500 nm^2, Z-scale: 2nm). (E) Profiles corresponding to the cross-section line shown in image A (E.1), B (E.2), C (E.3) and D (E.4). (F) Mean square root roughness of the background area as a function of the lipid concentration of the coating solution. The error bars indicate the standard deviation.

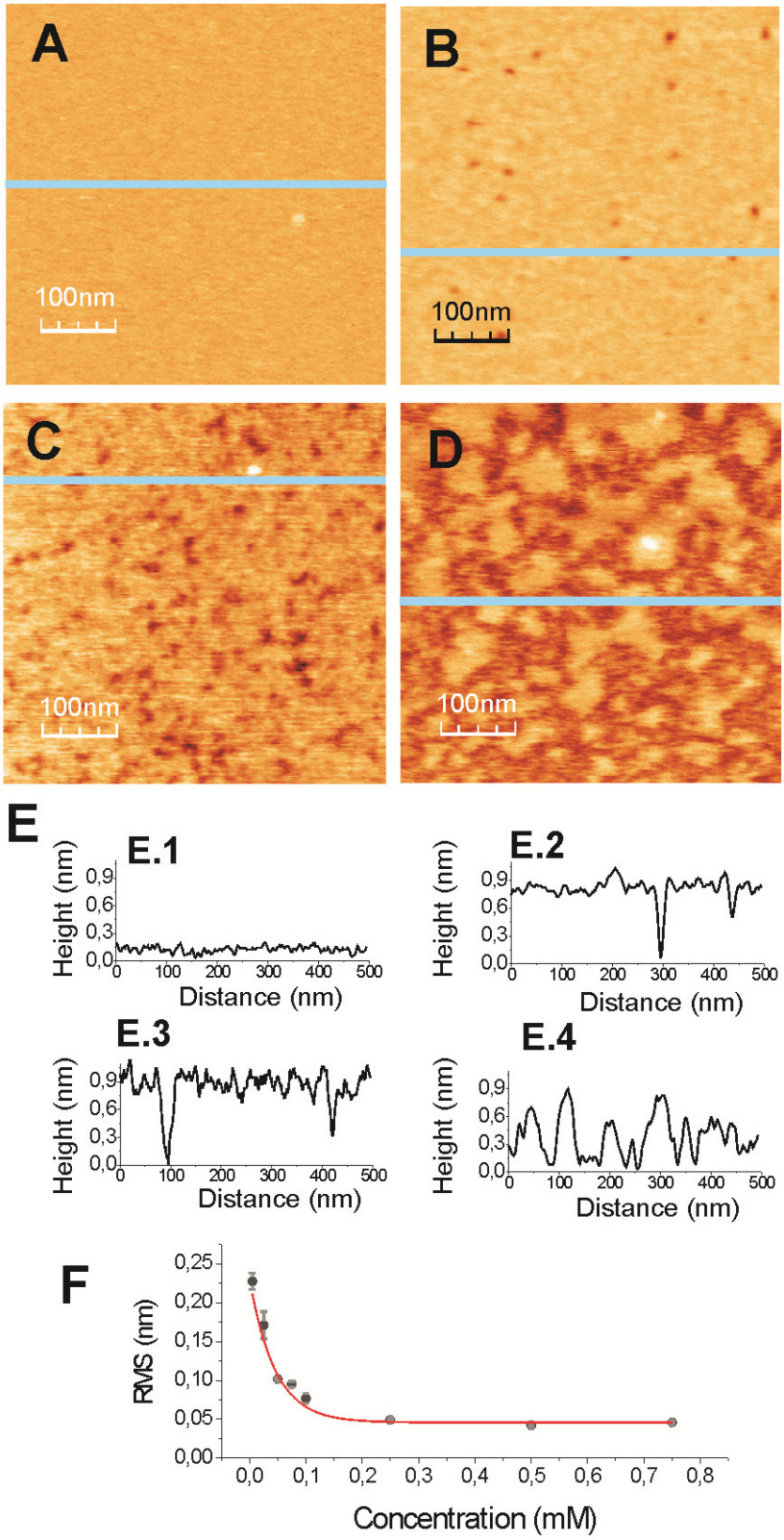
A
100nm
B
100nm
C
100nm
D
100nm
E
E.1
Height (nm)
0,0
0,3
0,6
0,9
0 100 200 300 400 500
Distance (nm)
E.2
Height (nm)
0,0
0,3
0,6
0,9
0 100 200 300 400 500
Distance (nm)
E.3
Height (nm)
0,0
0,3
0,6
0,9
0 100 200 300 400 500
Distance (nm)
E.4
Height (nm)
0,0
0,3
0,6
0,9
0 100 200 300 400 500
Distance (nm)
F
RMS (nm)
0,00
0,05
0,10
0,15
0,20
0,25
0,0 0,1 0,2 0,3 0,4 0,5 0,6 0,7 0,8
Concentration (mM)

By further lowering the concentration of the lipid solution to < 0.1 mM, we observed that the rims and patches disappear and that the uniform background starts distorting (Figure 3-2). The distortion of the background is reflected in a sharp increase in the roughness of the substrate as the lipid concentration decreases, as shown in Figure 3-2F.

These results reveal that the uniform background displayed in Figure 3-1 corresponds to a uniform lipid layer covering the mica substrate. This can be directly confirmed by performing a scratching experiment on the uniform background areas (Figure 3-3). After applying a force larger than 100nN, we observed the accumulation of material within the scratched region, which interestingly form flat islands instead of holes with a thickness of 4.5 ± 0.3 nm, identical to the thickness of the patches and rims discussed before. This result indicates that indeed a lipid layer is present in the background region, which can be moved with the tip to form thicker lipid structures.

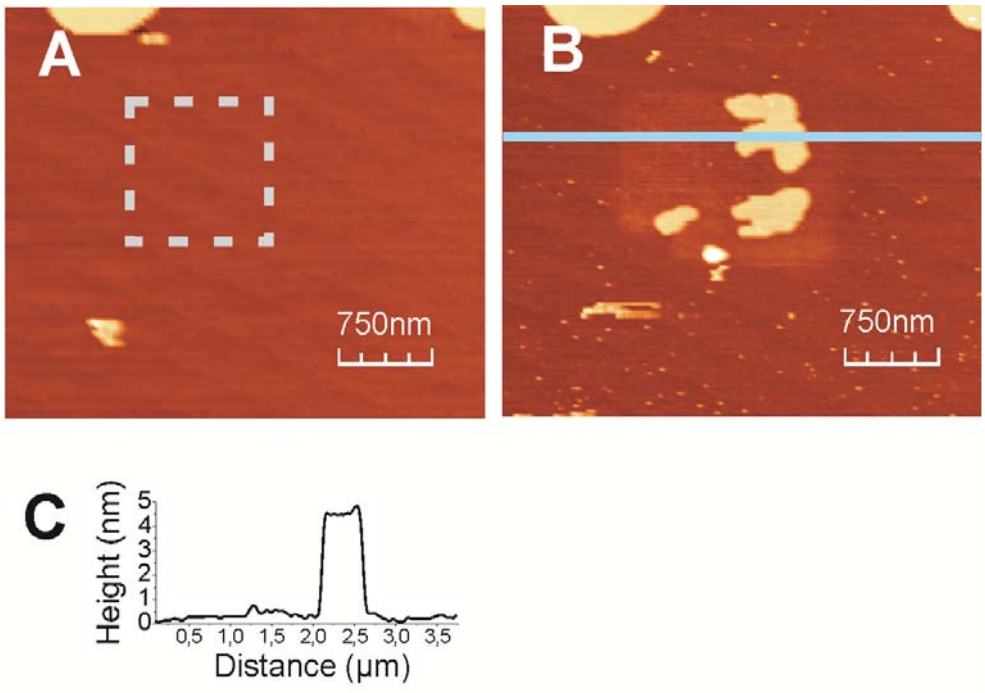

Figure 3-3 AFM topography image before (A) and after (B) scratching the background area of a 0.25mM DOPC spin-coated sample on mica. (3.750 x 3.250 μm^2, Z-scale: 10nm). (C) Profile corresponding to the cross-section line in Figure B.

The absence of any hole in the uniform background region displayed in Figure3-1A-D, including after scratching (Figure3-3), typically prevents from a direct measurement of the thickness of this first lipid layer. Isolated monolayer structures were rarely found in the low concentrated (~ 0.01mM) samples which allowed us to determine this parameter. In Figure 3-4A we show an isolated lipid patch found directly on the mica substrate, which reveals a thickness of ~1.3 nm. This first monolayer has the same properties as the background region described above, as shown by scratching on it and observing the formation of thicker lipid structures identical to the ones shown in Figure 3-3B (data not shown). Moreover, we found in the same area, shown in Figure 3-4B, the three types of lipid layers discussed until here, namely, the distorted background lipid layer, the packed lipid monolayer and the lipid bilayer, Note that the compact lipid monolayer is around ~0.5−0.7 nm thicker than the distorted one, as shown by the profile displayed in the inset of Figure 3-4B, probably as consequence of differences in molecular packing.

The results presented above indicate that in the range of concentrations from 0.1 mM to 1 mM and under dry conditions, spin coated DOPC lipid solutions on mica substrates form lipid layers consisting of a background of a packed and uniform lipid monolayer with thickness ~1.3 nm, on top of which lipid bilayer rims or patches are found with thicknesses ~4.6 nm and with lateral dimensions ranging from micrometers to nanometers depending upon the concentration used. For lower concentrations the background appears distorted, but due to local inhomogeneities it is possible to find isolated packed areas reminiscent of the uniform monolayer in the background of more concentrated samples. The lipid bilayers are expected to be configured with the acyl chains facing out, as suggested previously[65].

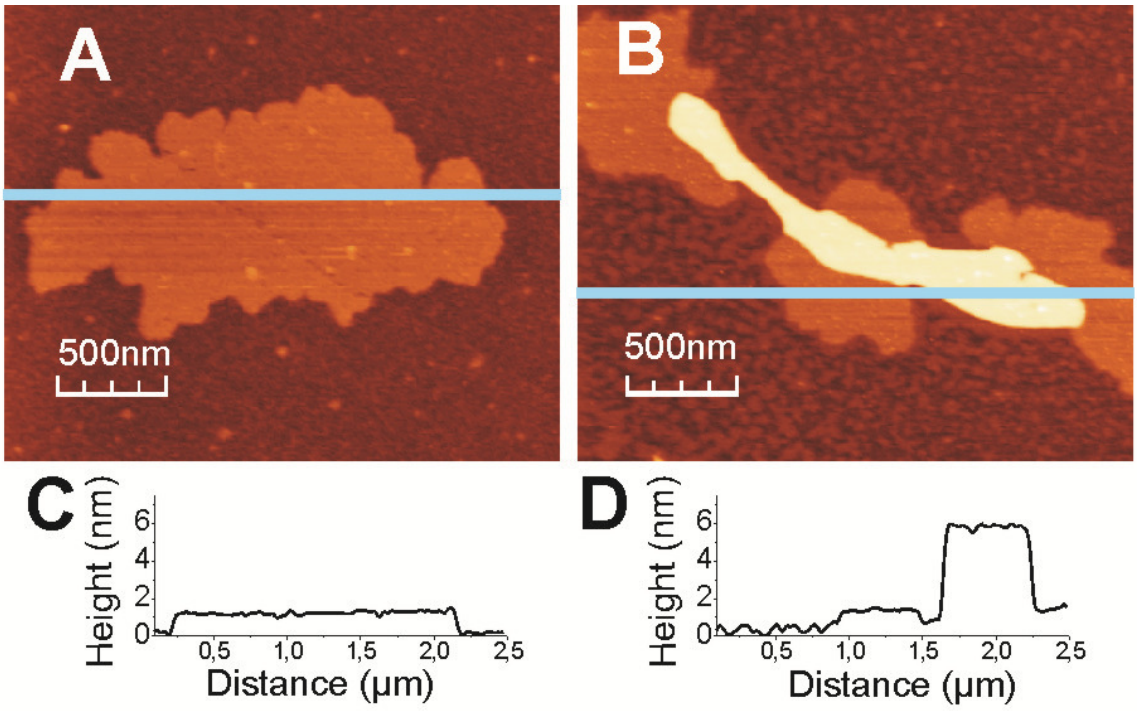

Figure 3-4 (A) AFM topography image of a lipid monolayer patch found in the background area directly on the mica substrate. (B) AFM topography image of another patch of lipids found on mica showing three types of lipid layers in the same area, namely a distorted layer, a compact monolayer and a bilayer of lipids.(C) Profile corresponding to the cross-section line in Figure A , showing a thickness of ~1.3 nm (D) Profile corresponding to the cross-section line in Figure B, showing the heights of the three layers (distorted layer: ~0.8nm, compact layer: ~1.3nm and bilayer ~4.6nm) (2500x2100 nm^2, Z-scale: 8nm).

Force spectroscopy measurements

The nanomechanical properties of the lipid layers, and their possible dependence on the lateral dimensions of the structures, have been analyzed by means of force spectroscopy measurements. Figure 3-5A shows the selected area, which consists of several patches of different radius ranging from 1.35 μm to 210 nm. Force curves have been performed on four different disc-shaped bilayer patches of different dimensions (numbered from 1 to 4) and on the background monolayer area (numbered 5) (see Figure 3-5A). Force curves were made only on the central region of the patches to obtain more reproducible results[82]. We have acquired force vs. piezo-displacement curves (Fz), and converted them into force vs. indentation curves (Fδ), as detailed in the methods section. Both approach and retraction curves have been analyzed. Figures 3-5C and 3-5D show two representative examples of Fz curves, corresponding to the background region and to a patch bilayer, respectively. In Figures 3-5E and 3-5F the same curves converted to Fδ curves are shown. As can be seen, in the case of Fz curves taken on disc-shaped structures (Figure3-5D and 3-5F), and after the jump-to-contact, a discontinuity is observed at low (negative) force values. This discontinuity is observable in all approaching curves taken on patch areas 1–4, and they are interpreted as rupture events of the lipid layers, as explained elsewhere [83]. In contrast, Fz curves taken on the background area do not display such rupture events (see Figure 3-5C and 3-5E).

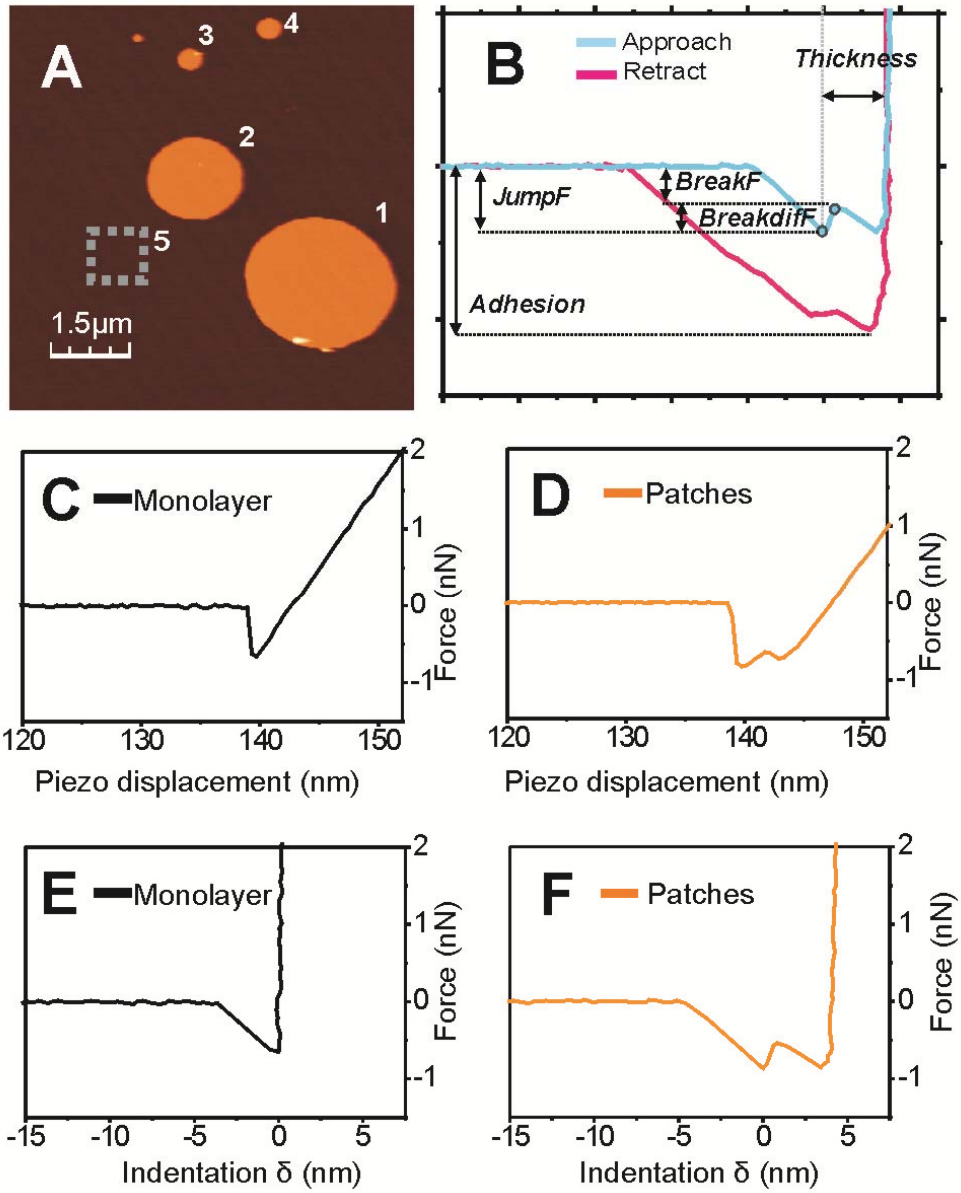

Figure 3-5. (A) AFM topography image of a spin-coated DOPC sample. Numbers correspond to the different areas selected for the force spectroscopy analysis. (B) Definition of the various parameters analyzed in each force versus indentation curve: "jump-into-contact" force (jumpF), the breakthrough force (breakF), the difference between the value of force at the contact and at the point of rupture of the layer (breakdifF), the thickness (thickness) and the adhesion force (adhesionF). (C and D) Representative force vs. piezo-scanner displacement curves on the monolayer and on the bilayer regions respectively. (E and F) Same force curves as given in C and D, but represented as a function of indentation.

In order to quantify the nanomechanical properties of the lipid layers from the measured force approach curves, we have extracted four parameters, namely, the value of force after the jump to contact of the tip (*jumpF*), the breakthrough force of the layers (*breakF*), the difference between the value of force at the contact and at the point of rupture of the layer (*breakdifF*) and the thickness of the layer (see Figure3-5B for a precise definition of the parameters). In addition, from the retraction force curves we have extracted the adhesion force. The average results for the different magnitudes for each of the five regions studied are shown in Table 1, while its statistical distribution with their Gaussian fit to the histograms is represented in Figure 3-6.

In the case of the curves taken on the background, no rupture events are observed, meaning that the breakthrough force, if present, is smaller than the *jumpF* force. As a consequence, in this region an estimation of the mechanical and topographic parameters from the force curves was not feasible. Only the values for the adhesion force and the jump-to-contact force could be retrieved, giving a mean value of −1.93 ± 0.03 nN and −0.64 ± 0.03 nN, respectively.

Instead, on the nanopatches rupture events are always observed in the force curves. In all cases rupture occurs at negative absolute force values, when the tip is still bend downwards after jump-to-contact, (see Table 1 and Figure 3-6A). The mean value of the *breakF* for the four patches is −0.64 ± 0.2 nN (n=200), assuming a Gaussian fit of the data, with *n* being the number of Fz included in the analysis. These rupture absolute force values correspond to net forces of rupture, *breakdifF*, (see Figure 3-5B) of 0.24 ± 0.09 nN (Table 3-1 and Figure 3-6B). The rupture forces on the nanopatches, as well as the other magnitudes analyzed, have been found to be independent from the diameter of the patch within the measurement error and for the patch diameters considered (see Table 3-1). Concerning thickness extraction from the force curves, the thickness values extracted from force curves are slightly lower than the thickness values obtained from the topography images, 4.1 ± 0.2 nm versus 4.6 ± 0.2 nm, respectively (see Table 3-1 and Figure 3-6C). Finally, with

respect to the adhesion force and the *jump-to-contact* force (*jumpF*) the values obtained on the patches, 2.2 ± 0.2nN, (n=200) and −0.88 ± 0.05 nN (n=200), respectively, are slightly smaller (in absolute values) than the corresponding values obtained on the background area (see Table 3-1 and Figure 3-6D and 3-6E).

Table 3-1 Height, thickness, breakthrough force (breakF), breakthrough force difference (breakdifF), adhesion force and force at the jump-to-contact (jumpF) measured on the four patches analyzed and on the background region. (n, number of force curves analyzed)

	Radius (μm)	Height (nm)	Thickness (nm)	BreakF (nN)	BreakdifF (nN)	AdhesionF (nN)	JumpF (nN)
Patch 1 (n=50)	1.35	4.5±0.2	4.1±0.2	-0.7±0.1	0.20±0.08	2.3±0.1	-0.89±0.05
Patch 2 (n=50)	0.85	4.6±0.2	4.2±0.3	-0.61±0.08	0.26±0.09	2.3±0.1	-0.87±0.04
Patch 3 (n=50)	0.21	4.6±0.2	4.2±0.3	-0.6±0.1	0.24±0.09	2.2±0.1	-0.87±0.04
Patch 4 (n=50)	0.21	4.7±0.3	4.1±0.3	-0.6±0.1	0.27±0.08	2.1±0.2	-0.89±0.06
Total (n=200)			4.1±0.2	-0.64±0.2	0.24±0.09	2.2±0.2	-0.88±0.05
Background (n=50)						1.93±0.03	-0.67±0.03

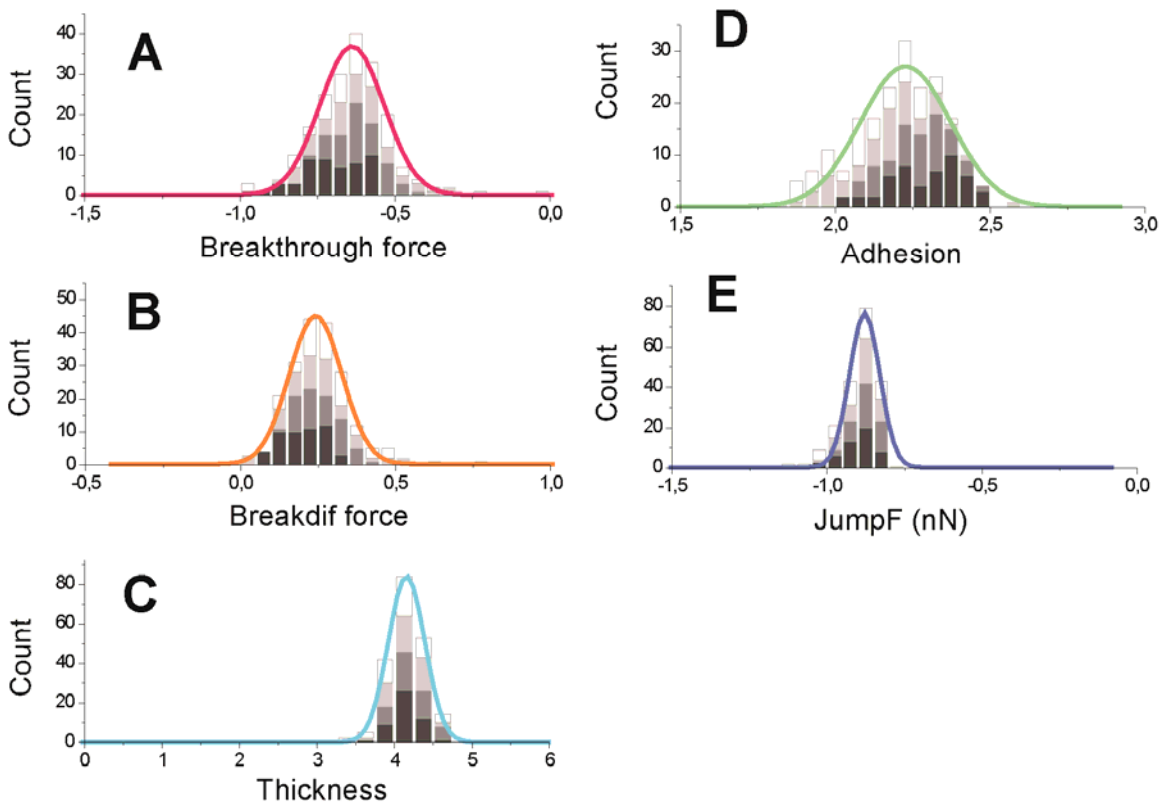

Figure 3-6 Histogram representation of the mechanical and topographic parameters extracted from the force curves performed on the lipid patches numbered 1-4 in Figure 5: (A) Breakthrough force, (B) breakthrough difference force, (C) thickness, (D) adhesion force, and (E) Jump-to-contact force. In all the histograms: dark grey: patch1, grey: patch2, light grey: patch3, white: patch4. Continuous lines correspond to the Gaussian fit of the whole data. The mean values and the standard deviation for each patch and the whole date are reported in Table 3-1.

3.4 Discussion

The results reported in the previous section reveals a number of interesting features of ultrathin spin-coated DOPC layers on mica substrates in dry environment unknown until now.

Firstly, the low concentrations used in this study allow one accessing to the single bilayer properties of dry spin coated lipids layers. Previous investigations, performed at higher concentrations, produced multilayered structures ranging from a few layers to hundreds of layers [65, 66]. Here we have shown that with lower concentrations one can obtain samples with the minimum possible number of layers, i.e. less than one complete bilayer sitting on top of a homogeneous monolayer. This low dimensionality system is defect-free and morphologically stable in dry air conditions.

The bilayer rims and patches displayed in Figure 3-1 show the characteristic dewetting pattern observed in thin polymer films, but the different levels of film breakup depend here on the concentration rather than on the proximity of the layer to the air interface as was described previously [65]. Thus the structures of more concentrated DOPC samples correspond to earlier stages in the dewetting process, when results are interpreted in terms of the standard dewetting [85-87]. Similarly the samples in which we have used a lower concentration display structures like those encountered in late stage polymer dewetting. The resulting structures with a disc shape are a consequence of the break-up of the rims between holes into droplets as described by Simonsen et al. [65].

The thickness of the bilayer structures observed in the AFM images (Figure 3-1) (~4.5 nm) is similar to values reported for supported fluid DOPC bilayers in liquid media measured by AFM [88, 89]. This good agreement is remarkable in view of the fact that the samples shown here are dried and the lipid layers forming the bilayer discs are expected to be inverted in comparison with hydrated membranes. This could indicate

that independently of the orientation of the lipids in the bilayers their internal interactions are preserved and hence the thickness of the bilayer.

Concerning the ordering of the lipids in the bilayer structures we suggest a lamellar structure because the height is equivalent to the values reported in lamellar phase in aqueous environment and because the low roughness values measured (0.078 nm) are not compatible with a non-lamellar phase [90]. This result should be contrasted with the results reported with multi-bilayers stacks where DOPC is expected to form non-lamellar structures for RH below 40% [91, 92] . We have shown that at the single bilayer level, lamellar structures can be found even at very low RH levels (~0%). Our results indicate that the presence of a planar solid support, as mica, strongly stabilizes the lamellar structures, and it contributes to the absence of non-lamellar phases described for multi-bilayers samples.

Regarding the force required to break the DOPC bilayers (*breakdifF*) the mean value reported (~0.24 nN) (Figure 3-6B) is surprisingly close to the breakthrough force values obtained in pure water measurements with DOPC supported lipid bilayers (SLBs). Dekkiche *et al.* [88] reported a value of 0.375nN for DOPC bilayers in ultrapure water. For bilayers prepared in water, Leonenko *et al.* reported an indentation of 6.1nm for 1nN while the value of a bilayer is 4.0nm in the same conditions, which indicates that the breakthrough force for the bilayer is smaller than 1nN [89]. Instead, breakthrough forces for DOPC obtained in buffer solutions are much larger (~15 nN) [93]. These results suggest that the maximum force the DOPC bilayers in dry environment are able to withstand before breaking is similar to the force in pure water, therefore suggesting a liquid phase state for these bilayers even in dry environment. The fluid phase nature of the bilayers is further supported by the fact that the force curves taken on the bilayers are very repeatable and do not induce any topographic modification, thus indicating that the lipids in the bilayer recover quickly their position after the indentation, as corresponding to a fluid phase.

Finally, concerning the properties of the uniform background observed on the AFM images (Figure 3-1) we have demonstrated it to correspond to a homogeneous lipid monolayer. Scratching experiments shown in Figure 3, which resulted in the formation of lipid bilayers from the displaced material, are a close evidence of this fact. In addition, AFM experiments performed at concentrations lower than 1 mM have shown a clear dependence of the distortion of these areas with the concentration of the coating solution (Figure 3-2). Moreover, this layer displayed a roughness almost identical to the one of the bilayer regions. In principle, the lack of phase contrast in the AFM images (Figure 3-1F) and absence of significant differences in the adhesion force (Table 3-1) would also suggest a similar composition and similar viscoelastic response for both regions. However, in dry air conditions phase contrast and adhesion forces are less sensitive to the hydrophobicity/ hydrophilicity of the materials. The thickness of this layer could not be determined neither from AFM images on samples with concentrations larger than 0.1mM nor from force spectroscopy curves. Instead, it has been possible to obtain it from samples prepared for lower concentrations (Figure 3-4) showing a value of around ~1.3 nm, smaller than the half of the value obtained for the bilayers. This could indicate a strong interaction of these lipid monolayers with the substrate. Concerning force spectroscopy measurements no rupture event was observed for the monolayer background region (Figure 3-5). Other authors have also mentioned the lack of special signatures (ruptures or non linearities) in the force curves on lipid monolayers. Garcia-Manyes *et al* [94] described a similar case in which force spectroscopy experiments on POPE monolayers prepared by the Langmuir-Blodgett technique did not revealed any rupture. This phenomenon was explained by the fact that the rupture force for the bilayer was already low in itself (around 1.6nN), so that the value of the breakthrough force for the monolayer was expected to be much smaller and hence difficult to reveal. In fact for some lipids (e.g. DPPC) it has been demonstrated that there are two orders of magnitude difference between the breakthrough forces on bi- and mono-layers [95, 96]. In the case of DOPC layers considered here we have obtained a low value of the breakthrough force for the bilayers (–0.64 ± 0.2 nN), thus the absence of

ruptures on the monolayer is not unexpected. This absence of ruptures also indicates that there are no more layers below the monolayer observed since in the case of multilayers multiple breaks would be observed. The force curves reported also permits to exclude the presence of lipids on the tip during the experiments, because in this case an additional rupture corresponding to the lipids on the tip would also be evident[97].

A final comment concerns the correlation of the thickness of the lipid bilayers estimated from topographic images with the one obtained from force spectroscopy curves. The results obtained from force curve and topographic measurements, 4.1 ± 0.2 nm versus 4.6 ± 0.2 nm, respectively, are in good agreement. At first sight this result can be surprising due to the presence of the bottom lipid monolayer which should contribute to the value probed by the force curves and not by the one obtained from the topography. However, on one hand, the bottom lipid monolayer does not contribute to the thickness determination from force curves for the reasons discussed above. On the other hand, the small difference (~0.5 nm) obtained between the two types of measurement could be due to tip penetration into the upper lipid layer during the jump-to-contact, as previously suggested by Garcia-Manyes et al. [94] for force spectroscopy curves displaying a jump to contact and rupture in the negative force range. We remark that this initial penetration depth is expected to be larger the higher is the jump-to-contact force, which is significant when AFM measurements are done in air. For this reason it is convenient to take into account the *jumpF* values to identify artifacts because of the measurement conditions. On the contrary, this might not be so relevant in force spectroscopy performed in water, since the snap-in event is much smaller or not evident at all. The presence of an evident snap-in in air is also the reason to use the *breakdifF* parameter (Figure 3-5B) as a measure of the breakthrough force comparable with the values obtained in different conditions, instead of the absolute break force at rupture (*breakF*), the difference between them being precisely the jump–to-contact force.

3.5 Conclusions

In the present Chapter the formation and nanoscale topographic and mechanical properties of mica supported ultrathin spin-coated DOPC layers in dry air ambient were studied. We have shown that under these conditions the lipid layers consist of a homogeneous lipid monolayer covering the whole substrate on top of which inverted lipid bilayer (or multilayer) rims and patches are formed. The shape of the micro/nanostructures observed is reminiscent of dewetting patterns in polymers. The nanomechanical and topographic properties of the lipid layers suggest a fluid phase state of the lipids. Remarkably similar properties are found for DOPC lipid bilayers studied in pure water. No dependence of the mechanical or topographic properties on the lateral bilayer size is observed in the range from 200 nm to 1.5 μm.

We have demonstrated that using the spin-coating technique for the deposition of lipids it is possible to obtain supported lipid bilayers morphologically stable in dry air conditions and whose mechanical properties are in accordance with a fluid state. This technique may provide researchers a simple and fast method to create ultrathin samples of lipids when it is required to study the samples in air for instrumental reasons. Thus the samples can be used to study the intrinsic properties of these lipids under very low humidity conditions as we have done studying the mechanical properties of the bilayers in air.

3.6 Appendix: Additional properties of DOPC samples prepared by the spin-coating technique.

Besides the results reported in the chapter, during the work with DOPC samples we observed a number of properties of these samples which are worth mentioning, although they have not been investigated in depth. In what follows we briefly mention them.

3.6.1 Deposition on conductive substrates

Apart from mica, spin-coating technique enables to create ultrathin layers on different substrates. Since the sample is spin-coated with organic solvents, the hydrophilic character of the substrate is not a prerequisite to use this technique (as it is in the case of the vesicle fusion technique described in the Appendix of Chapter 2) , although it may have an effect on the shape of the bilayer patches formed. An example is shown below for the case of a DOPC sample prepared on ultraflat gold substrates (obtained by the replica method) (Figrue 3-7). As can be seen DOPC bilayers are formed, whose thickness ~4.7nm is in agreement with the thickness obtained on mica. However we note that the shape of the bilayers instead of the round shapes observed on mica, it is of a dendrite nature meaning that the interaction with the substrate has important effects on the bilayer structure.

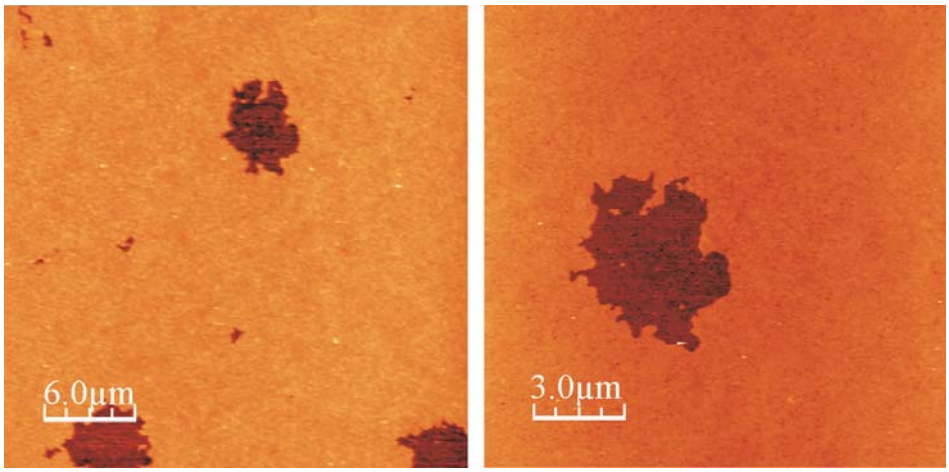

Figure 3-7. AFM topography image in dry air conditions of a DOPC sample prepared by spin-coating on a gold substrate.

3.6.2 Sample mobility

We have observed that DOPC samples showed mobility at ambient humidity, specially, in the multilayer regions, contrary to what happens in dry air conditions where they showed no evolution with time. This can be seen explicitly in Figure 3-8, here we show successive scans of a given region of the sample during 90 min. Changes in the extension of the first bilayer and in the number of layers can be appreciated.

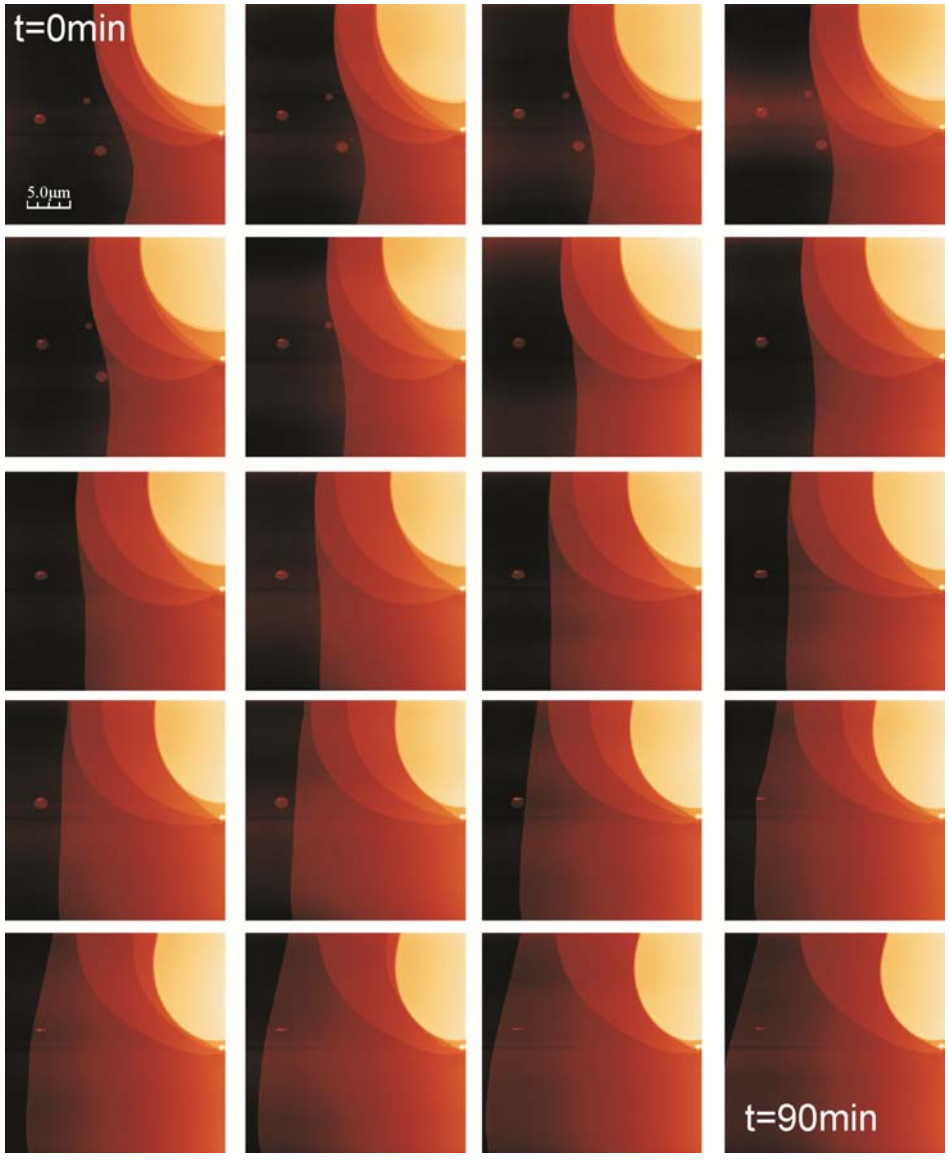

Figure 3-8. Successive AFM topography images of a DOPC sample (1mM) on mica prepared by the spin coating technique and imaged at ambient humidity during 90min.

3.6.3 Instability of multilayers stacks

All the samples analyzed in the chapter showed single or few DOPC bilayers with an almost atomically flat surface. However we have observed that when the number of bilayers is higher, and they are exposed to low humidity (RH=0%) for a long period of time a significant reorganization of the upper lipid bilayers can be observed. In Figure 3-9 we show a DOPC sample with a multilayered structure of height >30nm (corresponding to more than 6 bilayers) whose surface structure changed its appearance from flat to a rough surface made of cylinders.

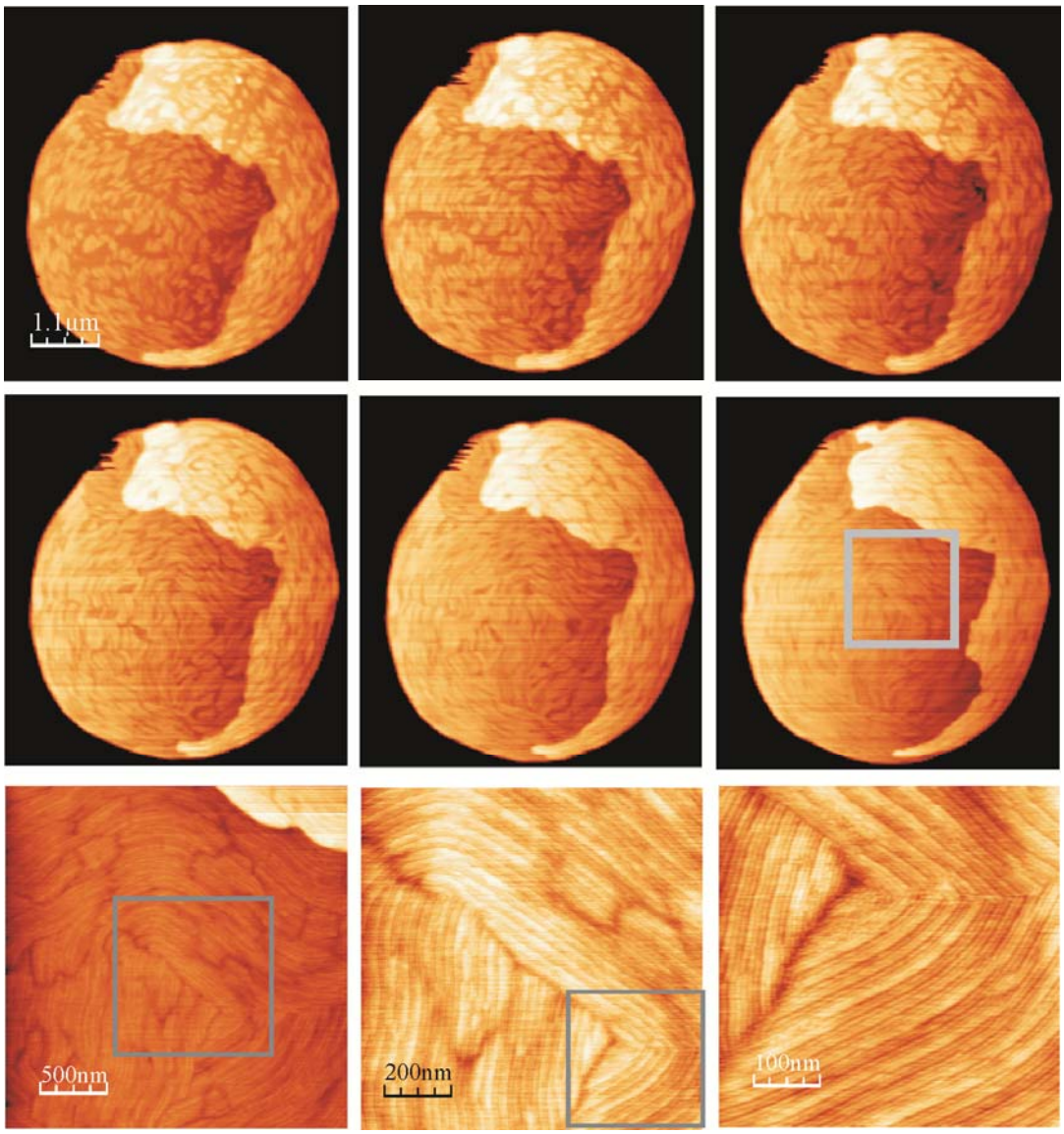

Figure 3-9. Successive AFM topography images of a DOPC multilayer patch after long exposure to a very low humidity conditions (time period 180min)

The final structures observed may correspond to a non-lamellar phase, probably inverted hexagonal phase (H_{II}) or rhombohedral, which is expected for multilayer DOPC samples at low humidity[92, 98]. The cylinders observed in the final images, and which are zoomed in Figure 3-10, have a diameter of ~10nm.

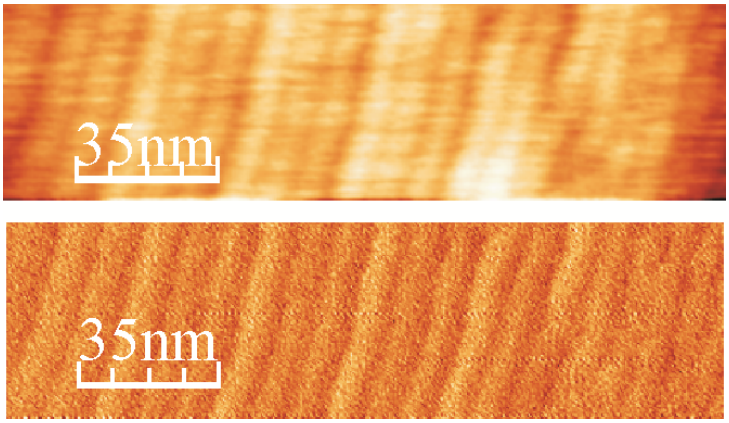

Figure 3-10. Zoomed region in which cylinders can be visualized. Upper image corresponds to AFM topography image and lower image corresponds to the error image.

Chapter 4. Nanoscale structural properties of monocomponent ultrathin spin-coated layers: saturated phosphocholines

Summary: In the present chapter the nanoscale structural properties of ultrathin dry layers of saturated phosphocholines on mica is investigated. Lipid bilayers are obtained with the use of dilute Dilauroylphosphatidylcholine (DLPC), Dimyristoyl-phosphatidylcholine (DMPC), Dipalmitoyl-phosphatidylcholine (DPPC) and Distearoyl-phosphatidylcholine (DSPC) solutions (1 mM). A complete topographic Atomic Force Microscopy (AFM) study is carried out. We demonstrate that some dry saturated phosphocholine bilayers exhibit interdigitated regions as a consequence of the preparation procedure. Interdigitation can be avoided by changing the parameters used in the sample preparation.

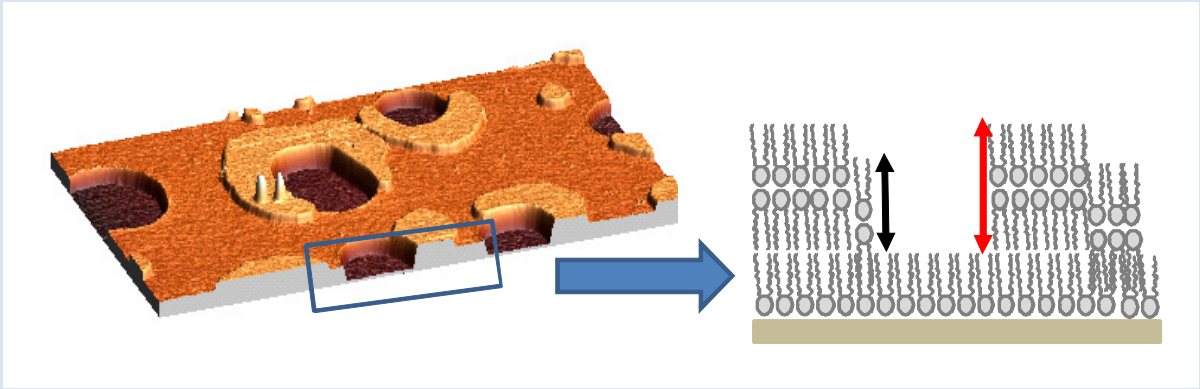

(*)This chapter reproduces almost literally the contents of an article currently under preparation by Aurora Dols-Perez, Laura Fumagalli, and Gabriel Gomila.

4.1 Introduction

The adequacy of the spin-coating technique to create air-stable samples of unsaturated lipids, such as DOPC, was demonstrated in previous chapter. In this chapter, the preparation of other monocomponent samples is considered, specifically the fabrication of monocomponent samples of lipids with saturated acyl chains. To this aim different phospholipids with different longitudes in their chains (from 12 to 18 carbons) were considered. DLPC and DMPC presented a flat structure with a thickness that is in accordance with the values reported in literature for the bilayer thickness measured in liquid media. However for DPPC and DSPC the behavior was different, they showed interdigitated areas apart from the conventional areas with the usual bilayer thickness. The influence of alcohols and lateral tension were studied to check the origin of this effect. Finally, the rotation speed was demonstrated to be the responsible for the interdigitation. By changing the rotation speed and adding a previous step in the sample preparation the interdigitated area can be reduced notably.

4.2 Materials and Methods

Materials: The lipid layers have been prepared with 1,2-dilauroyl-*sn*-glycero-3-phosphocholine (DLPC), 1,2-dimyristoyl-*sn*-glycero-3-phosphocholine (DMPC), 1,2-dipalmitoyl-*sn*-glycero-3-phosphocholine (DPPC) and 1,2-distearoyl-*sn*-glycero-3-phosphocholine (DSPC) purchased from Sigma-Aldrich and used as received without further purification. Hexane, LC-MS grade (Sigma-Aldrich), Isopropanol (Sigma-Aldrich) and Methanol, HPLC grade (Sigma-Aldrich), were used as solvent in the experiments. Lipid layers were formed on Hi-grade freshly cleaved mica substrates (Ted Pella,Inc).

Sample preparation and AFM imaging: Air-stable lipid layers have been obtained by the spin-coating technique following the methodology developed by Simonsen et al[65] further optimized to produce ultrathin (single) bilayer samples as described in the previous chapter. In here, the concentration of lipid used in the coating solution is 1mM. Using this concentration the spin-coated sample of lipids is composed by an homogeneous monolayer background with a single inverted bilayer on top forming patches or rims, and occasionally some multilayer patch[99]. At higher concentrations the number of layers increases [65, 66, 99].

AFM imaging was performed in dry environment, relative humidity RH ~ 0%, with calibrated AFM probes (PPP-CONTR, Nanosensors, spring constant 0.2 N/m, tip radius < 7 nm) using a commercial AFM (Nanotec Electronica S.L). Height analysis was performed using histogram analysis of the pixels over image areas of 1000 nm x 1000 nm (N = 3-7). The small size of the areas is selected to avoid systematic errors in height determination associated with image flattening. The obtained value is the mean of the values extracted at different areas and the error corresponds to the standard deviation (SD) of the means.

4.3 Results and discussion

AFM imaging was used to show how acyl chain longitude affects to the lipid organization and sample appearance in the spin-coating samples in dry environment. The large-scale topography images of the DLPC, DMPC, DPPC and DSPC samples prepared following the conventional spin-coating protocol are given in Figure 4-1.

As it can be seen the sample appearance changes depending on the lipid considered. For all the saturated lipids tested the bottom layer consists of a lipid monolayer as we demonstrated previously with other phosphocholine samples[99]. The DLPC and DMPC presented single or multiple bilayers formed on top of the background layer (Figure 4-1A-B). These layers showed a homogeneous surface. However, the DPPC and DSPC samples presented a non-homogeneous surface as can be seen in Figure 4-1C-D, in which "domains" with slightly different heights are observed.

Using the spin-coating technique it is possible to form incomplete layers that allows the access to the bottom monolayer; this fact allows measuring directly the bilayer thickness. The heights obtained by histogram and profile analysis are ~4.5 nm and ~4.9 nm, for DLPC and DMPC, respectively. These values are consistent with previous studies in hydrated samples[100, 101]. For the DPPC and DSPC the behavior is different, they present two different heights per layer. The lower heights are ~3.7 nm and ~3.8 nm, while the thicker ones are ~5.6nm and ~6.3nm, for DPPC and DSPC, respectively. In accordance to literature the higher thicknesses correspond to the bilayer height reported for hydrated samples [24]. Furthermore, it is well known that the bilayer thickness varies linearly with acyl chain length[102] and this phenomenon is also observable in Figure 4-1-E when the values of the thicker membranes are used.

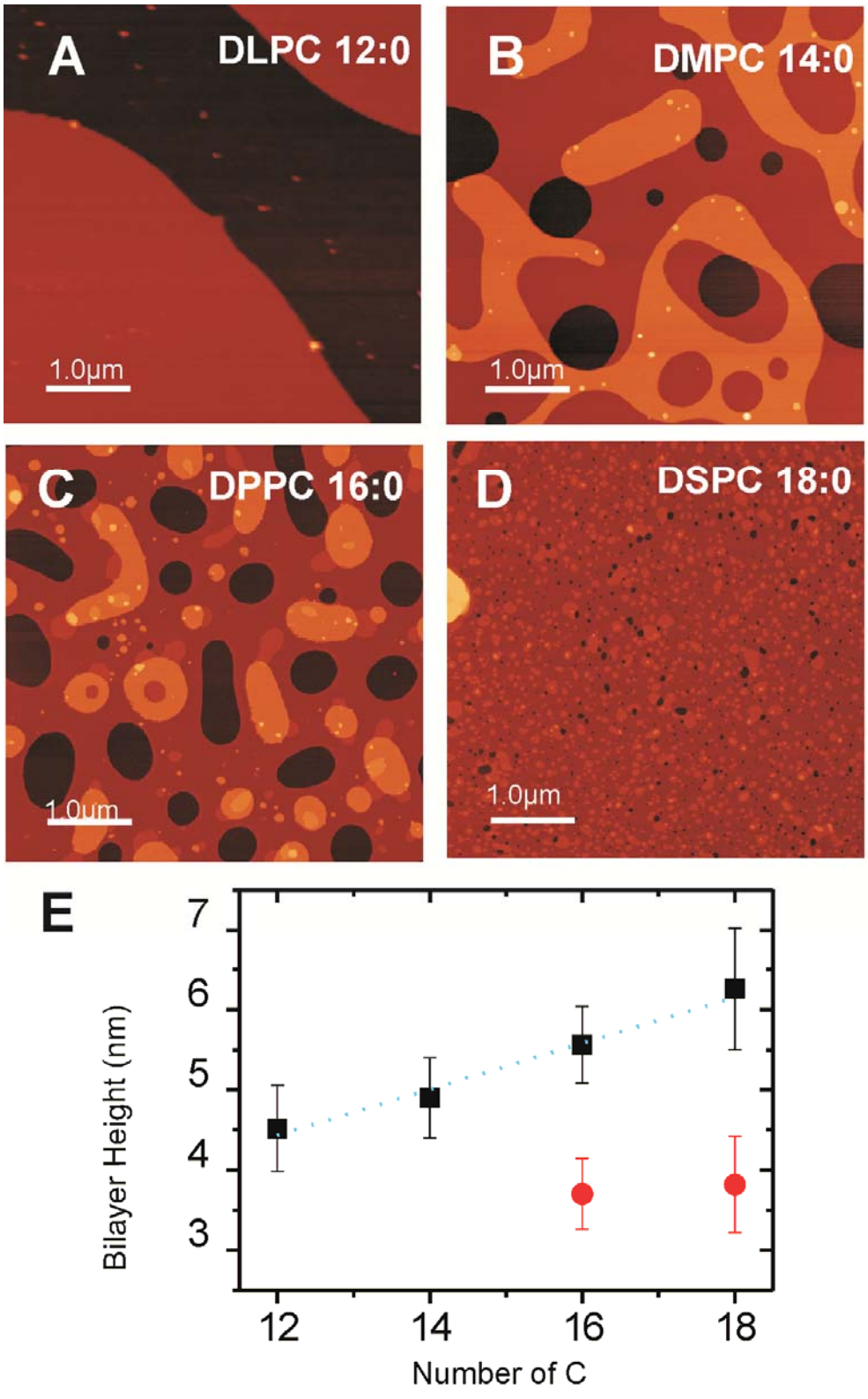

Figure 4-1 Representative AFM topography images of spin-coated samples of DLPC (A), DMPC (B), DPPC (C) and DSPC (D) in dry air conditions. (E) Bilayer height as a function of the acyl chain length (number of C).

Therefore the DPPC and DSPC samples present an intermediate height apart from the expected bilayer height. The thickness value of these regions is higher than the monolayer value whereby the partial delamination was discarded as hypothesis. However, as can be seen in Figure 4-2, the thickness values matched perfectly with values reported for interdigitated phases in liquid media.

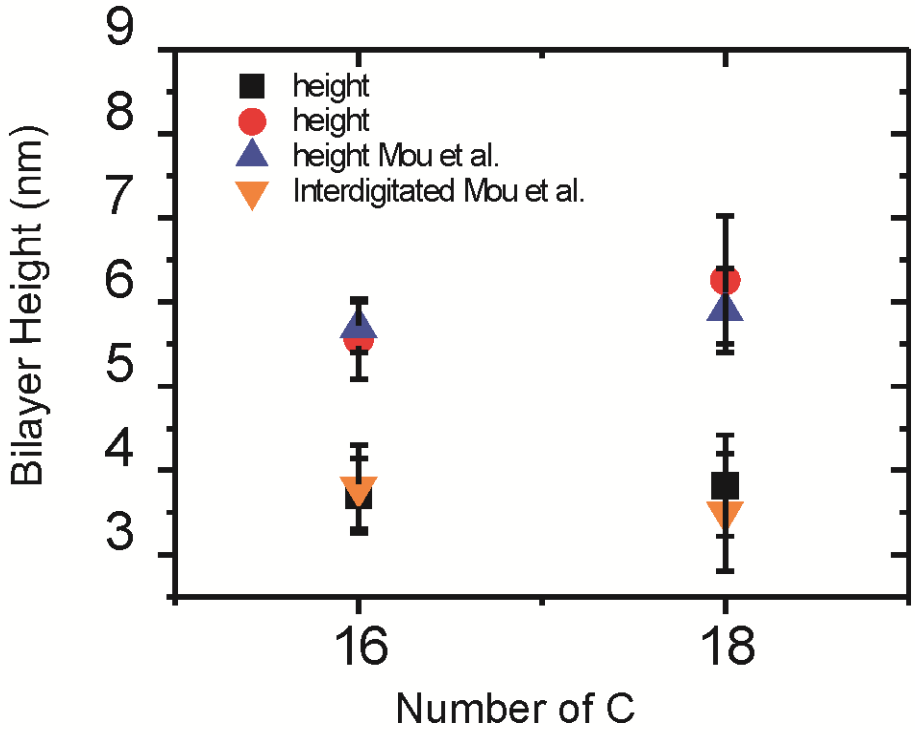

Figure 4-2 Bilayer thicknesses values for the dried samples of DPPC and DSPC compared with the values present in literature for these bilayers in liquid (blue triangle) and for the interdigitated regions (orange triangle)

The interdigitated phase (L_β'I) is produced in phosphatidylcholines in liquid due the presence of alcohols or volatile anesthetics or the presence of an abnormal pressure such as lateral tension[103]. Due to the absence of previous results in dried lipid layers presenting this phenomenon both effects were considered. The corresponding results are described below.

Effect of the presence of alcohol in the coating solution.

The presence of alcohols in the coating solutions is necessary due to the difficulty to dissolve saturated phospholipids in hydrocarbonated solvents (in contrast to what observed previously with unsaturated phospholipids[99]). Simonsen and coworkers proposed ~3% of methanol in hexane to dissolve correctly these lipids[65].

To check the effect of alcohols in the coating solutions different alcohols and proportions were used: solution A (hexane + methanol (98:2)) (Figure 4-1), solution B (pure methanol), solution C (pure isopropanol) and solution D (isopropanol + hexane + water (60:20:20)). During this procedure the same speed (3000rpm) and time (1min) was used. The results obtained for solvents B, C and D for the different lipids are represented in Figure 4-3.

As it can be seen, although the appearance of the layer changes depending on the solvent used, the presence of interdigitated areas is still observed independently of the coating solution used and the total amount of alcohol. The thickness of the bilayers is also maintained independently of the solvent used in both areas, interdigitated and non-interdigitated.

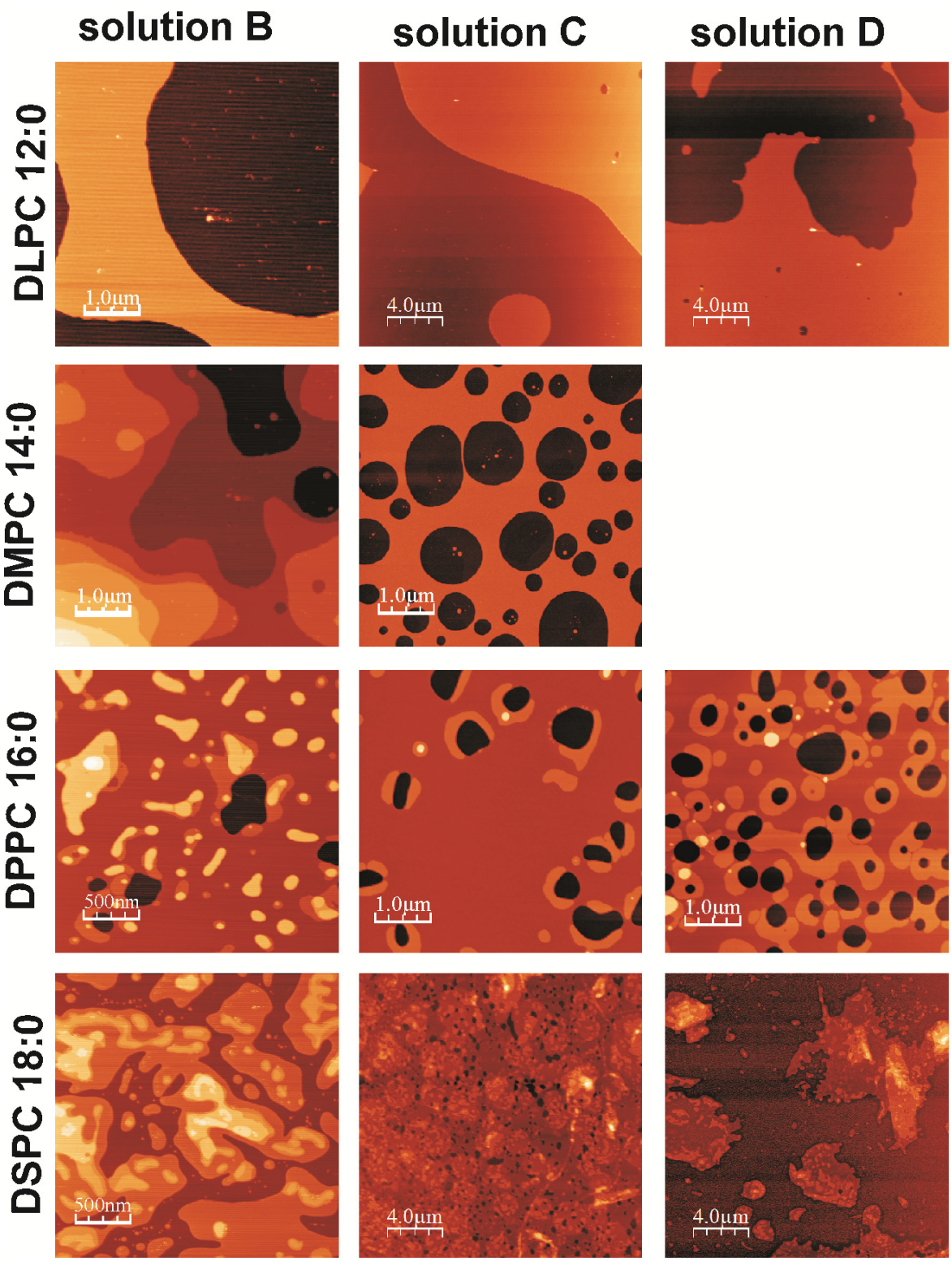

Figure 4-3 Representative AFM topography images of spin-coated samples of DLPC, DMPC, DPPC and DSPC in air for different solvents.

In hydrated samples the effect of alcohols is different. DMPC is also affected by the presence of alcohols in solution [104] showing also a thinning of its thickness. In hydrated samples the proportion of alcohol used is related to the area interdigitated and may induce the interdigitation of the total area of the bilayer[24]. In our results no dependency of the area affected was observed, and solutions with 100% of alcohols in the coating solution did not show a complete interdigitation, contrary to what expected.

These results suggested that the interdigitation in the DPPC and DSPC surface was not induced by the presence of alcohols in the coating solutions in the case of dry samples.

Effect of the lateral tension

In hydrated samples the interdigitated phase induced by lateral tension (L_β'I_T) is produced when the sample is exposed to a temperature above the Tm and after it is rapidly cooled below the Tm. The interdigitation is then produced due to the action of two factors: the substrate surface-lipid interaction[105] and the tension created by having to pass to cover a large area to cover a smaller one in a short period of time. If the transition is not slow enough, the area covered is larger than the expected for a solid phase and the bilayer cannot maintain its structure. For this reason the interdigitation, with a higher area per molecule, is induced occupying a larger area.

In the spin-coating the temperature is not changed during the process, so that another parameter should affect the lateral tension of the sample. A clear candidate is the rotation speed and the acceleration present during the spin-coating process. This hypothesis is compatible with the absence of interdigitated regions in DLPC and DMPC samples because these

samples are in fluid phase at the working temperature and then their mobility is higher than the solid samples. Then DLPC and DMPC can recover their position easily independently of the effect of the lateral pressure.

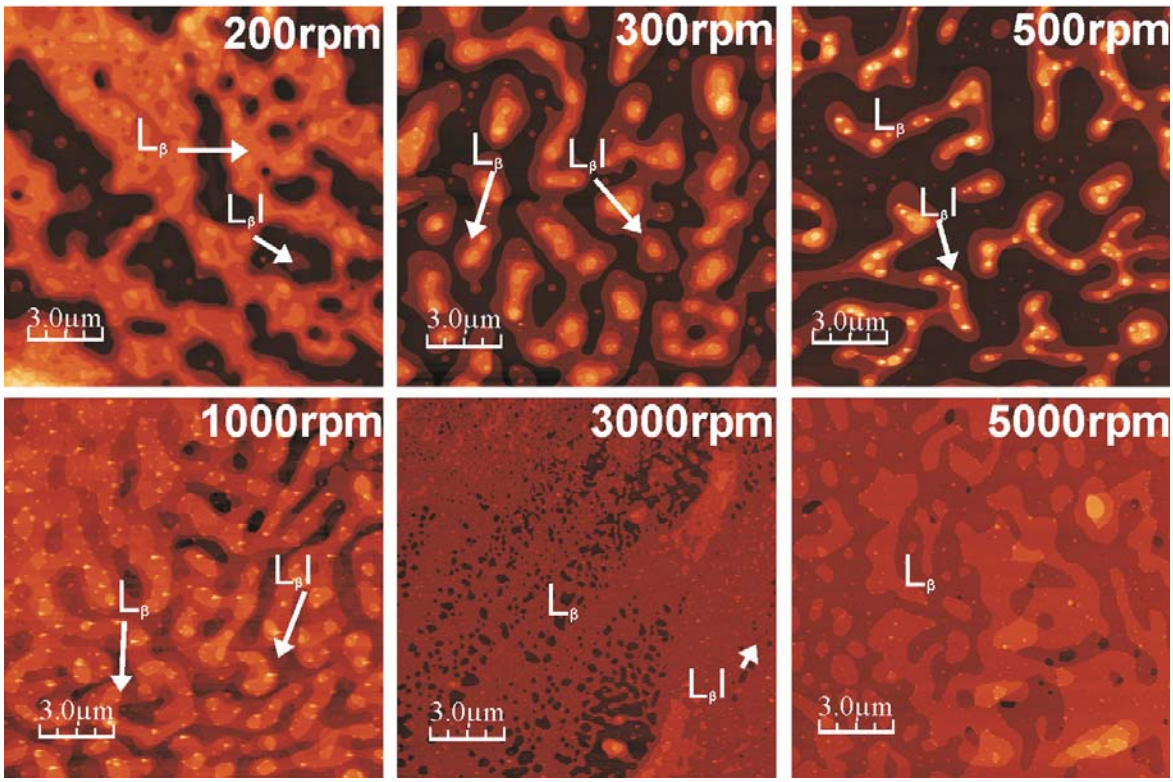

Figure 4-4 AFM topography images in function of the rotation speed used during the sample preparation. For higher speeds (3000rpm, 5000rpm the interdigitated regions disappear).

Here, we have decided to change the rotation speed and add an initial step to the process, in which the sample rotates at low speed (200rpm 15s), to avoid effects due to the interaction with the substrate. To check the effects of these parameters we have used DPPC. The results obtained with the different rotation speeds are shown in Figure 4-4.

The results demonstrate that the interdigitated area depends on the rotation speed used to prepare the sample and can be reduced adjusting these parameters properly.

4.4 Conclusions

In the present Chapter the nanoscale topographic properties of mica supported ultrathin spin-coated saturated lipid layers in dry air ambient have been studied. We have shown that the thickness of the bilayers increases proportionally to the number of carbons of the lipids used, in good agreement with what observed for hydrates samples. Additionally we have observed for the lipids with higher melting temperature the presence of bilayers with an intermediate thickness, which it is in accordance with an interdigitated phase observed also sometimes in liquid media. The effect of the alcohols and the lateral pressure were studied to ascertain the responsible of this effect. Finally the lateral tension due to the rotation speed was demonstrated to be the responsible of interdigitation in dried bilayers. We showed that by adjusting the preparation procedure interdigitation can be reduced drastically.

This study shows that in addition to the case of unsaturated lipids, studied in the previous chapter, it is also possible to prepare lipid bilayer samples stable in dry environment with saturated lipids. This opens the possibility to create multicomponent lipid sample combining both types of lipids.

4.5 Appendix: Layers formed with other monocoponent samples (cholesterol and sphingomyelin)

Besides the results reported in this chapter, other monocomponent samples with different components used in the next chapter for multicomponent samples were analyzed. This is the case of Cholesterol and Sphingomyelin, used in the formation of binary and ternary mixtures relevant for lipid raft models. Here, we briefly outline their main topographic properties for further reference.

4.5.1 Spin coated cholesterol layers

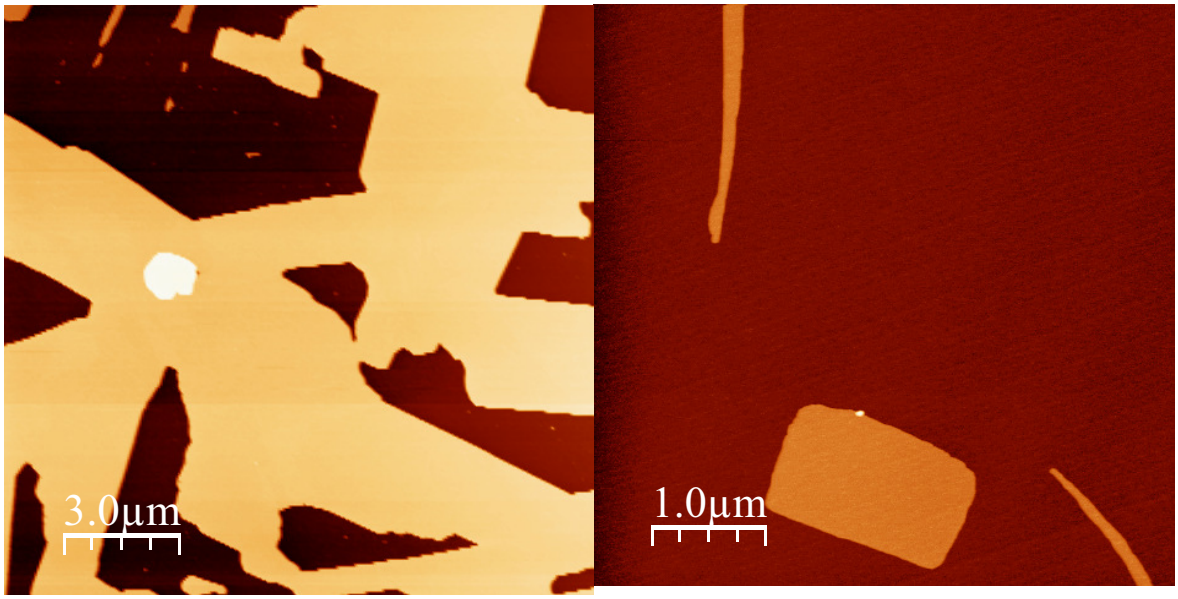

Figure 4-5 AFM topography images of a Cholesterol sample on mica prepared by spin-coating

In Fig. 4-5 we show AFM topographic images of dry cholesterol layers prepared by the spin-coating technique on mica (Cholesterol concentration 1mM). The cholesterol samples presented flat surfaces with straight edges and a thickness of ~3.5 nm per layer. The presence of straight edges was attributed to the structure of the molecule and its rigidity. These samples were prepared only to check the quality of the lipid aliquot previous to the mixture elaboration and were not studied exhaustively.

4.5.2 Spin coated Sphingomyelin layers

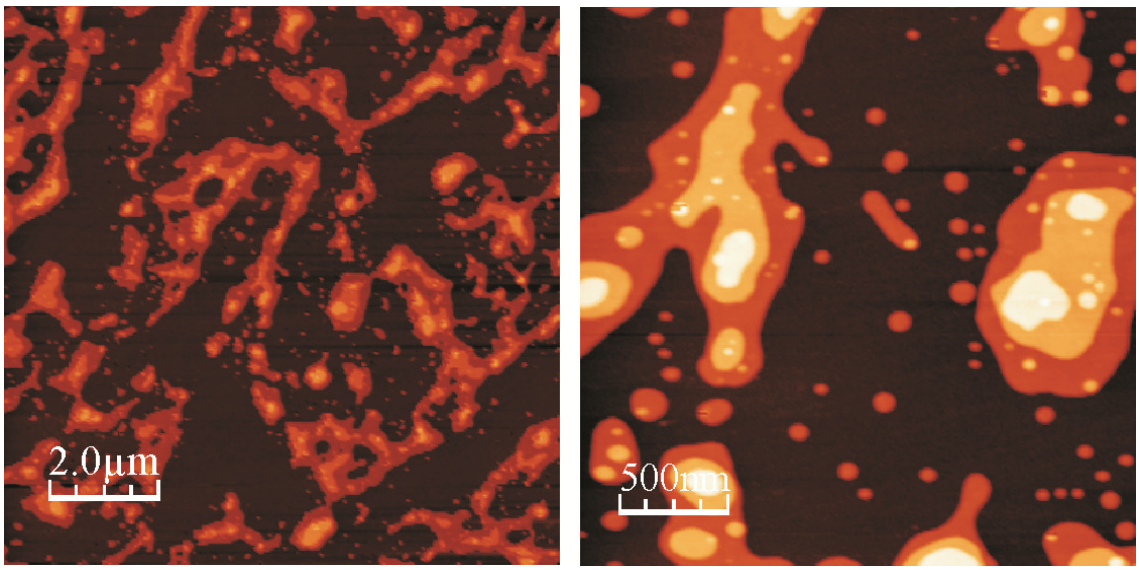

Figure 4-6 AFM topography image of a monocomponent sphingomyelin sample prepared by spin-coating on mica.

Figure 4-6 show AFM topographic images of a Sphingomyelin layer on mica prepared by the spin-coating technique (concentration 1mM). Sphingomyelin layers presented a multilayered structure similar to the described for phosphocholines. The bilayer thickness was homogeneous, without interdigitation, and was ~6nm in height.

Chapter 5. Nanoscale properties of multicomponent lipid bilayers of DOPC, Sphingomyelin and Cholesterol in dry air environment

Summary: In this chapter we demonstrate that lipid raft models morphologically stable in dry air environment can be prepared by the spin-coating technique. To this end we investigate the nanoscale structural and mechanical properties of binary and ternary mixtures of Dioleoylphosphatidylcholine (DOPC), Sphingomyelin (SM) and Cholesterol (Chol) by AFM, and show that they exhibit phase separation properties, bilayer thicknesses, rupture forces and cholesterol effects similarly to the corresponding values reported for equivalent models in aqueous solutions.

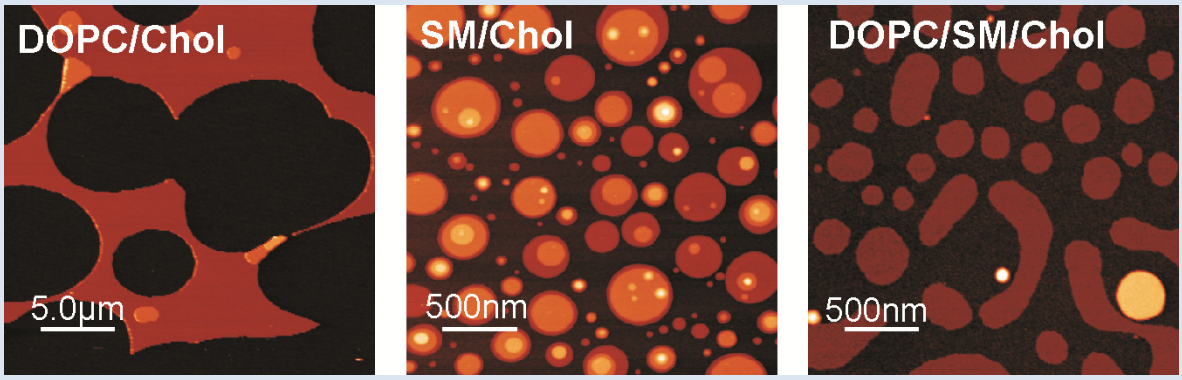

This chapter reproduces almost literally the article: *Nanoscale properties of multicomponent lipid bilayers of DOPC, Sphingomyelin and Cholesterol in dry air environment* by Aurora Dols-Perez, Laura Fumagalli and Gabriel Gomila, which has been submitted for publication.

In this article I was in charge of performing all the experiments and processing the results. In this part of the work I followed some technical suggestions from L. Fumagalli. The article was written by me with the collaboration of the other co-authors.

5.1 Introduction

In this chapter we investigate the nanoscale structural and mechanical properties of multicomponent supported lipid bilayers made of DOPC, Sphingomyelin and Cholesterol in dry air conditions. This ternary mixture has been chosen because of its relevance in the study of lipid raft models. As it is well known lipid raft models are usually based on ternary mixtures composed by a phosphocholine of low melting temperature (Tm), a sphingolipid (or a phosphocholine of high Tm) and cholesterol, and previous studies have shown that these mixtures under liquid conditions have liquid-ordered domains of ~ 10-200 nm (lipid rafts), enriched in sphingolipids and cholesterol, and a liquid-disordered phase enriched in phosphocoline. In Chapter 3, we have shown that dry monocomponent bilayers made of DOPC prepared by the spin coating technique showed nanomechanical and structural properties resembling those of DOPC lipid bilayers in pure water (but distinct of DOPC lipid bilayers in buffer). In the present chapter, we extend this study to the much more complex case of multicomponent lipid bilayers, including ternary mixtures relevant for lipid raft studies, in order to investigate if the parallelism between dry and hydrated samples is also maintained for multicomponent samples showing phase segregated domains.

5.2 Materials and Methods

Materials:

The lipid layers have been prepared with 1,2-Dioleoyl-sn-glycero-3-phosphocholine (DOPC), Egg Sphingomyelin (SM) and Cholesterol (Chol) purchased from Sigma-Aldrich and used as received without further purification. A 98:2 (v/v) solution of Hexane, LC-MS grade (Sigma-Aldrich), and Methanol, HPLC grade (Sigma-Aldrich), was used as solvent in all the experiments. Lipid layers were formed on hi-grade freshly cleaved mica substrates (Ted Pella,Inc).

Sample preparation, AFM imaging and Force Spectroscopy Measurements:

Air-stable lipid layers have been obtained by the spin-coating technique following the methodology developed by Simonsen et al[65] further optimized to produce ultrathin (single) bilayer samples as described in reference[99]. In here, the concentration of lipid used in the coating solution is 1mM. Using this concentration the spin-coated sample of lipids is composed by an homogeneous monolayer background with a single inverted bilayer on top forming patches or rims, and occasionally some multilayer patch[99]. At higher concentrations the number of layers increases [65, 66, 99]. Both binary mixtures of Chol and DOPC or SM, as well as ternary mixtures of DOPC/SM/Chol, have been prepared in order to elucidate the effect of Chol. We have obtained binary mixtures combining DOPC or SM with Cholesterol from 10 mol% to 50 mol%. Ternary mixtures (DOPC/SM/Chol) were prepared using the ratios 1:1:1, 2:1:1 and 2:2:1. These samples were prepared using the same stock solutions to avoid discrepancies in their characteristics. Sample preparation by spin-coating were performed following the methods that we previously detailed[99].

AFM imaging was performed in dry environment, relative humidity RH ~ 0%, with calibrated AFM probes (PPP-CONTR, Nanosensors, spring

constant 0.2 N/m, tip radius < 7 nm) using a commercial AFM (Nanotec Electronica S.L). Height analysis was performed using histogram analysis of the pixels over image areas of 500 nm x 500 nm (N = 3-7). The small size of the areas is selected to avoid systematic errors in height determination associated with image flattening. The obtained value is the mean of the values extracted at different areas and the error corresponds to the standard deviation (SD) of the means. Additionally, force curves (Fz) were taken individually on selected locations of the sample to obtain the local mechanical properties (approach velocity 1.6 μm/s). They were systematically taken at different locations to avoid the effects of any plastic deformation of the sample. Fz curves were measured with two different probes to check the reproducibility of the data. Breakthrough forces, defined as the maximum force the layer is able to withstand before its rupture, have been determined from the force curves. This parameter is a direct measure of the mechanical stability of the membrane, and hence it is considered a fingerprint of the sample state, composition and environment conditions[79]. Mean values, and standard deviations, of breakthrough forces have been obtained from 40 force curves taken with the two different probes used. Independent sets of experiments were performed with different samples and probes to demonstrate the reproducibility of the results reported here.

5.3 Results

Binary mixtures of DOPC/Chol and SM/Chol

The large-scale topography of the binary DOPC/Chol samples are given in Figure 5-1A-D at increasing concentration of Chol (for 0 mol% content, see chapter 3). As can be seen the sample consists of a uniform background, on top of which single (or multiple) bilayers are formed. The background consists of a lipid monolayer as we demonstrated previously[99]. The Chol content influences the morphology of the bilayers as well as the total height of the structures. For low concentrations of Chol, 10 mol%, single lipid bilayers formed a network of rims with holes of different sizes, and occasionally some multibilayers (Figure 5-1A). When the concentration of Chol increased to 20 mol%, these networks broke up forming isolated patches with a multilayered structure with the presence of some single bilayers (Figure 5-1B). For higher concentrations, 30-40 mol%, the samples tended to form thicker multilayered structures with a limited presence of structures formed by a single bilayer, as can be appreciated in Figures 5-1C-D. Single bilayer regions are hardly appreciated on the large scale images but they can be easily identified on specific parts from zoomed images (Figures 5-1A.1-D.1) or from a height distribution analysis of the images (Figure 5-2).

Figure 5-1 Representative AFM topography images of spin-coated samples of DOPC/Chol in air with different concentrations of Chol. (A) 10 mol % of Chol, (B) 20 mol% of Chol, (C) 30 mol % of Chol and (D) 40 mol % of Chol. (25μm X 25 μm, Z-scale: 40nm). (A.1-D.1) Zoomed topography images on specific regions of DOPC/Chol samples for different Chol concentrations showing the presence of single bilayers (marked with an arrow) (Z-scale:20nm). (E) Bilayer height as function of the Cholesterol concentration in the coating solution.

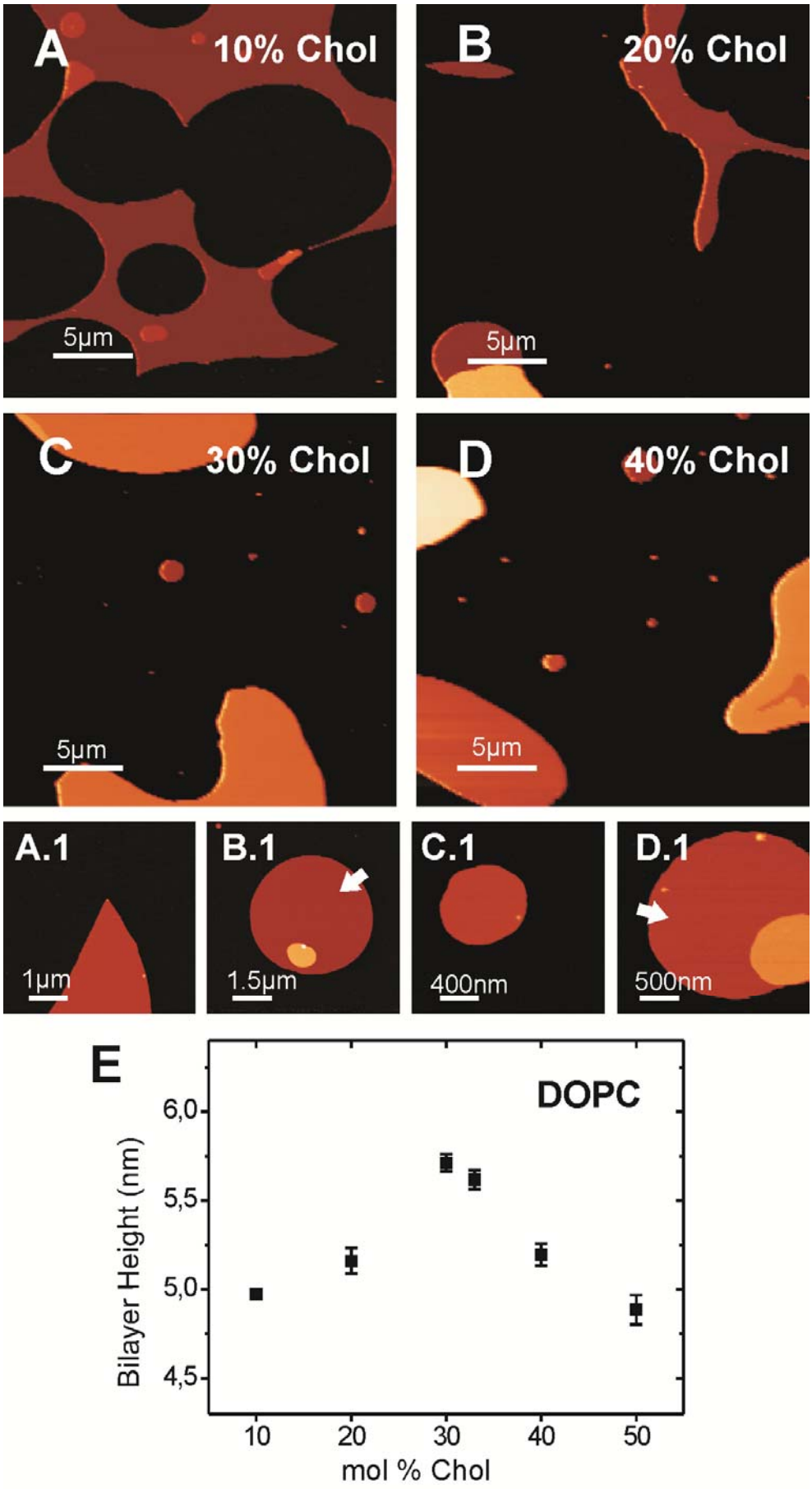
A
10% Chol
5µm
B
20% Chol
5µm
C
30% Chol
5µm
D
40% Chol
5µm
A.1
1µm
B.1
1.5µm
C.1
400nm
D.1
500nm
E
DOPC
Bilayer Height (nm)
6,0
5,5
5,0
4,5
10
20
30
40
50
mol % Chol

The measured height of the single bilayers of the binary DOPC/Chol depends on Chol content. We show it in Figure 5-1E, where the height of the single bilayers is given as a function of the Chol concentration. The data, obtained from histogram analysis of the height, indicate that the height of DOPC/Chol bilayer first increased from ~ 5 nm to ~ 5.7 nm with increasing the cholesterol concentration up to ~ 30 mol%. For larger concentrations the bilayer height decreased to lower values to reach about ~ 4.8 nm, at Chol concentration of ~ 50 mol % (Figure 5-1E).

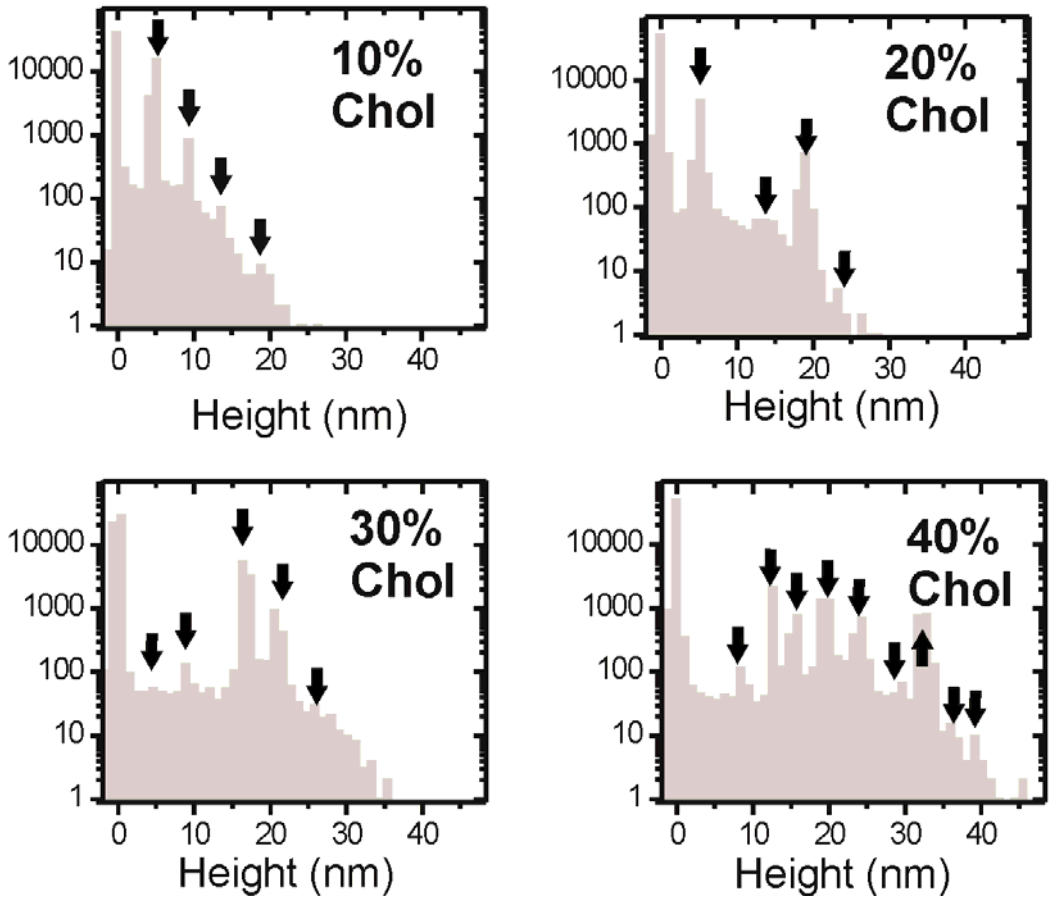

Figure 5-2 Height analysis of the DOPC/Chol images in Figure 1A-D for different concentrations of Chol. Histograms represent the height of the pixels in the topography images. Arrows indicate the peaks corresponding to single or multi-bilayers. An increment of the number of layers, when the Chol content increases, is observed. The initial peak (without arrow) corresponds to the background of the image.

In Figure 5-3 we show the morphological properties of the SM/Chol binary mixture. They were also affected by the Chol content, but in a different manner. Samples of low concentration of Chol, 10–20 mol%, showed multilayered structures similar to lipid aggregates, with heights up to 50 nm and a mean surface coverage of ~ 30% (Figures 5-3A-B). Single bilayers were difficult to appreciate in the large scale image but they could be easily identified by zooming in specific regions (Figures 5-3A.1-D.1) or by the histogram analysis of the height (Figure 5-4). The initial morphology evolved to round patches with a smaller number of layers and larger mean surface coverage, around 50%, when the concentration of Chol was increased to 30–40 mol% (Figure 5-3C-D). The evolution of the number of layers, and their thickness, can be easily appreciated from height histogram analysis at the different concentrations (Figure 5-4). The height of a single SM/Chol bilayer is also affected by the Chol content but to a lesser extent than for the case of DOPC/Chol bilayers. Specifically, the membrane bilayer height remains constant at ~ 6 nm for a molar concentration of Chol up to ~ 40 mol%, then slightly decreases to ~ 5.6 nm for 50 mol% of Chol (see Figure 5-3E).

Figure 5-3 Representative AFM topography images of spin-coated samples of SM/Chol in air with different concentrations of Chol. (A) 10 mol % of Chol, (B) 20 mol % of Chol, (C) 30 mol % of Chol and (D) 40 mol % of Chol. (2.5μm X 2.5 μm Z-scale: 50nm). (A1-D1) Zoomed topography images on specific regions of SM/Chol samples for different Chol concentrations showing the presence of single bilayers (marked with an arrow) (Z-scale: 40nm) (E) Bilayer height as function of the Cholesterol concentration in the coating solution.

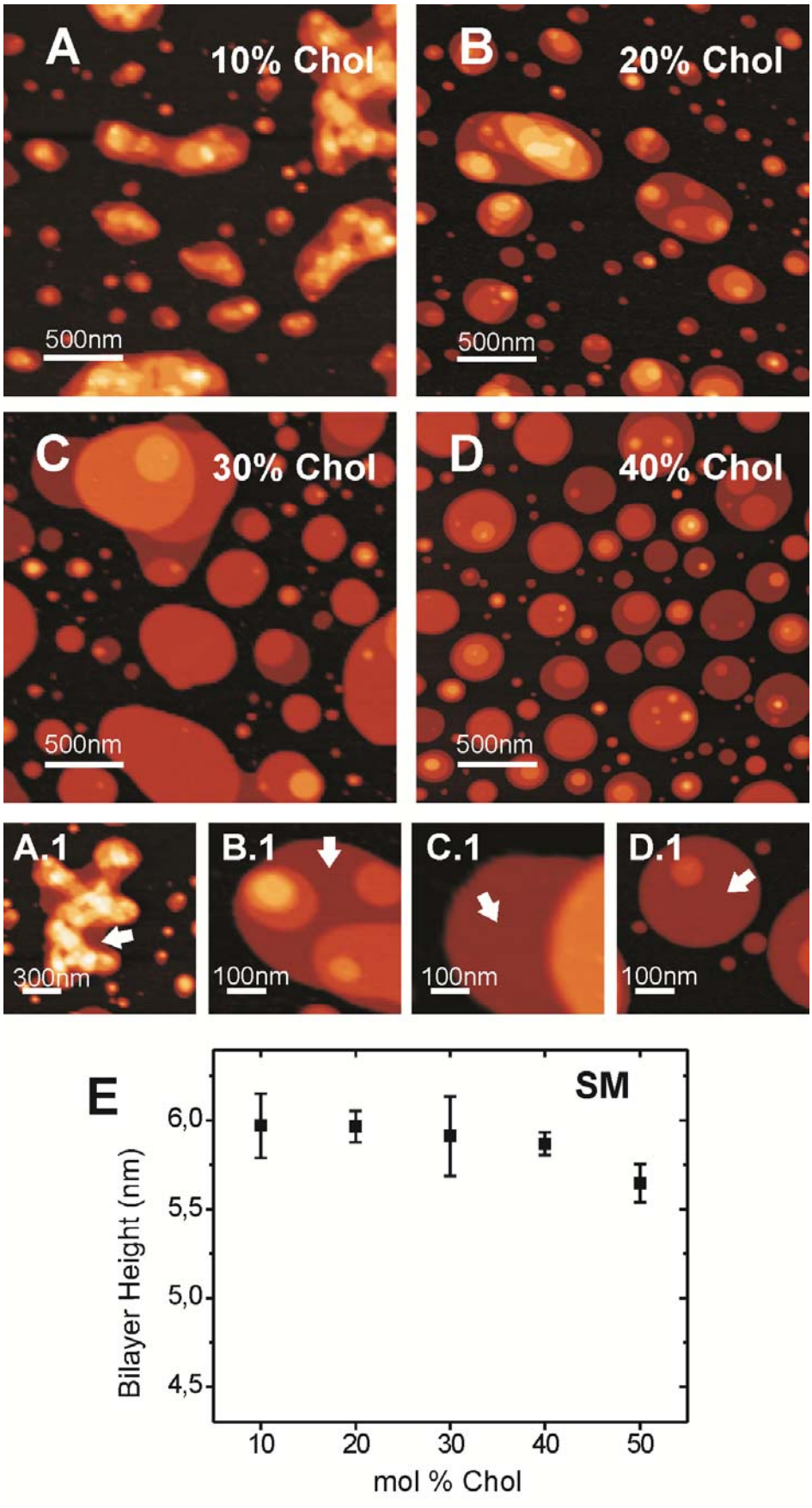
A
10% Chol
500nm
B
20% Chol
500nm
C
30% Chol
500nm
D
40% Chol
500nm
A.1
300nm
B.1
100nm
C.1
100nm
D.1
100nm
E
SM
Bilayer Height (nm)
6,0
5,5
5,0
4,5
10
20
30
40
50
mol % Chol

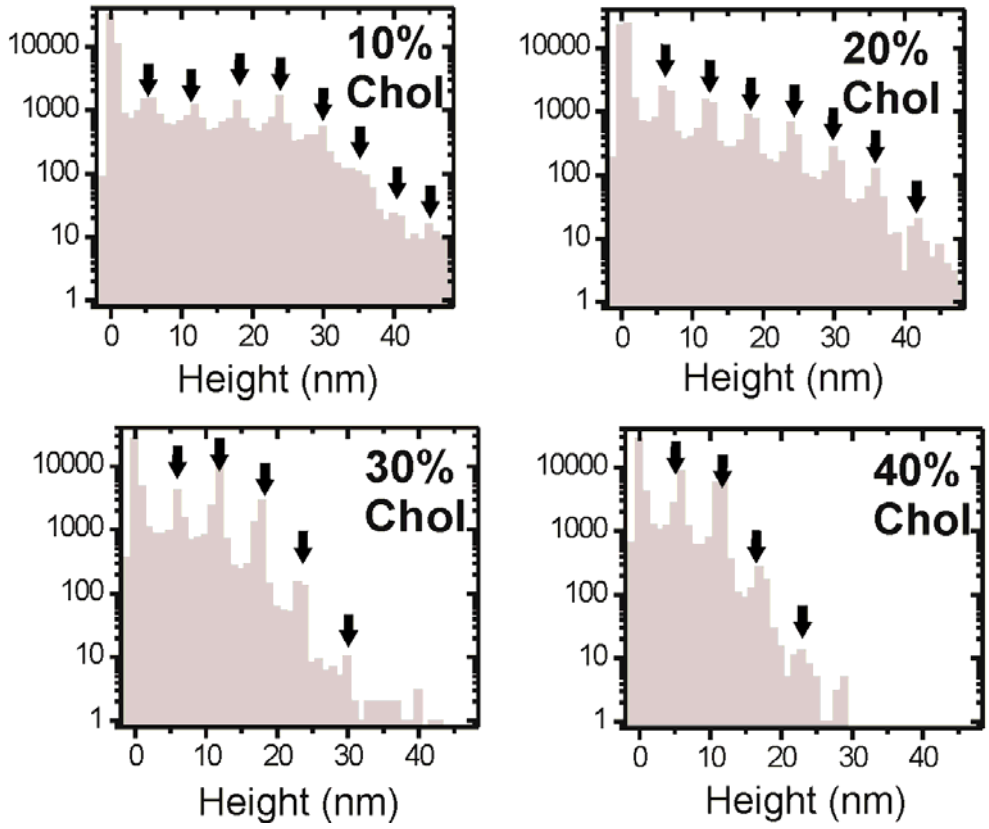

Figure 5-4 Height analysis of the SM/Chol images in Figure 5-3 for different concentrations of Chol. Histograms represent the height of the pixels in the topography images. Arrows indicate the peaks corresponding with single or multi bilayers. A decrease of the number of layers, when the Chol content increases, is observed. The initial peak (without arrow) corresponds to the background of the image.

Phase separation or domain formation was not observed in the AFM images for both binary mixtures.

In Figure 5-5, we report on the rupture forces of both binary bilayers as a function of their Chol content measured by force spectroscopy. Fz curves taken on the background showed no ruptures for both DOPC/Chol and SM/Chol samples (data not shown), similarly to what we observed earlier for pure DOPC layers[99]. Instead, bilayers showed clear rupture events with well defined breakthrough forces (Figure 5-5A). In the case of DOPC/Chol bilayers ruptures are present at negatives values of force ~–0.6 nN, with no significant dependence on the Chol content (Figure 5-

5B, red circles). For SM/Chol bilayers the rupture forces showed positive values and a slight dependence on Chol concentration up to a Chol concentration of ~ 50%. At this concentration an important decrease in the breakthrough force, from ~9 nN to ~3 nN, was observed (Figure 5-5B, black squares).

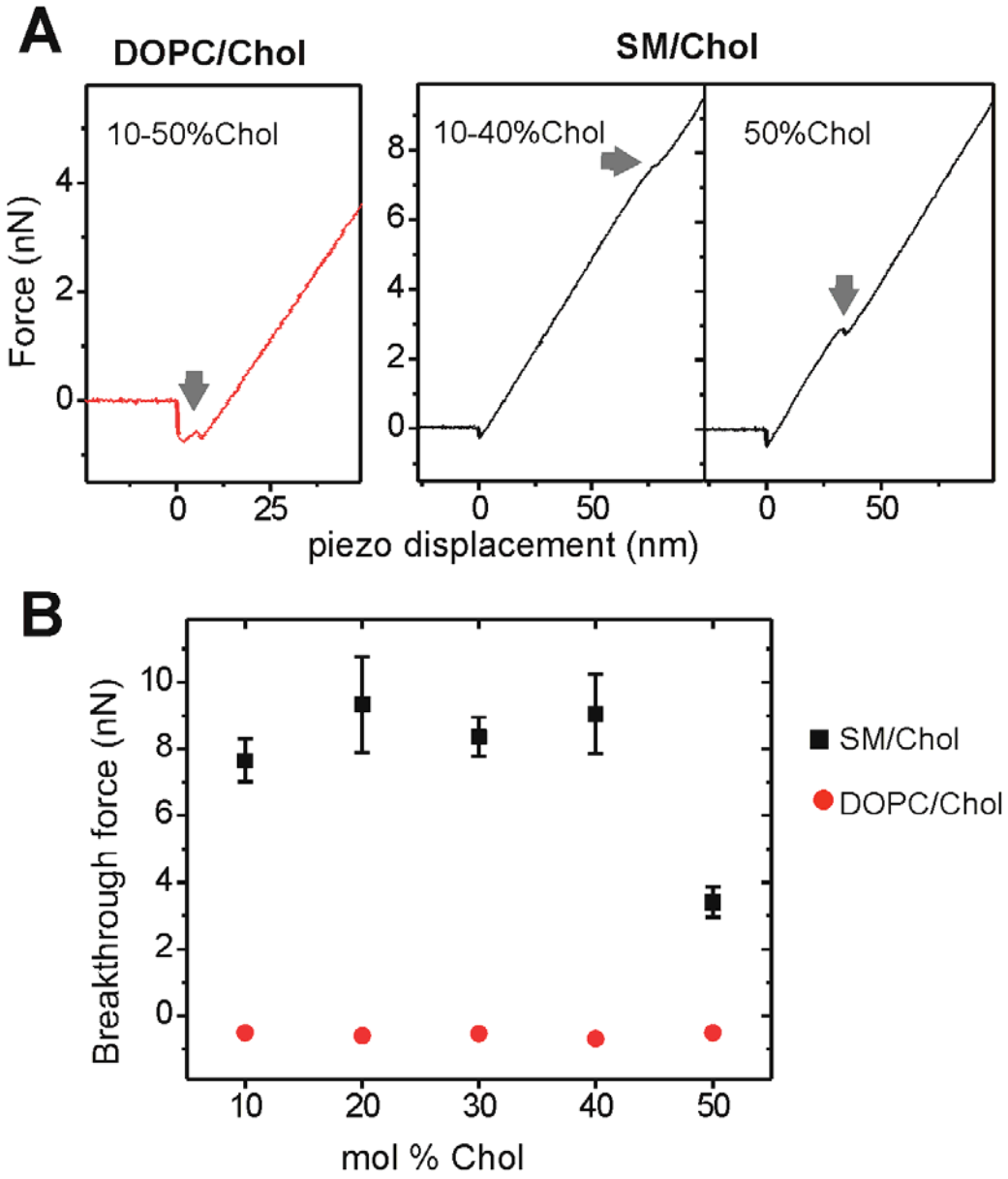

Figure 5-5(A) Representative force versus piezo-scanner displacement curves on DOPC/Chol (red), and on SM/Chol, (black) single bilayers. Arrows indicate rupture events. (B) Plot of breakthrough forces for DOPC/Chol (red circles) and SM/Chol (black squares) single bilayers as a function of Cholesterol content.

Ternary mixtures

The morphology of the ternary mixtures of DOPC/SM/Chol showed the characteristic dewetting pattern with extended single (and multi-) bilayer networks of rims with large holes on top of a background monolayer (Figure 5-6A-C).

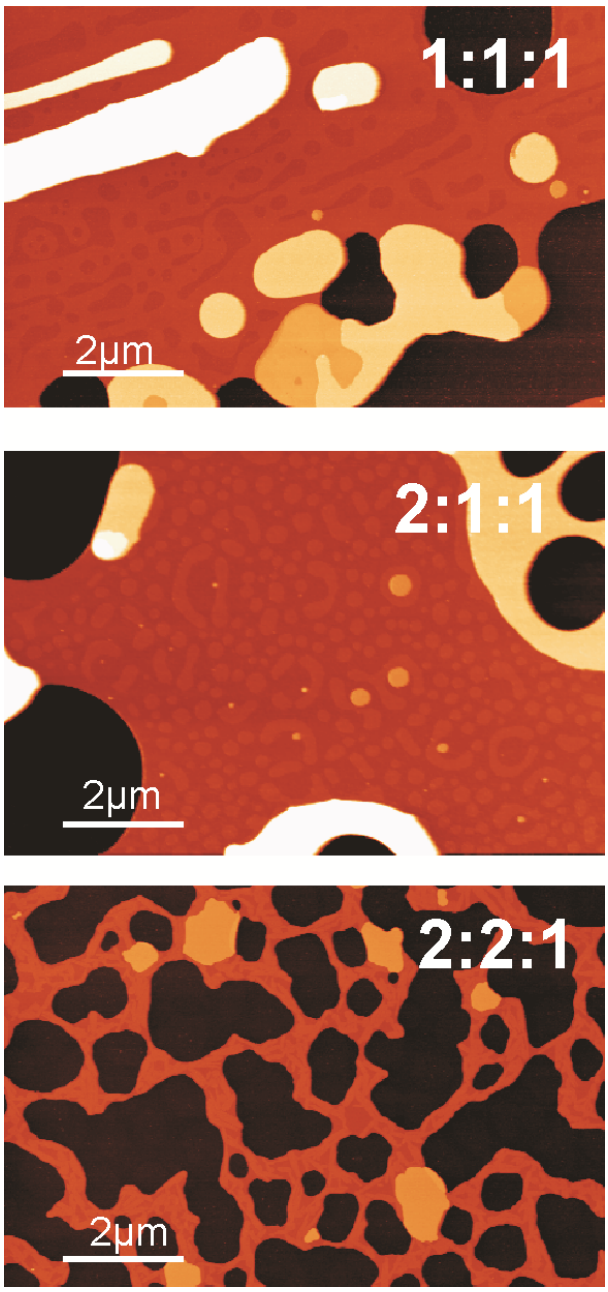

Figure 5-6. Representative AFM topography images of single bilayers of DOPC/SM/Chol, in different ratios, in air. (A) 1:1:1 (B) 2:1:1 and (C) 2:2:1

No domain was observed in the background monolayer for two of the compositions analyzed, 1:1:1 and 2:1:1, while they were observed for the composition 2:2:1, with a very small domain height difference (~ 0.1 nm) (Figure 5-7).

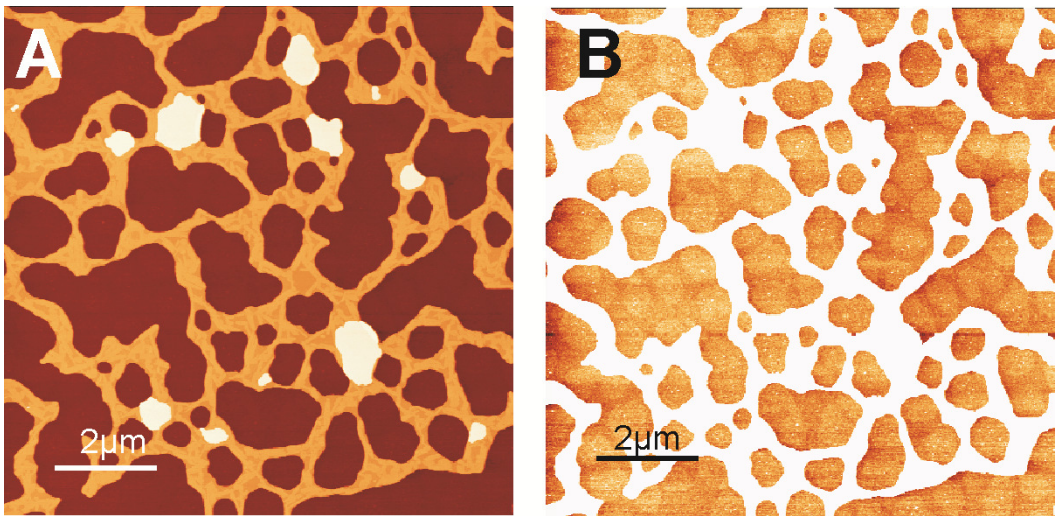

Figure 5-7. Representative AFM topography image of a sample of DOPC/SM/Chol (2:2:1) with different Z-scales (A) Z-scale 15nm (B) Z-scale 1.5nm. In the later case the presence of domains on the background layer can be visualized, with a very small height difference (~0.1 nm). For the other two concentrations tested (1:1:1 and 2:1:1) no domains were observed on the background.

Instead, single bilayers showed in all the cases the formation of domains (Figures 5-8A-C), indicating the coexistence of two phases. Lower regions (blue arrow in Figures 5-8A-C) and higher regions (red arrow in Figures 5-8A-C) were ascribed to DOPC-enriched and SM-enriched regions respectively. Note that the darker regions in Figures 5-8A-C indicated with white arrows correspond to the bottom background monolayer. We remark that direct access to the background layer in this type of samples is an advantage, because it allows measuring the height of the different domains directly and not simply the difference between regions (see profiles in Figure 5-8). The obtained heights of the different phases of the bilayers for the compositions analyzed here are given in Figure 5-8D.

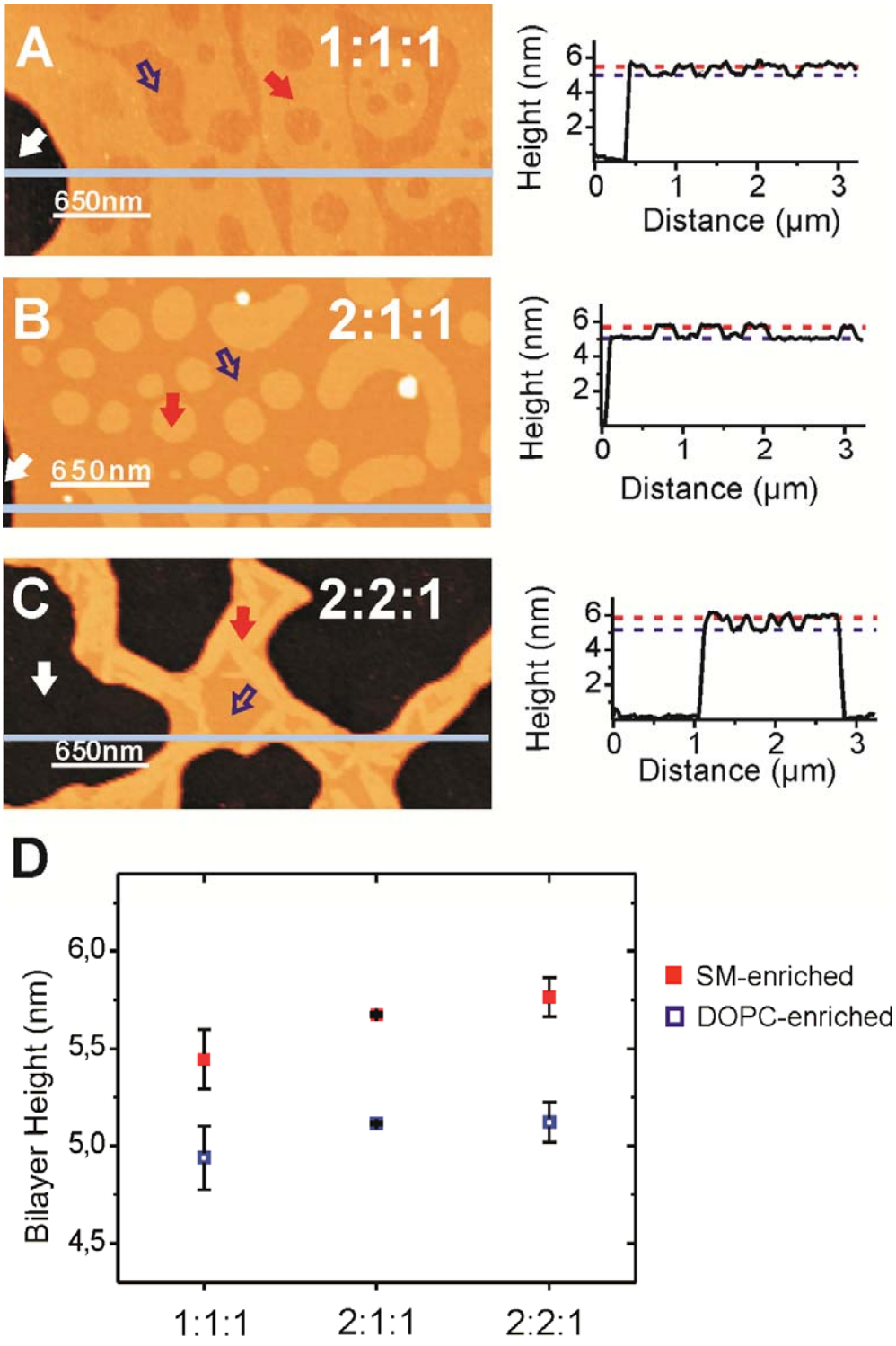

Figure 5-8 Zoomed topography images on specific regions (3.25µm X 1.7 µm, Z-scale: 10nm). Profiles corresponding to the cross-section line are shown beside the corresponding topography image. (D) Bilayer heights as a function of lipid mixture composition. Red filled squares correspond to SM-enriched regions, while blue open squares to DOPC-enriched regions.

To assess the mechanical properties of the two phases of the bilayers, Fz curves were taken on each sample composition and phase regions. Figure 5-9A gives representative Fz curves taken on different regions shown in Figure 5-8. Rupture events were observed on both phases on the bilayers but on the background monolayer. The two phases of the bilayers showed remarkable differences in their rupture forces, as shown in Figure 5-9B where the mean values of the measured rupture forces are given. The mean values of the breakthrough force of the DOPC-enriched region were 0.2 ± 0.8nN, 3.7 ± 0.9nN and −0.7 ± 0.1nN, while for the SM-enriched region we obtained 4.4 ± 0.9nN, 8.0 ± 0.4nN and 5.8 ± 0.9nN for the compositions 1:1:1, 2:1:1 and 2:2:1, respectively. In all the samples that we analyzed the thinner region (DOPC-enriched) showed lower rupture forces, while the thicker domains (SM-enriched), showed higher rupture forces. Therefore, the two coexisting phases in the single bilayers showed both thickness differences as well as mechanical differences.

Figure 5-9.(A) Representative force versus piezo-scanner displacement curves measured on the background, DOPC-enriched region and SM-enriched region for the different samples and areas shown in Figure 5-8. Arrow indicates rupture events. (B) Breakthrough forces for DOPC/SM/Chol bilayers as a function of the lipid ratio. Red filled square, SM-enriched region; blue open square, DOPC-enriched region.

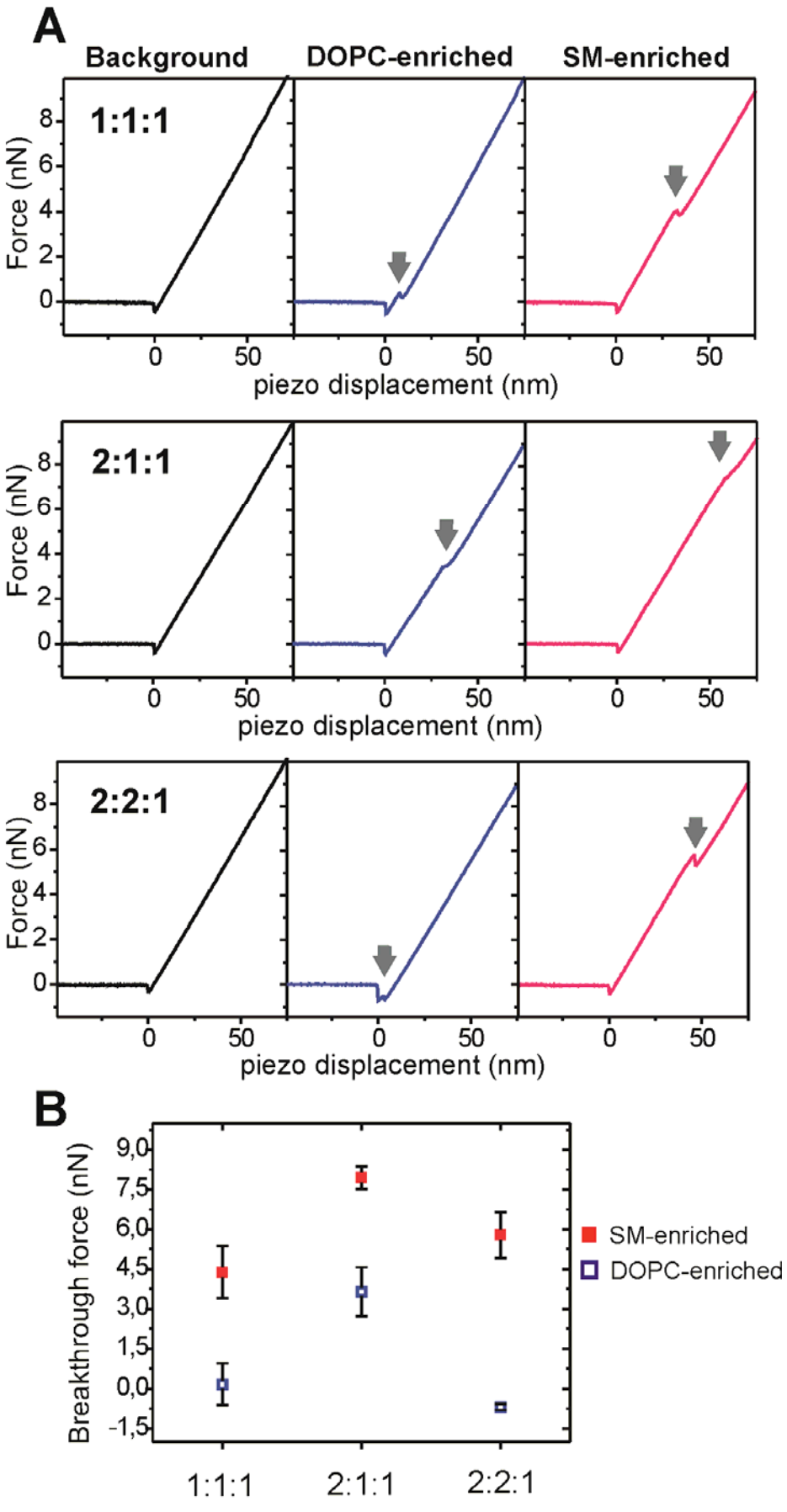
A
Background
DOPC-enriched
SM-enriched
1:1:1
2:1:1
2:2:1
Force (nN)
piezo displacement (nm)
B
Breakthrough force (nN)
SM-enriched
DOPC-enriched
1:1:1
2:1:1
2:2:1

5.4 Discussion

In the previous section we have demonstrated the possibility to form air-stable lipid bilayers of binary and ternary mixtures by the spin-coating technique. We have also shown that the composition of these mixtures affects the lateral morphology of the bilayers, their thickness, their mechanical properties and their phase segregation properties. In particular, we have shown lipid raft-like structures in the case of ternary mixtures. Below, we compare the properties of the dry bilayers in relation with their equivalent systems studied in the liquid environment.

Binary mixtures

The influence of Cholesterol in phosphocholines and in sphingomyelins *in liquid* environment has been highly studied in recent years. Many studies demonstrate that the presence of Chol causes a change in the order of the layers. Chol addition has shown to have a direct influence in the lipid packing and as a consequence on the area per molecule, on the phase, on the lateral diffusion, on the thickness and on the breakthrough force of the mixture among others. In the study presented here, we observed similar effects in the lipid layers under dry conditions.

With increasing the cholesterol content, dry DOPC/Chol bilayers evolved from a single bilayer extended configuration, similar to the one obtained for pure DOPC [99], to a compact multi-bilayer configuration (Figure 5-1). This change in morphology is compatible with a reduction of the lateral diffusion and with the well-known effect of cholesterol on the area per molecule of a binary mixture. In particular, it gives lower area per molecule than the expected from an ideal mixture ("condensing effect")[106-108]. The change in the ordering normally promotes the thickening of the phosphocholine layers[109]. In our results this thickening effect is observed only for Chol concentrations < 30% mol, while for higher concentrations the bilayer thickness decreases (Figure 5-1E). Although AFM experimental data of for hydrated DOPC/Chol samples are not available at similar Chol concentrations, molecular dynamics

simulations clearly support the experimental behaviour that we observed [107]. According to simulations, the thickness of the bilayer should increase with Chol concentration and reach a maximum at 35% mol, after which the thickness should suffer a gradual decrease. This is explained by the reorganization of the DOPC headgroups at higher Chol concentrations in order to cover more cholesterol in accordance with the umbrella model, thus causing the decrease in the bilayer thickness.

Concerning the mechanical properties of the DOPC/Chol bilayers, the breakthrough forces took very small values (< 1nN), similar to reported values for samples of pure DOPC in air prepared by spin-coating[99]. In aqueous solution DOPC does not form liquid-ordered phase (L_o). Despite the addition of cholesterol and the consequent change in the lipid chain order, it remains in a liquid-disordered phase (L_d). Figure 5-5B demonstrates that the mechanical properties of DOPC/Chol samples are not significantly affected by the Chol content. This suggest that similarly to hydrated samples, there is no change in the phase of dry DOPC/Chol samples in this range of Chol concentrations.

In hydrated samples of SM/Chol bilayers, on the other hand, the addition of increasing amounts of Chol causes the change them from solid (S_o) to liquid-ordered phase (L_o)[20, 110, 111]. The later phase has intermediate characteristics between solid and fluid phase. For the results that we obtained here with dry SM/Chol bilayers, they showed an increase of the surface covered by the inverted bilayers and a decrease of the total number of layers when the Chol concentration increases. This indicates an increased fluidity with increasing the content of cholesterol. Moreover, we observed a slight reduction of the bilayer thickness at Chol concentrations above 40 % mol. This is another effect consistent with a "fluidization" of the SM/Chol bilayers due to the increase of cholesterol. These results are in agreement with reported observations on *hydrated* liquid-ordered lipids, which also show a fluidization and bilayer thinning at relatively high concentrations of cholesterol[60, 112]. Remarkably, the thinning of ~ 0.5 nm that we obtained in air when increasing the Chol content is very similar to results previously reported for hydrated

samples (~ 0.9 nm reported by An *et al*[112] and ~ 0.6 nm reported by Maulik *et al.*[113].

The measured breakthrough forces of *dry* SM/Chol bilayers showed a significant variation for Chol concentrations above 40%, a result that further supports the “fluidization" effect of cholesterol on SM at high cholesterol content. An *et al.*[112] also reported the presence of thinner areas showing smaller breakthrough forces when Cholesterol is added to *hydrated* SM layers. In their experiments these areas, with a lower packing density, have a breakthrough force smaller than in pure SM samples[112].

Finally, we note that domains or differences in height were not observed in any of the binary samples considered (DOPC/Chol and SM/Chol).

In summary, the binary mixtures of dry DOPC/Chol and dry SM/Chol show remarkable similarities with their equivalent hydrated systems, thus supporting the fact that dry single bilayers prepared by spin-coating can be good models of the corresponding hydrated samples for studies under dry conditions[99].

Ternary mixtures

The mixtures of DOPC/SM/Chol examined in this study, 1:1:1, 2:1:1 and 2:2:1; are the most commonly studied in the context of lipid rafts.[58, 60, 114, 115] In the *hydrated* state, these mixtures show liquid-ordered domains (L_o) coexisting with a liquid-disordered phase (L_d) [60, 116]. Although these three lipids are present in both phases, L_o phase is enriched in SM (SM-enriched region) while L_d is rich in DOPC (DOPC-enriched region) [110]. In fact, compared with other ternary mixtures that mimic lipid rafts, e.g. POPC/SM/Chol, the proportion of SM in the liquid-disordered phase is smaller[110, 117]. In the AFM images the thicker regions are ascribed to the L_o regions, while the thinner one to the L_d region [55, 60]. The height difference and the shape of these domains depend on the Chol amount[60].

In the AFM images shown here and taken in *dry* environment, the air-stable ternary DOPC/SM/Chol mixtures showed the coexistence of two different phases (Figure 5-8) as for the hydrated case. The absence of intermediate heights indicate that the two leaflets of the bilayer are coupled, in agreement with reported observations on hydrated samples[118]. The morphology of these phases depended on the composition. It showed isolated domains for lower concentration of Chol and domain coalescence with phase inversion for the higher concentration of Chol. The difference in height between the two phases measured in the *dry* samples for the different lipid ratios is in remarkably quantitative agreement with their analogues measured in *aqueous* solution, as shown in Figure 5-10.

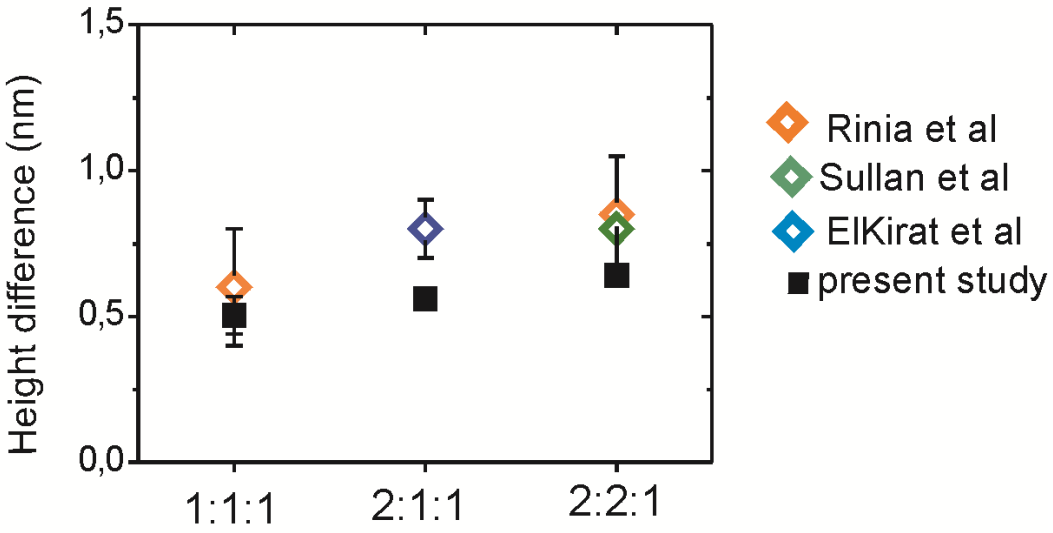

Figure 5-10(Black solid squares) Measured height difference between DOPC-enriched region and SM-enriched region in *dry* DOPC/SM/Chol bilayers for the different compositions tested. (Empty rhombs) Measured height difference between DOPC-enriched region and SM-enriched region in *hydrated* DOPC/SM/Chol bilayers reported by other authors. Rinia *et al.* refers to Ref. [118], Sullan *et al.* to Ref. [60] and Elkirat *et al.* to Ref. [115].

Previous studies demonstrated that the height difference between the two phases is Chol-dependent, decreasing with increasing Chol content[60, 118]. This smaller height difference was attributed to the fluidization of the

SM-enriched region, giving a thinner phase, and the simultaneous thickening of DOPC-enriched region. However, no direct measurement of the thickness of the DOPC-enriched region was reported, probably due to the difficulty to create holes or to find defects in this layer.

Owing to the characteristics of our samples we have access to the bottom monolayer and we can measure the total height of the two phases and not only their difference (Figure 5-8). By changing the total proportion of Chol from 20 mol%, 2:2:1 sample, to 33 mol%, 1:1:1 sample, we observed a reduction in the height of the SM-rich region of 0.4 ± 0.2nm while for the DOPC-enriched region we practically did not observe any variation (0.2 ± 0.2nm, see Figure 5-8D). Then, the effect of fluidization of the SM-enriched region is higher than the thickening of the DOPC-enriched region. Comparing these results with data obtained in the binary samples, they suggest that the concentration of Chol in the DOPC-enriched region is very low (< 20 mol %), otherwise the height would increase according to Figure 5-1E, while the concentration of Chol in the SM-enriched region has to be very high (above 40%). This interpretation suggests a preferential location of the Chol in the SM-rich regions in equimolar mixtures in accordance with previous results in *hydrated* samples [119-121].

Force spectroscopy measurements showed two different behaviors completely separated for the SM-enriched and DOPC-enriched regions (Figure 5-9B). The regions showing higher rupture forces in the three ternary mixtures that we analyzed are the SM-enriched domains. The same behavior was reported in *hydrated* samples.[60] The higher rupture force for the SM-rich domains is attributed to a major compactness between the components of these regions compared with the DOPC-enriched regions.

Interestingly the values measured for the breakthrough forces of the two phases in the case of samples with equimolar concentrations of DOPC and SM (samples 2:2:1 and 1:1:1) support the interpretation made above about the preferential separation of the Chol into the SM-enriched phase. Indeed, the rupture force for the SM-enriched phase in sample 2:2:1 is

about ~ 6 nN and decreases to ~ 4.5 nN in the 1:1:1. These values are compatible with Chol concentrations above 40 mol % in the SM-rich region (see Figure 5-5B) and show the fluidization effect of Chol in the L_o phase. For the DOPC-enriched phase, the breakthrough forces are ~-0.7 nN and ~0.2 nN compatible with a liquid-disordered phase measured in air.[99] Interestingly, *hydrated* samples of DOPC/SM/Chol 1:1:1 showed a poor proportion of SM (< 8%) in the liquid-disordered phase.[117] These observations are in agreement with our results and also with the comparison of the phase of the equimolar ternary mixtures with the binary mixtures of DOPC/Chol and SM/Chol.

In the case of non-equimolar samples (DOPC/SM/Chol 2:1:1), the SM-rich regions show rupture forces similar to the binary SM/Chol mixture with Chol content < 40% while the DOPC-enriched region presents higher rupture force than the one described for DOPC/Chol binary mixtures. Our interpretation is that for the non-equimolar sample, DOPC/SM/Chol 2:1:1, domains show different characteristics from the binary DOPC/Chol and SM/Chol samples. This supports the idea that the DOPC-enriched phase in this case is richer in SM than equimolar samples, giving higher mechanical consistency to this phase. Then the major presence of SM in the lower phase could be the responsible for the higher rupture forces in the thicker phase indicating a minor proportion of Chol.

All the similarities between dry and hydrated samples that we have discussed above are quite remarkable. This suggest that many characteristics of lipid raft are due to lateral interactions between the lipids and not very much dependent on the orientation of the lipids, because the bilayers should be inverted in dry samples.[65]

5.5 Conclusions

In this chapter we have studied the nanoscale morphological and mechanical properties of multicomponent lipid bilayers prepared by spin-coating in dry air environment. In particular, binary and ternary mixtures of lipids containing DOPC, SM and Cholesterol were examined. For the DOPC/Chol binary mixtures we have observed an initial increase of the bilayer thickness, followed by a reorganization process that leads to a decrease of the bilayer height for concentrations above 30% Chol. In this case, the mechanical response of the bilayer was not sensitive to the Chol content. For the SM/Chol bilayers we have observed a fluidization for high contents of Chol, above 40 mol%, which was reflected in the thinning of the bilayer as well as in the decrease of the force necessary to break the bilayer. No phase separation has been observed on these binary layers.

For ternary mixtures different ratios of DOPC/SM/Chol have been used, 1:1:1, 2:1:1 and 2:2:1. In all the cases two phases were observed in the single bilayers with different mechanical and structural properties. The properties of the domains resemble those of the lipid rafts observed in hydrated ternary lipid samples, thus supporting the idea that these systems could be used as lipid raft models in dry environment. These results then open the possibility to probe chemical and physical properties of *dry* lipid rafts models using a range of nanoscale characterization techniques that so far have not been applied due to the difficulties in operating them in liquid environment.

Chapter 6. Conclusions and perspectives

6.1 Conclusions

The objective of the present thesis was to develop a procedure to prepare model lipid bilayers stable in air environment and showing physico-chemical properties as close as possible to their equivalent in liquid media.

We have demonstrated that sample preparation methods based on the spin-coating technique present the desired properties, and offered fundamental advantages on what concerns reliability and reproducibility over alternative methods suggested in the current literatures, such as the freeze-drying method.

For the first experiments DOPC was selected as model to adapt the existing protocols for hydrated spin-coated samples to the new protocol for dried samples. In the structural study it was demonstrated that the dewetting pattern described by previous authors not only depends on the proximity of the layer to the substrate because also depends on the lipid concentration on the coating solution. Apart from that the presence of a continuous monolayer in contact with the mica substrate was demonstrated contrary to previous results with other lipids. The force spectroscopy measurements represented the first study on single bilayers in air and, surprisingly, demonstrated that the lipid layers in air presented similar mechanical properties than hydrated samples.

Secondly, the preparation protocol was adapted for phospholipids with different characteristics, the saturated phosphocholines. Contrary to unsaturated lipids, which present in general a high fluidity at ambient temperature, this is not always true for saturated lipids. For phosphocholines with short hydrocarbonated chains the melting temperature is low and then they are fluid, but for long hydrocarbonated chains the melting temperature is high and they can present a non-fluid

behavior. For this reason, different saturated lipids with different chain lengths were studied (DLPC, DMPC, DPPC and DSPC). The results with these lipids demonstrate that the conventional protocol of spin-coating induces the interdigitation of certain areas of the samples for DPPC and DSPC. The effect of the presence of alcohols and lateral tension were studied, being the rotation speed determined as causative of this phenomenon.

Finally, we studied the more important case of multicomponent samples. In this study, ternary samples made of DOPC, Sphyngomelin and Cholesterol, relevant for lipid raft models, were selected. The corresponding binary samples with Cholesterol were also studied to determine separately the effect of Cholesterol in each of the components (DOPC and SM). Results unambiguously showed that air stable multicomponent lipid bilayers can be prepared by the spin-coating technique with structural and mechanical properties remarkably resembling those of the equivalent systems in liquid media, specially on what concerns phase segregation phenomena. In particular, and more importantly, we showed that the ternary mixtures of DOPC/SM/Chol under dry conditions showed also the presence of lipid rafts.

In summary, the present thesis has showed that it is possible to prepare lipid bilayer model systems morphologically stable in dry air conditions that present similar topography and mechanical properties than hydrated samples. Therefore, it opens the possibility to characterize these systems with nanoscale techniques that until now have not been applied to them, thus offering the possibility to clarify physicochemical properties of lipid bilayer model systems that still today remain unexplored, in spite of the vast literature of lipid bilayer model systems.

6.2 Perspectives

A research work is never complete, especially thesis works. This thesis is a demonstration of a hypothesis of work, namely it is possible to prepare lipid bilayers stable in air and to study the influence of different components locally.

Now this kind of samples are ready to be analyzed with nanoscale techniques that have never been applied to this type of systems and extract important physical parameters of them, such as electric or dielectric properties, with nanometric lateral scale. An example of what could be obtained starting from this work of thesis is shown below in Figure 6-1, where the topography and dielectric response of a nanometric DOPC bilayer patch prepared following the methods presented in the present thesis are reported. From these images the dielectric constant of the lipid bilayer could be determined with nanoscale spatial resolution, something that has never been reported for any lipid bilayer system.

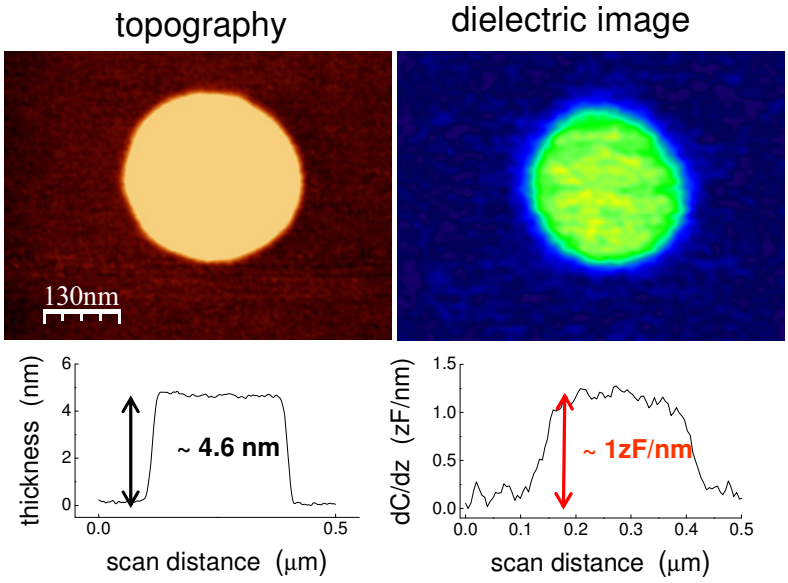

Figure 6-1 (a) Topography and (b) dielectric image of a dry nanometric DOPC bilayer patch prepared by the spin-coating technique following the methods developed in this work of thesis. Image courtesy of L. Fumagalli.

The next steps to improve the samples would be to incorporate proteins to reproduce more truly the plasma membrane structure and also to incorporate fluorophores to make this system compatible with optical techniques.

Apart from that, the dried bilayers are an interesting system itself to their study. The effect of low humidity in single bilayers is something that has not been studied until now due to the difficulty to dry samples with good results.

6.3 Summary in Catalan/ Resum en Català

La nanotecnologia és un dels principals exemples d'interdisciplinarietat en el camp de la ciència, es basa en l'estudi dels fenòmens a la nanoescala en tots els àmbits científics com són la física, la biologia i la química. De fet, un gran esforç per combinar aquestes disciplines és necessari. No només es necessari desenvolupar noves tècniques físiques que permetin estudiar certes propietats fisicoquímiques o estudiar noves estructures cel·lulars, sinó que és necessari també fer un esforç per adaptar i fer convergir la recerca de tots els àmbits en un interès comú. Per aquest motiu a vegades és necessari adaptar les tècniques més "físiques" a les mostres biològiques o adaptar les mostres biològiques a les tècniques.

El meu treball d'aquests últims quatre anys s'ha basat en el desenvolupament de preparacions de mostres que permetin apropar l'estudi de la membrana cel·lular a un ampli ventall de tècniques. En particular, l'objectiu va ser desenvolupar una tècnica per crear model de membrana estables en aire amb estructures, composició i propietats mecàniques similars a les observades en solucions aquoses.

Aquesta tesi està organitzada en 8 capítols. En el primer es fa una breu introducció de la membrana cel·lular, els models de membrana, les fases lipídiques i es segueix amb un llistat de les tècniques a la nanoescala i les tècniques que existeixen fins ara per a la deshidratació de membranes. Seguidament hi ha un capítol dedicat a les tècniques experimentals emprades que són el *spin-coating* (recobriment per rotació) i la microscòpia de forces atòmiques (AFM segons les seves sigles en anglès). Després d'aquesta introducció la secció dedicada a resultats comença. Aquí els resultats estan separats en capítols en funció dels lípids utilitzats per preparar les mostres: lípids insaturats (tercer capítol), lípids saturats (quart capítol) i barreges multicomponent (cinquè capítol). Finalment en el sisè capítol s'extreuen les conclusions del treball i es troba el resum en català. En el setè i vuitè capítols es troben l'apèndix i les referències utilitzades al llarg d'aquest treball.

Introducció i objectius

Les membranes cel·lulars són sistemes fluids 2D heterogenis que presenten estructures a la nanoescala de gran interès degut a la seva importància en les funcions de membrana. A causa de la inherent complexitat de les membranes naturals és essencial estudiar models de membrana per poder obtenir informació.

Les petites dimensions laterals i les escasses variacions en alçada de les estructures lipídiques requereixen l'ús de tècniques de caracterització a la nanoescala. No obstant, el requeriment d'un medi líquid per preservar la integritat de la membrana limita el nombre de tècniques que poden ser usades en l'estudi de les propietats de les membranes i els seus dominis. A la pràctica l'AFM és la tècnica més usada ja que permet treballar en aquest medi. Altres exemples importants com la Espectrometria de masses d'ions secundaris (NanoSIMS segons les seves sigles en anglès) que identifica la composició d'un material a la nanoescala; tècniques per a la caracterització elèctrica com el microscopi de forces atòmiques conductiu (C-AFM segons les seves sigles en anglès) i el microscopi d'escombratge d'efecte túnel (STM segons les seves sigles en anglès) que mesuren la conductivitat elèctrica, el microscopi d'impedància a la nanoescala (NIM segons les seves sigles en anglès) i el microscopi de forces electrostàtiques (EFM segons les seves sigles en anglès) que mesuren les propietats dielèctriques a la nanoescala. Així, varies propietats físiques dels lípids romanen desconegudes degut a la dificultat que tenen aquestes tècniques per operar en líquid.

Per solventar aquesta limitació, seria adequat preparar models de lípids que es mantinguessin estables en aire amb propietats estructural y físiques el més properes possible a les observades en medi aquós.

Amb aquest objectiu s'ha de tenir en compte les tècniques existents per deshidratar o assecar les mostres lipídiques. El secat directe no és vàlid ja que indueix irreversibles inestabilitats a la mostra i produeix la modificació de la seva estructura. Alguns autors han proposat afegir molècules com a crioprotectors o lioprotectors , però aquest tipus

d'agents tenen tendència a precipitar durant l'eliminació de l'aigua. La tècnica del *freeze-drying* (secat ultracongelat) ha demostrat que se poden obtenir bons resultats per bicapes lipídiques però requereix un acurat entrenament en la preparació de mostres.

Per aquests motius és necessari desenvolupar tècniques de secat que permetin l'estabilitat de la mostra sense generar gaires inconvenients durant la preparació de la mostra i les mesures.

El principal objectiu d'aquest treball de tesi és preparar mostres de models de membranes lipídiques amb aquests requeriments (tant monocomponents com multicomponents) i comprovar que les seves propietats són similars a les que es troben en medi líquid.

Per aquest fi el AFM ha sigut escollit com la tècnica de caracterització adequada per demostrar que les propietats són similars. El principal avantatge d'aquesta tècnica és que pot operar tant en aire com en líquid i certes aplicacions com la espectroscòpia de forces pot fer-se també en els dos medis. D'aquesta manera, tant les mesures topogràfiques com les mecàniques dels dos medis poden ser comparades.

En resum, els objectius principals són:

1- Preparar mostres de bicapes lipídiques mono- i multicomponents estables en aire.

2- Estudiar les característiques estructurals de les capes ultrafines formades en aire.

3- Estudiar les propietats mecàniques de les bicapes en aire en funció de la seva composició

4- Establir les semblances i diferències en les propietats estructurals i mecàniques entre les membranes lipídiques en aire i les hidratades

Tècniques experimentals utilitzades

Durant el temps d'aquesta tesi doctoral es varen considerar diferents protocols per a la creació de capes lipídiques. De fet, els primers intents varen consistir en preparar capes hidratades, mitjançant la tècnica de fusió de vesícules, i tractar de secar-les sense deteriorar la seva estructura. Però cap de les tècniques utilitzades donava bons resultats pel que es va optar per preparar les mostres per la tècnica de *spin-coating*.

Aquesta tècnica consisteix en el depòsit d'una solució sobre un substrat que es rotat a una alta velocitat. Com a conseqüència de les forces centrifugues el fluid recobreix el substrat i forma una capa molt fina de material.

En el cas dels lípids aquesta tècnica va començar a utilitzar-se per a estudis de reflectivitat de raigs X. Temps després va ser adaptada per al seu ús amb microscòpia de forces atòmiques i microscòpia confocal. En aquest cas el que feien era hidratar la mostra després del pas de creació de multicapes per mitjà del *spin-coating*.

En el nostre cas hem modificat el protocol eliminant el pas d'hidratació de la mostra i també reduint considerablement la concentració de lípid utilitzada en la solució de recobriment.

D'aquesta forma el que obtenim són capes ultrafines de lípids en aire.

En aquest estudi , en general, s'han utilitzat fosfatidilcolines per a la formació de les bicapes ja que són un dels lípids majoritaris en les membranes de les cèl·lules eucariotes. També s'han utilitzat esfingomielina i colesterol. Com a solvent per a dissoldre'ls s'ha utilitzat una barreja de hexà i metanol (98:2, v/v) ja que dissol bé els lípids, mulla la superfície de la mica correctament i és volàtil. La mica ha estat el substrat escollit per preparar les mostres gràcies a la seva capacitat de produir capes atòmicament planes per simple exfoliació de la superfície i la seva facilitat d'ús.

Els lípids eren dissolts en el solvent fins a una concentració <1mM, aquesta solució d'estoc era dipositada a sobre dels substrat de mica que era posteriorment rotat a una velocitat de 3000rpm durant 1min. Després d'això la mostra era sotmesa al buit per assegurar la correcta evaporació dels solvents.

Com tècnica per caracteritzar les mostres es va escollir la microscòpia de forces atòmiques (AFM) degut a la seva capacitat per cartografiar la superfície de la mostra tant lateralment com verticalment amb resolució nanomètrica.

El seu funcionament es basa en la interacció entre una punta que rastreja la mostra. La força d'interacció entre la mostra i la punta indueix la flexió de la palanca de la punta que pot ser mesurada gràcies al ús d'un laser i un fotodíode. El làser està enfocat al final de la palanca i la senyal és reflectit al fotodíode. La posició del punt en el fotodíode depèn de la deflexió de la sonda. Durant la formació de la imatge, el sistema de retroalimentació canvia l'elongació del escàner per mantenir constant la força entre la punta i la mostra. La imatge final és la reconstrucció del moviment adquirit en la direcció z en funció de la seva posició en x/y.

Per aquesta tesi s'ha utilitzat el sistema dinàmic per fer imatges topogràfiques. En aquest mode la punta es oscil·lada a la seva freqüència de ressonància i es manté l'amplitud d'oscil·lació constant (quan la punta interacciona amb la mostra la amplitud disminueix). El sistema de retroalimentació i el controlador ajusten l'elongació del escàner per mantenir l'amplitud d'oscil·lació constant durant l'escaneig de la mostra, basant-se en això la imatge topogràfica es reconstruïda.

Apart de la topografia també s'ha estudiat l'espectroscòpia de forces per mitjà de les corbes de forces. En el cas de les bicapes lipídiques això permet estudiar les propietats mecàniques de la mostra localment. El paràmetre més important és el que en anglès s'anomena *Breakthrough force*, que és la força màxima que la capa és capaç d'aguantar abans de la seva ruptura.

El fet de que el AFM pugui utilitzar-se tant en aire com en líquid el fan una tècnica idònia per comparar l'estat de les capes lipídiques en aire, ja que així es pot comparar fàcilment amb les mesures existents en líquid.

Mesures sobre lípids insaturats

El primer exemple estudiat és el de bicapes monocomponents fetes de dioleoilfosfatidilcolina (DOPC) per mitjà de la tècnica de *spin-coating*. El AFM s'ha emprat per fer l'estudi de les propietats estructurals i mecàniques a la nanoescala en ambient sec (humitat relativa ~ 0%). S'ha vist que per concentracions de lípid de 0.1-1mM les estructures de DOPC preparades per spin-coating consten d'una monocapa homogènia del voltant de 1.3nm, cobrint tota la superfície dels substrat, a sobre de la qual es troben bicapes o multicapes amb forma de micro- i nano- illes o estructures anellades.

El gruix d'aquestes estructures és de 4.6nm (o múltiples d'aquesta alçada), encara que les dimensions laterals estan tant en el rang dels micròmetres com de les desenes de nanòmetres en funció de la concentració de lípid utilitzada.

En quant als experiments d'espectroscòpia de forces, la força requerida per trencar la bicapa (la *breakthrough force*) s'ha vist que és de ~0.24nN. No s'ha vist cap tipus de dependència de la força de ruptura amb les dimensions laterals de les estructures. Cal remarcar que tant la alçada de la bicapa com la seva força de ruptura són molt similar a les reportades a la literatura per bicapes de DOPC en aigua pura.

S'ha demostrat que utilitzant la tècnica de *spin-coating* per dipositar els lípids es possible obtenir capes lipídiques morfològicament estable en aire i que les seves propietats mecàniques coincideixen amb una fase fluida dels lípids.

Mesures sobre lípids saturats

La adequació de la tècnica de *spin-coating* per crear mostres de lípids insaturats, com ara DOPC, estables aire es va demostrar en el capítol anterior.

En aquest capítol, la preparació d'altres mostres d'un sol component es considera, específicament la fabricació de mostres d'un sol component de lípids amb cadenes saturades. Per aquest objectiu es van considerar diferents fosfolípids amb diferents longituds en les seves cadenes (de 12 a 18 àtoms de carboni). Hem demostrat que el gruix de les bicapes augmenta proporcionalment amb el nombre de carbonis a les cadenes dels lípids utilitzats, d'acord amb el que s'observa per les mostres hidratades.

Les mostres de DLPC i DMPC presenten una estructura plana amb un gruix que coincideix amb els valors reportats en la literatura per al gruix mesurat de la bicapa en líquid. No obstant això, per DPPC i DSPC el comportament va ser diferent, mostraven àrees interdigitades a més de les àrees convencionals amb el gruix de la bicapa esperat. Es van estudiar la influència dels alcohols utilitzats en la solució solvent i la tensió lateral per verificar l'origen d'aquest efecte. Finalment, la velocitat de rotació es va demostrar que era la responsable de la interdigitació. Mitjançant el canvi de la velocitat de rotació i l'addició d'una etapa anterior a la preparació de la mostra de la zona interdigitada es pot reduir notablement.

Aquest estudi mostra que, a més del cas dels lípids insaturats, estudiats en el capítol anterior, també és possible preparar mostres de bicapes lipídiques estables en ambient sec amb lípids saturats. Això obre la possibilitat de crear qualsevol mostra lípids multicomponent combinant ambdós tipus de lípids.

Mesures sobre mostres multicomponents

En aquest capítol s'investiga les propietats estructurals I mecàniques de les mostres multicomponents de Dioleoylfosfatidilcolina (DOPC), esfingomielina (SM) i colesterol (Chol) en aire. Aquesta mostra ternària s'ha escollit a causa de la seva rellevància en l'estudi dels models de lipid raft.

Com se sap el models de lipid raft estan basats en barreges ternàries compostes d'un lípid de baixa temperatura de transició, esfingomielina (o un fosfolípid amb alta temperatura de transició) i colesterol. Estudis previs en líquid han demostrat que aquestes barreges presenten dominis de fase líquida ordenada d'uns ~10-200 (lipid rafts), enriquits en esfingomielina i colesterol, i envoltats per una matriu en fase líquida desordenada enriquida en fosfolípids.

En aquest estudi s'han analitzat tres barreges diferents de barreges ternàries (DOPC/SM/ Chol, 1:1:1, 2:1:1, 2:2:1) i barreges binàries de DOPC i SM amb colesterol a diferents proporcions.

Per la mescla de DOPC/Chol es va observar un increment inicial de l'alçada de les bicapes seguit d'un procés de reorganització que produeix un descens de l'alçada de la capa per concentracions per sobre d'un 30% de colesterol. La seva resposta mecànica es va veure que no va ser sensible a la proporció de Chol a la mostra.

Per les mostres de SM/Chol es va veure un procés de fluïdització per concentracions per sobre del 40%, que es va veure en un descens de l'alçada de la bicapa i ,a la vegada, en un descens de la força necessària per trencar la capa.

En cap de les barreges binàries es va veure separació de fases.

En el cas de les mostres ternàries es varen veure dues fases en totes les barreges utilitzades i a més, aquestes varen presentar propietats mecàniques diferenciades.

Les propietats dels dominis observat varen tenir propietats molt similars a les observades en líquid, corroborant la idea que aquests sistemes poden ser usats com a models de lipid raft en aire.

Aquests resultats obren la possibilitat d'estudiar propietats fisicoquímiques dels lipid rafts en aire mitjançant tècniques a la nanoescala que necessitin operar en aire.

Conclusions

En resum, aquesta tesi demostra que es possible preparar models membrana morfològicament estables en aire i presenten propietats mecàniques i estructurals similars a les observades en líquid.

Per tant obre la possibilitat a la utilització de tècniques de caracterització que fins ara no podien ser aplicades. Això permetrà estudiar propietats físico-químiques de les membranes cel·lulars que romanen desconegudes fins ara.

Chapter 7. Appendix

7.1 Acronyms

AFM: Atomic Force Microscopy

BLM: Black lipid Membranes

BreakdifF: Breakthrough force difference

BreakF: Breakthrough force

C-AFM: Conductive- AFM

Chol: Cholesterol

DLPC: 1,2-dilauroyl-*sn*-glycero-3-phosphocholine

DMPC: 1,2-dimyristoyl-*sn*-glycero-3-phosphocholine

DOPC: 1,2-dioleoyl-*sn*-glycero-3-phosphocholine

DPPC: 1,2-dipalmitoyl-*sn*-glycero-3-phosphocholine

DSPC: 1,2-distearoyl-*sn*-glycero-3-phosphocholine

EFM: Electrostatic Force Microscopy

Fz: force vs distance curve

GUV: Giant Unilamellar Vesicle

JumpF: jump-to-contact force

KPFM: Kelvin Probe Force Microscopy

LB: Langmuir-Blodgett

LS: Langmuir-Schaefer

LUV: Large Unilamellar Vesicle

MLV: Multilamellar Large Vesicle

NanoSIMS: Nanoscale Secondary Ion Mass Spectrometer

NIM: Nanoscale Impedance Microscopy

NSOM: Near-field Scanning Optical Microscopy

POPC: 1-palmitoyl-2-oleoyl-sn-glycero-3-phosphocholine

SLB: Supported lipid Bilayer

SM: Sphingomyelin

SPM: Scanning Probe Microscopy

STM: Scanning Tunnelling Microscopy

SUV: Small Unilamellar Vesicles

Tm: Transition Temperature

7.2 List of publications

- *Ultrathin Spin-Coated Dioleoylphosphatidylcholine Lipid Layers in Dry Conditions: A Combined Atomic Force Microscopy and Nanomechanical Study, Langmuir* 27, 13165-13172 (2011) by **Aurora Dols-Perez**, Laura Fumagalli, Adam Cohen Simonsen, and Gabriel Gomila.

- *Nanoscale properties of multicomponent lipid bilayers of DOPC, Sphingomyelin and Cholesterol in dry air environment* by **Aurora Dols-Perez**, Laura Fumagalli and Gabriel Gomila, Submitted.

- *Visualization of ultrathin mica flakes on gold substrates* by **Aurora Dols-Pérez**, Xavier Sisquella, Laura Fumagalli, and Gabriel Gomila. In preparation.

- *Effects of spinner parameters on lipid bilayers of saturated phospholipids* by **Aurora Dols-Perez**, Laura Fumagalli and Gabriel Gomila. In preparation

- *Nanoscale measurement of the dielectric constant of supported lipid bilayers in electrolyte solutions with electrostatic force microscopy* by Georg Gramse, **Aurora Dols-Perez**, Martin A. Edwards, Laura Fumagalli, and Gabriel Gomila. In preparation.

- *Dielectric properties of supported lipid layers at the nanoscale* by L. Fumagalli, **Aurora Dols-Perez** and Gabriel Gomila. In preparation.

7.3 Congress participations

- AFM BioMed Conference 2011.Paris 2011 *Nanomechanical properties of DOPC nano-patches in dry environment* **A. Dols-Perez**, L.Fumagalli, A.C. Simonsen, and G. Gomila. Poster.

- Nanomeasure 2010. Krakow 2010 Quantifying the low frequency dielectric constant at the nanoscale.L. Fumagalli, G. Gramse, D. Esteban, **A. Dols-Perez,** M. Edwards and G. Gomila. Oral communication

- IRUN symposium on Nanotechnology Barcelona 2010 *Dielectric properties of supported lipid layers at the nanoscale* **A. Dols-Perez**, L. Fumagalli and G. Gomila. Oral communication

- Spanish portuguese biophysics Zaragoza 2010 *Dielectric constant of planar supported biomembranes measured at the nanoscale* Laura Fumagalli, **Aurora Dols**, Georg Gramse, Daniel Esteban, Martin Edwards Gabriel Gomila. Poster.

- Seeing at the Nanoscale 2010 Basel 2010 *Quantifying the dielectric constant at the nanoscale using electrostatic force microscopy* Laura Fumagalli, Georg Gramse, **Aurora Dols**, Daniel E. Ferrer, Martin A. Edwards and Gabriel Gomila. Oral communication

- Fuerzas y túnel Tarragona 2010: *Quantifying the low frequency dielectric constant at the nanoscale* L. Fumagalli, G. Gramse, D. Esteban, **A. Dols**, M. Edwards and G. Gomila. Oral communication

- 3rd IBEC Symposium Barcelona 2010 *Dielectric properties of supported biomembranes at the nanoscale.* **A. Dols-Perez**,, L.Fumagalli & G.Gomila. Poster & Flash Presentation

- AFM BioMed Conference 2010 Red Island (Croatia) 2010 *Quantifying the dielectric constant of biomembranes and lipids bilayers with atomic force microscopy on insulating substrates* L. Fumagalli, G. Gramse, **A. Dols**, D. E. Ferrer, M. A. Edwards, G. Gomila. Oral communication

- 1st Winter Workshop on Functional Scanning Probe Microscopy Módena (Italia) 2010 *Dielectric constant of planar supported biomembranes at the nanoscale* L. Fumagalli, G. Gramse, **A. Dols-Pérez**, , G. Gomila. Oral communication

- European Biophysics Congress Genoa 2009 Genova 2009. *Quantitative Nanoscale Dielectric Microscopy of Supported Biomembrane* **A. Dols-Perez**, L.Fumagalli & G.Gomila. Poster.

- 2nd IBEC Symposium Barcelona 2009 *Nanoscale Dielectric Microscopy applied to biological samples: sample preparation and numerical simulations* **A. Dols-Perez**, D. Esteban-Ferrer, L.Fumagalli & G.Gomila. Poster.

- 2nd IBEC Symposium Barcelona 2009 *Dielectric properties of biomembranes measured at the nanoscale* L. Fumagalli, G. Gramse, **A. Dols-Perez**, D. Esteban, J. Toset and G. Gomila. Oral communication

- 7th International Symposium on Scanning Probe Microscopy in Life Science Berlin 2008. *Quantitative measurement of dielectric-constant and thickness of supported biomembranes by nanoscale capacitance microscopy.* Dols-Perez A. Poster.

- XXIII Reunión bienal Sociedad Microscopía de España Bilbao 2007 *Aplicación de la microscopía electrónica en la evaluación ecotoxicológica de mamíferos silvestres expuestos a contaminación atmosférica.* Sánchez-Chardi A, Bohils F, Cardoso F, Dols-Pérez A, Roldán M, Rossinyol E, Castell O, Baró, MD. Oral communication

7.4 Acknowledgments

Ara que la tesi està acabada m'agradaria donar les gràcies a molta gent que directa o indirectament són responsables de que hagi fet aquest treball (si em deixo algú... ho sento...sóc així).

Gràcies a la meva família per ser qui són, escoltar-me i saber sempre el moment adequat per pegar-me una estirada d'orelles i fer-me recordar com sóc.

Gràcies al meu grup per tota la feina, la ajuda, les rialles i les vivències junts, i en especial al Gabriel Gomila per haver-me confiat aquest treball i haver-me ajudat a realitzar-ho.

Gràcies al Pere Company per la seva paciència amb totes les preguntes dintre i fora de temari i per fer que em volgués dedicar a això.

Gràcies als meus amics per estar-hi en els mals moments i fer que acabin sent bons moments.

I gràcies a la gent de l'Ibec , la Marina i la Yolanda de la Plataforma de Nano, las "jefas" del laboratori Isa, Laura i Cristina, la gent d'administració i secretaria,… per fer el que els experiments i el dia a dia al laboratori fos una mica més fàcil i divertit.

Finalment, gràcies al xiquet per aguantar-me

Chapter 8. References

8.1 References

(1)Edidin, M. Lipids on the frontier: a century of cell-membrane bilayers. *Nature reviews. Molecular cell biology* **2003,** 4, 414-8.
(2)Singer, S. J.; Nicolson, G. L. The Fluid Mosaic Model of the Structure of Cell Membranes. *Science* **1972,** 175, (4023), 720-731.
(3)Gong, K. Effects of pH on the stability and compressibility of DPPC/cholesterol monolayers at the air–water interface. *Colloids and Surfaces A: Physicochemical and Engineering Aspects* **2002,** 207, 113-125.
(4)Bhattacharya, S.; Haldar, S. Interactions between cholesterol and lipids in bilayer membranes. Role of lipid headgroup and hydrocarbon chain-backbone linkage. *Biochim. Biophys. Acta* **2000,** 1467, 39-53.
(5)Cooper, G., *The Cell: A Molecular Approach.* . 2nd edition. ed.; Sinauer Associates: Sunderland (MA), 2000.
(6)Marguet, D.; Lenne, P.-F.; Rigneault, H.; He, H.-T. Dynamics in the plasma membrane: how to combine fluidity and order. *The EMBO journal* **2006,** 25, 3446-57.
(7)Edidin, M. Lipid microdomains in cell surface membranes. *Current opinion in structural biology* **1997,** 7, 528-32.
(8)Simons, K.; Ikonen, E. Functional rafts in cell membranes. *Nature* **1997,** 387, 569-72.
(9)Simons, K.; Toomre, D. Lipid rafts and signal transduction. *Nature reviews. Molecular cell biology* **2000,** 1, 31-9.
(10)Lindholm-sethson, B.; Lindholm-sethson, B. SUPPORTED LIPID MEMBRANES FOR RECONSTITUTION OF MEMBRANE PROTEINS. *Physics*, 131-165.
(11)Chan, Y.-H. M.; Boxer, S. G. Model membrane systems and their applications. *Current Opinion in Chemical Biology* **2007,** 11, (6), 581-587.
(12)Seantier, B.; Giocondi, M.; Grimellec, C.; Milhiet, P. Probing supported model and native membranes using AFM. *Curr Opin Colloid In* **2008,** 13, 326-337.
(13)Mueller, P.; Rudin, D. O.; Ti Tien, H.; Wescott, W. C. Reconstitution of Cell Membrane Structure in vitro and its Transformation into an Excitable System. *Nature* **1962,** 194, (4832), 979-980.

(14)Tamm, L. K.; McConnell, H. M. Supported phospholipid bilayers. *Biophys. J.* **1985,** 47, (1), 105-113.
(15)Kim, Y.; Rahman, M.; Zhang, Z.; Misawa, N.; Tero, R.; Urisu, T. Supported lipid bilayer formation by the giant vesicle fusion induced by vesicle–surface electrostatic attractive interaction. *Chemical Physics Letters* **2006,** 420, 569-573.
(16)Richter, R. P.; Bérat, R.; Brisson, A. R. Formation of solid-supported lipid bilayers: an integrated view. *Langmuir* **2006,** 22, 3497-505.
(17)Girard-Egrot, A. P.; Godoy, S.; Blum, L. J. Enzyme association with lipidic Langmuir-Blodgett films: interests and applications in nanobioscience. *Advances in colloid and interface science* **2005,** 116, 205-25.
(18)Picas, L.; Suárez-Germà, C.; Teresa Montero, M.; Hernández-Borrell, J. Force spectroscopy study of Langmuir-Blodgett asymmetric bilayers of phosphatidylethanolamine and phosphatidylglycerol. *J. Phys. Chem. B* **2010,** 114, 3543-9.
(19)Heimburg, T., Membrane Structure. In *Thermal Biophysics of Membranes*, Wiley-VCH Verlag GmbH & Co. KGaA: 2007; pp 15-27.
(20)Marsh, D. Liquid-ordered phases induced by cholesterol: A compendium of binary phase diagrams. *Biochim.Biophys.Acta.Biomem.* **2010,** 1798, (3), 688-699.
(21)Subczynski, W. K.; Wisniewska, A.; Hyde, J. S.; Kusumi, A. Three-dimensional dynamic structure of the liquid-ordered domain in lipid membranes as examined by pulse-EPR oxygen probing. *Biophys. J.* **2007,** 92, 1573-84.
(22)Brown, D. a.; London, E. Structure and function of sphingolipid- and cholesterol-rich membrane rafts. *The Journal of biological chemistry* **2000,** 275, 17221-4.
(23)Adachi, T.; Takahashi, H.; Ohki, K.; Hatta, I. Interdigitated structure of phospholipid-alcohol systems studied by x-ray diffraction. *Biophys. J.* **1995,** 68, 1850-5.
(24)Mou, J.; Yang, J.; Huang, C.; Shao, Z. Alcohol induces interdigitated domains in unilamellar phosphatidylcholine bilayers. *Biochemistry* **1994,** 33, 9981-5.
(25)de Vries, A. H.; Yefimov, S.; Mark, A. E.; Marrink, S. J. Molecular structure of the lecithin ripple phase. *Proceedings of the National Academy of Sciences of the United States of America* **2005,** 102, (15), 5392-5396.

(26)Domènech, O.; Morros, A.; Cabañas, M. E.; Teresa Montero, M.; Hernández-Borrell, J. Supported planar bilayers from hexagonal phases. *Biochim. Biophys. Acta* **2007,** 1768, 100-6.
(27)Alessandrini, A.; Muscatello, U. AFM and FTIR spectroscopy investigation of the inverted hexagonal phase of cardiolipin. *J. Phys. Chem. B* **2009,** 113, 3437-44.
(28)Kent, B.; Garvey, C. J.; Cookson, D.; Bryant, G. The inverse hexagonal - inverse ribbon - lamellar gel phase transition sequence in low hydration DOPC:DOPE phospholipid mixtures. *Chemistry and physics of lipids* **2009,** 157, 56-60.
(29)Armstrong, C. L.; Kaye, M. D.; Zamponi, M.; Mamontov, E.; Tyagi, M.; Jenkins, T.; Rheinstadter, M. C. Diffusion in single supported lipid bilayers studied by quasi-elastic neutron scattering. *Soft Matter* **2010,** 6, (23), 5864-5867.
(30)Koynova, R.; Caffrey, M. An index of lipid phase diagrams. *Chemistry and physics of lipids* **2002,** 115, 107-219.
(31)Veatch, S. L.; Keller, S. L. Seeing spots: Complex phase behavior in simple membranes. *Biochimica et Biophysica Acta (BBA) - Molecular Cell Research* **2005,** 1746, (3), 172-185.
(32)Johnston, L. J. Nanoscale imaging of domains in supported lipid membranes. *Langmuir* **2007,** 23, 5886-95.
(33)Shaw, J. E.; Epand, R. F.; Epand, R. M.; Li, Z.; Bittman, R.; Yip, C. M. Correlated fluorescence-atomic force microscopy of membrane domains: structure of fluorescence probes determines lipid localization. *Biophys. J.* **2006,** 90, 2170-8.
(34)Binnig, G.; Rohrer, H.; Gerber, C.; Weibel, E. Surface Studies by Scanning Tunneling Microscopy. *Phys. Rev. Lett.* **1982,** 49, (1), 57.
(35)Haggerty, L.; Lenhoff, A. M. STM and AFM in biotechnology. *Biotechnology Progress* **1993,** 9, (1), 1-11.
(36)Heim, M.; Cevc, G.; Guckenberger, R.; Knapp, H. F.; Wiegräbe, W. Lateral electrical conductivity of mica-supported lipid bilayer membranes measured by scanning tunneling microscopy. *Biophys. J.* **1995,** 69, 489-97.
(37)Casuso, I.; Fumagalli, L.; Samitier, J.; Padrós, E.; Reggiani, L.; Akimov, V.; Gomila, G. Electron transport through supported biomembranes at the nanoscale by conductive atomic force microscopy. *Nanotechnology* **2007,** 18, 465503.
(38)Hane, F.; Moores, B.; Amrein, M.; Leonenko, Z. Effect of SP-C on surface potential distribution in pulmonary surfactant: Atomic force

microscopy and Kelvin probe force microscopy study. *Ultramicroscopy* **2009,** 109, (8), 968-973.
(39)Fumagalli, L.; Ferrari, G.; Sampietro, M.; Gomila, G. Quantitative nanoscale dielectric microscopy of single-layer supported biomembranes. *Nano letters* **2009,** 9, 1604-8.
(40)Gramse, G.; Casuso, I.; Toset, J.; Fumagalli, L.; Gomila, G. Quantitative dielectric constant measurement of thin films by DC electrostatic force microscopy. *Nanotechnology* **2009,** 20, 395702.
(41)Galli Marxer, C.; Kraft, M. L.; Weber, P. K.; Hutcheon, I. D.; Boxer, S. G. Supported membrane composition analysis by secondary ion mass spectrometry with high lateral resolution. *Biophys. J.* **2005,** 88, 2965-75.
(42)Kraft, M.; Fishel, S.; Marxer, C.; Weber, P.; Hutcheon, I.; Boxer, S. Quantitative analysis of supported membrane composition using the NanoSIMS. *Appl. Surf. Sci.* **2006,** 252, 6950-6956.
(43)Kraft, M. L.; Weber, P. K.; Longo, M. L.; Hutcheon, I. D.; Boxer, S. G. Phase separation of lipid membranes analyzed with high-resolution secondary ion mass spectrometry. *Science* **2006,** 313, 1948-51.
(44)Crowe, J. H.; Crowe, L. M.; Carpenter, J. F.; Aurell Wistrom, C. Stabilization of dry phospholipid bilayers and proteins by sugars. *The Biochemical journal* **1987,** 242, 1-10.
(45)Holden, M. a.; Jung, S.-Y.; Yang, T.; Castellana, E. T.; Cremer, P. S. Creating fluid and air-stable solid supported lipid bilayers. *J. Am. Chem. Soc.* **2004,** 126, 6512-3.
(46)Crowe, J. H.; Crowe, L. M. Induction of Anhydrobiosis : Membrane Changes during Drying. *Cryobiology* **1982,** 19, 317-328.
(47)Chiantia, S.; Kahya, N.; Schwille, P. Dehydration damage of domain-exhibiting supported bilayers: an AFM study on the protective effects of disaccharides and other stabilizing substances. *Langmuir* **2005,** 21, 6317-23.
(48)Bennun, S. V.; Faller, R.; Longo, M. L. Drying and rehydration of DLPC/DSPC symmetric and asymmetric supported lipid bilayers: a combined AFM and fluorescence microscopy study. *Langmuir* **2008,** 24, 10371-81.
(49)Ricker, J. V.; Tsvetkova, N. M.; Wolkers, W. F.; Leidy, C.; Tablin, F.; Longo, M.; Crowe, J. H. Trehalose maintains phase separation in an air-dried binary lipid mixture. *Biophys. J.* **2003,** 84, 3045-51.
(50)Albertorio, F.; Chapa, V. A.; Chen, X.; Diaz, A. J.; Cremer, P. S. The alfa , alfa- (1f1) Linkage of Trehalose Is Key to Anhydrobiotic Preservation. *Langmuir* **2007**, 10567-10574.

(51)Wetzer, B.; Pum, D.; Sleytr, U. B. S-Layer Stabilized Solid Supported Lipid Bilayers. *Journal of Structural Biology* **1997,** 119, (2), 123-128.
(52)Goksu, E. I.; Vanegas, J. M.; Blanchette, C. D.; Lin, W.-C.; Longo, M. L. AFM for structure and dynamics of biomembranes. *Biochim. Biophys. Acta* **2009,** 1788, 254-66.
(53)Vockenroth, I.; Ohm, C.; Robertson, J.; McGillivraya, D.; Lösche, M.; Köper, I. Stable insulating tethered bilayer lipid membranes. *Biointerphases* **2008,** 3, (2), FA68-FA73.
(54)Milhiet, P. E.; Vié, V.; Giocondi, M.-C.; Le Grimellec, C. AFM Characterization of Model Rafts in Supported Bilayers. *Single Molecules* **2001,** 2, 109-112.
(55)Giocondi, M.-C. c.; Milhiet, P. E.; Dosset, P.; Grimellec, C. L. Use of Cyclodextrin for AFM Monitoring of Model Raft Formation. *Biophys. J.* **2004,** 86, (2), 861-869.
(56)Chiantia , S.; Ries , J.; Kahya, N.; Schwille, P. Combined AFM and Two-Focus SFCS Study of Raft-Exhibiting Model Membranes. *ChemPhysChem* **2006,** 7, (11), 2409-2418.
(57)Chiantia, S.; Kahya, N.; Schwille, P. Raft Domain Reorganization Driven by Short- and Long-Chain Ceramide:A Combined AFM and FCS Study. *Langmuir* **2007,** 23, (14), 7659-7665.
(58)Connell, S. D.; Smith, D. A. The atomic force microscope as a tool for studying phase separation in lipid membranes (Review). *Molecular Membrane Biology* **2006,** 23, (1), 17-28.
(59)Simonsen, A. C. Activation of phospholipase A2 by ternary model membranes. *Biophys. J.* **2008,** 94, 3966-75.
(60)Sullan, R. M. a.; Li, J. K.; Hao, C.; Walker, G. C.; Zou, S. Cholesterol-dependent nanomechanical stability of phase-segregated multicomponent lipid bilayers. *Biophys. J.* **2010,** 99, 507-16.
(61)El Kirat, K.; Morandat, S.; Dufrêne, Y. F. Nanoscale analysis of supported lipid bilayers using atomic force microscopy. *Biochim. Biophys. Acta* **2010,** 1798, 750-65.
(62)Wang, T.; Shogomori, H.; Hara, M.; Yamada, T.; Kobayashi, T. Nanomechanical Recognition of Sphingomyelin-Rich Membrane Domains by Atomic Force Microscopy. *Biochemistry* **2012,** 51, (1), 74-82.
(63)Picas, L.; Rico, F.; Scheuring, S. Direct Measurement of the Mechanical Properties of Lipid Phases in Supported Bilayers. *Biophys. J.* **2012,** 102, (1), L01-L03.

(64)Cremer, P. S.; Boxer, S. G. Formation and Spreading of Lipid Bilayers on Planar Glass Supports. *J. Phys. Chem. B* **1999,** 103, 2554-2559.
(65)Simonsen, A. C.; Bagatolli, L. a. Structure of spin-coated lipid films and domain formation in supported membranes formed by hydration. *Langmuir* **2004,** 20, 9720-8.
(66)Mennicke, U.; Salditt, T. Preparation of Solid-Supported Lipid Bilayers by Spin-Coating. *Langmuir* **2002,** 18, 8172-8177.
(67)Perino-Gallice, L.; Fragneto, G.; Mennicke, U.; Salditt, T.; Rieutord, F. Dewetting of solid-supported multilamellar lipid layers. *Eur. Phys. J. E* **2002,** 8, 275-82.
(68)Ngwa, W.; Chen, K.; Sahgal, a.; Stepanov, E.; Luo, W. Nanoscale mechanics of solid-supported multilayered lipid films by force measurement. *Thin Solid Films* **2008,** 516, 5039-5045.
(69)Yamada, N.; Torikai, N. Additive-induced phase transition of a spin-coated lipid film. *Thin Solid Films* **2007,** 515, 5683-5686.
(70)Domenici, F.; Castellano, C.; Congiu, a.; Pompeo, G.; Felici, R. Ordering and lyotropic behavior of a silicon-supported cationic and neutral lipid system studied by neutron reflectivity. *Appl. Phys. Lett.* **2008,** 92, 193901.
(71)Jurak, M.; Chibowski, E. Wettability and topography of phospholipid DPPC multilayers deposited by spin-coating on glass, silicon, and mica slides. *Langmuir* **2007,** 23, 10156-63.
(72)Pompeo, G.; Girasole, M.; Cricenti, a.; Cattaruzza, F.; Flamini, a.; Prosperi, T.; Generosi, J.; Castellano, a. C. AFM characterization of solid-supported lipid multilayers prepared by spin-coating. *Biochim. Biophys. Acta* **2005,** 1712, 29-36.
(73)Krapf, L.; Dezi, M.; Reichstein, W.; Köhler, J.; Oellerich, S. AFM characterization of spin-coated multilayered dry lipid films prepared from aqueous vesicle suspensions. *Colloid Surface B* **2011,** 82, 25-32.
(74)Hoopes, M. I.; Faller, R.; Longo, M. L. Lipid Domain Depletion at Small Localized Bends Imposed by a Step Geometry. *Langmuir* **2012,** 27, (6), 2783-2788.
(75)Ogunyankin, M. O.; Torres, A.; Yaghmaie, F.; Longo, M. L. Lipid Domain Pixelation Patterns Imposed by E-beam Fabricated Substrates. *Langmuir* **2012,** 28, (18), 7107-7113.
(76)van Meer, G.; Voelker, D. R.; Feigenson, G. W. Membrane lipids: where they are and how they behave. *Nature Reviews Molecular Cell Biology* **2008,** 9, (2), 112-124.

(77)Butt, H.-J. Measuring electrostatic, van der Waals, and hydration forces in electrolyte solutions with an atomic force microscope. *Biophys. J.* **1991,** 60, (6), 1438-1444.
(78)Dufrêne, Y. F.; Boland, T.; Schneider, J. W.; Barger, W. R.; Lee, G. U. Characterization of the physical properties of model biomembranes at the nanometer scale with the atomic force microscope. *Faraday discussions* **1998**, 79-94; discussion 137-57.
(79)Garcia-Manyes, S.; Sanz, F. Nanomechanics of lipid bilayers by force spectroscopy with AFM: a perspective. *Biochim. Biophys. Acta* **2010,** 1798, 741-9.
(80)Redondo-Morata, L.; Giannotti, M. I.; Sanz, F., Stability of Lipid Bilayers as Model Membranes: Atomic Force Microscopy and Spectroscopy Approach. In *Atomic Force Microscopy in Liquid*, Wiley-VCH Verlag GmbH & Co. KGaA: 2012; pp 259-284.
(81)Brian, a. a.; McConnell, H. M. Allogeneic stimulation of cytotoxic T cells by supported planar membranes. *Proceedings of the National Academy of Sciences of the United States of America* **1984,** 81, 6159-63.
(82)Nussio, M. R.; Oncins, G.; Ridelis, I.; Szili, E.; Shapter, J. G.; Sanz, F.; Voelcker, N. H. Nanomechanical characterization of phospholipid bilayer islands on flat and porous substrates: a force spectroscopy study. *J. Phys. Chem. B* **2009,** 113, 10339-47.
(83)Franz, V. Tip penetration through lipid bilayers in atomic force microscopy. *Colloid Surface B* **2002,** 23, 191-200.
(84)Horcas, I. F., R.; Gomez-Rodriguez, J. M.; Colchero, J.; Gomez-Herrero, J.; and Baro, A. M. *Rev. Sci. Instrum.* **2007,** 78, 013705.
(85)M ller-Buschbaum, P. Dewetting and pattern formation in thin polymer films as investigated in real and reciprocal space. *J. Phys-Condens. Mat.* **2003,** 15, R1549-R1582.
(86)Sharma, a. Instability of Thin Polymer Films on Coated Substrates: Rupture, Dewetting, and Drop Formation. *J. Colloid Interface Sci* **1996,** 178, 383-399.
(87)Sharma, A.; Khanna, R. Pattern formation in unstable thin liquid films under the influence of antagonistic short- and long-range forces. *J. Chem. Phys.* **1999,** 110, 4929.
(88)Dekkiche, F.; Corneci, M. C.; Trunfio-Sfarghiu, a.-M.; Munteanu, B.; Berthier, Y.; Kaabar, W.; Rieu, J.-P. Stability and tribological performances of fluid phospholipid bilayers: Effect of buffer and ions. *Colloid Surface B* **2010,** 80, 232-239.
(89)Leonenko, Z. V.; Finot, E.; Ma, H.; Dahms, T. E. S.; Cramb, D. T. Investigation of temperature-induced phase transitions in DOPC and

DPPC phospholipid bilayers using temperature-controlled scanning force microscopy. *Biophys. J.* **2004,** 86, 3783-93.
(90)Picas, L.; Montero, M. T.; Morros, A.; Oncins, G.; Hernández-Borrell, J. Phase changes in supported planar bilayers of 1-palmitoyl-2-oleoyl-sn-glycero-3-phosphoethanolamine. *J. Phys. Chem. B* **2008,** 112, 10181-7.
(91)Binder, H. The Molecular Architecture of Lipid Membranes—New Insights from Hydration-Tuning Infrared Linear Dichroism Spectroscopy. *Appl. Spectrosc. Rev.* **2003,** 38, 15-69.
(92)Yang, L.; Ding, L.; Huang, H. W. Accelerated Publications New Phases of Phospholipids and Implications to the Membrane Fusion Problem †. *Biochemistry* **2003,** 42, (22), 6631-6635.
(93)Garcia-Manyes, S.; Redondo-Morata, L.; Oncins, G.; Sanz, F. Nanomechanics of lipid bilayers: heads or tails? *J. Am. Chem. Soc.* **2010,** 132, 12874-86.
(94)Garcia-Manyes, S.; Domènech, O.; Sanz, F.; Montero, M. T.; Hernandez-Borrell, J. Atomic force microscopy and force spectroscopy study of Langmuir-Blodgett films formed by heteroacid phospholipids of biological interest. *Biochim. Biophys. Acta* **2007,** 1768, 1190-8.
(95)Oncins, G.; Picas, L.; Hernández-Borrell, J.; Garcia-Manyes, S.; Sanz, F. Thermal response of Langmuir-Blodgett films of dipalmitoylphosphatidylcholine studied by atomic force microscopy and force spectroscopy. *Biophys. J.* **2007,** 93, 2713-25.
(96)Garcia-Manyes, S.; Oncins, G.; Sanz, F. Effect of temperature on the nanomechanics of lipid bilayers studied by force spectroscopy. *Biophys. J.* **2005,** 89, 4261-74.
(97)Pera, I.; Stark, R.; Kappl, M.; Butt, H.-J.; Benfenati, F. Using the atomic force microscope to study the interaction between two solid supported lipid bilayers and the influence of synapsin I. *Biophys. J.* **2004,** 87, 2446-55.
(98)Marrink, S.-J.; Mark, A. E. Molecular view of hexagonal phase formation in phospholipid membranes. *Biophys. J.* **2004,** 87, 3894-900.
(99)Dols-Perez, A.; Fumagalli, L.; Simonsen, A. C.; Gomila, G. Ultrathin Spin-Coated Dioleoylphosphatidylcholine Lipid Layers in Dry Conditions: A Combined Atomic Force Microscopy and Nanomechanical Study. *Langmuir* **2011,** 27, (21), 13165-13172.
(100)Tokumasu, F.; Jin, A. J.; Feigenson, G. W.; Dvorak, J. a. Nanoscopic lipid domain dynamics revealed by atomic force microscopy. *Biophys. J.* **2003,** 84, 2609-18.

(101)Garciamanyes, S.; Oncins, G.; Sanz, F. Effect of pH and ionic strength on phospholipid nanomechanics and on deposition process onto hydrophilic surfaces measured by AFM. *Electrochimica Acta* **2006,** 51, 5029-5036.
(102)Lewis, B. A.; Engelman, D. M. Lipid bilayer thickness varies linearly with acyl chain length in fluid phosphatidylcholine vesicles. *Journal of Molecular Biology* **1983,** 166, (2), 211-217.
(103)Vanegas, J. M.; Faller, R.; Longo, M. L. Influence of Ethanol on Lipid/Sterol Membranes: Phase Diagram Construction from AFM Imaging. *Langmuir* **2010,** 26, (13), 10415-10418.
(104)Gedig, M.; Faiß, S.; Janshoffa, A. Melting and interdigitation of microstructured solid supported membranes quantified by imaging ellipsometry. *Biointerphases* **2008,** 3, (2), FA51-FA58.
(105)Xing, C.; Ollila, O. H. S.; Vattulainen, I.; Faller, R. Asymmetric nature of lateral pressure profiles in supported lipid membranes and its implications for membrane protein functions. *Soft Matter* **2009,** 5, (17), 3258-3261.
(106)Dynarowicz-Latka, P.; Hac-Wydro, K. Interactions between phosphatidylcholines and cholesterol in monolayers at the air/water interface. *Colloid Surface B* **2004,** 37, 21-25.
(107)Alwarawrah, M.; Dai, J.; Huang, J. A Molecular View of the Cholesterol Condensing Effect in DOPC Lipid Bilayers. *J. Phys. Chem. B* 114, (22), 7516-7523.
(108)Smaby, J. M.; Brockman, H. L.; Brown, R. E. Cholesterol's Interfacial Interactions with Sphingomyelins and-Phosphatidylcholines: Hydrocarbon Chain Structure Determines the Magnitude of Condensation. *Biochemistry* **1994,** 33, (31), 9135-9142.
(109)Pan, J.; Mills, T. T.; Tristram-Nagle, S.; Nagle, J. F. Cholesterol Perturbs Lipid Bilayers Nonuniversally. *Phys. Rev. Lett.* **2008,** 100, (19), 198103.
(110)de Almeida, R. F. M.; Fedorov, A.; Prieto, M. Sphingomyelin/phosphatidylcholine/cholesterol phase diagram: boundaries and composition of lipid rafts. *Biophys. J.* **2003,** 85, 2406-16.
(111)Ramstedt, B.; Slotte, J. P. Sphingolipids and the formation of sterol-enriched ordered membrane domains. *Biochim. Biophys. Acta* **2006,** 1758, 1945-56.
(112)An, H.; Nussio, M. R.; Huson, M. G.; Voelcker, N. H.; Shapter, J. G. Material Properties of Lipid Microdomains: Force-Volume Imaging Study of the Effect of Cholesterol on Lipid Microdomain Rigidity. *Biophys. J.* **2010,** 99, (3), 834-844.

(113)Maulik, P. R.; Shipley, G. G. Interactions of N-stearoyl sphingomyelin with cholesterol and dipalmitoylphosphatidylcholine in bilayer membranes. *Biophys. J.* **1996,** 70, (5), 2256-2265.
(114)Sullan, R. M. A.; Li, J. K.; Zou, S. Direct Correlation of Structures and Nanomechanical Properties of Multicomponent Lipid Bilayers. *Langmuir* **2009,** 25, (13), 7471-7477.
(115)El Kirat, K.; Morandat, S. Cholesterol modulation of membrane resistance to Triton X-100 explored by atomic force microscopy. *Biochim.Biophys.Acta.Biomem.* **2007,** 1768, (9), 2300-2309.
(116)Marsh, D. Cholesterol-induced fluid membrane domains: A compendium of lipid-raft ternary phase diagrams. *Biochim.Biophys.Acta.Biomem.* **2009,** 1788, (10), 2114-2123.
(117)Gandhavadi, M.; Allende, D.; Vidal, A.; Simon, S. A.; McIntosh, T. J. Structure, Composition, and Peptide Binding Properties of Detergent Soluble Bilayers and Detergent Resistant Rafts. *Biophys. J.* **2002,** 82, (3), 1469-1482.
(118)Rinia, H. A.; Snel, M. M. E.; van der Eerden, J. P. J. M.; de Kruijff, B. Visualizing detergent resistant domains in model membranes with atomic force microscopy. *FEBS Letters* **2001,** 501, (1), 92-96.
(119)Simons, K.; Ikonen, E. How Cells Handle Cholesterol. *Science* **2000,** 290, 1721-1726.
(120)Silvius, J. Role of cholesterol in lipid raft formation: lessons from lipid model systems. *Biochim.Biophys.Acta.Biomem.* **2003,** 1610, 174-183.
(121)Crane, J. M.; Tamm, L. K. Role of cholesterol in the formation and nature of lipid rafts in planar and spherical model membranes. *Biophys. J.* **2004,** 86, 2965-79.

8.2 Figure index